The Functional Relevance of Tensin1 in Chronic Obstructive Pulmonary Disease

Thesis submitted for the degree of

Doctor of Philosophy

at the University of Leicester

by

Panayiota Stylianou MSc (Hons)

Department of Infection Immunity and Inflammation

University of Leicester

August 2017

Abstract

Panayiota Stylianou

The Functional Relevance of Tensin1 in Chronic Obstructive Pulmonary Disease

Background
Chronic obstructive pulmonary disease (COPD) constitutes a major cause of morbidity and mortality. Genome wide association studies (GWAS) have shown significant associations between airflow obstruction or COPD with a non-synonymous single nucleotide polymorphism (SNP) in the TNS1 gene (which encodes tensin1) with COPD. This SNP generates the amino acid change R1197W in the tensin1 protein. R1197W is associated with reduced FEV1.

Aim
To examine tensin1 genotype, expression and function in human airways and cells from healthy controls and patients with smoking-related COPD or asthma.

Methods
Lung resections were immunostained for tensin1. Tensin1 expression in cultured human airway smooth muscle cells (HASMCs) and bronchial epithelial cells (HBECs) was evaluated using qRT-PCR, western blotting and immunofluorescent staining. siRNAs were used to downregulate tensin1 expression, and cells from healthy subjects and patients were genotyped using restriction fragment length polymorphism (RFLP) analysis.

Results
Immunohistochemical staining demonstrated increased tensin1 expression in the airway smooth muscle and lamina propria in COPD tissue, but not in asthma, when compared to healthy controls. Tensin1 was expressed in HASMCs and upregulated by TGFβ1. TGFβ1 and fibronectin increased the localisation of tensin1 to fibrillar adhesions. Tensin1 and α-smooth muscle actin (αSMA) were strongly co-localised in actin stress fibres. Tensin1 depletion in HASMCs attenuated αSMA expression and their contraction of collagen gels, but not proliferation. RFLP analysis revealed the presence of R1197W in predominantly people with COPD and asthma, but rarely in healthy controls.

Conclusions
Tensin1 may promote airway obstruction by enhancing the expression of contractile proteins and their localisation to stress fibres in HASMCs. R1197W is associated predominantly with COPD and asthma suggesting that the polymorphism may promote dysfunction in HASMCs.

Acknowledgements

The path towards this dissertation has been circuitous. Its completion is thanks in large part to the special people who challenged, supported and stuck with me along the way. First and foremost, I am grateful to my supervisor, Prof Peter Bradding, whose expertise, understanding, generous guidance and support made it possible for me.

I am grateful to Dr Katherine Clark for her immense interest and for providing me with materials and support. I would like to thank my colleagues within the Department of Respiratory Medicine, who supported me and challenged me throughout the project. This work would not materialise without the financial support of Biomedical Research Unit. I also thank the University of Leicester for the opportunity to study for a PhD degree.

These acknowledgments would not be complete without mentioning my friends and family. My deepest appreciation belongs to my friends for their patience and understanding, Finally, I would like to acknowledge with gratitude, the support and love of my family. They kept me going, and this would not have been possible without them. Thank you for standing behind me through this study.

Table of Contents

List of tables

List of figures

List of abbreviations

αSMA	alpha smooth muscle actin
AAT	α_1-antitrypsin deficiency
ABD	Actin-binding domain
ASM	Airway smooth muscle
BEBM	Bronchial Epithelial Basal medium
BEGM	Bronchial Epithelial Growth medium
CD	Cluster of differentiation
COPD	Chronic obstructive pulmonary disease
DAB	3,3'-diaminobenzidine
DAMPs	Damage-associated molecular patterns
DAPI	4',6-diomidino-2-phenylindole
DLC-1	Deleted in liver cancer-1
DMEM	Dulbecco's Modified Eagle medium
ECM	Extracellular matrix
EGF	Endothelial growth factor
FAB	Focal adhesion-binding
FAK	Focal adhesion kinase
FEV_1	Forced expiratory volume at second 1
FITC	Fluorescein conjugates
FSP	Fibroblast surface protein

FVC	Forced vital capacity
GM-CSF	Granulocyte macrophage colony stimulating factor
GMA	Glycolmethacrylate
GOLD	Global initiative for chronic obstructive lung disease
HASMCs	Human airway smooth muscle cells
IL	Interleukin
IFN	Interferon
IKK	IκB kinase
IPP	Integrin linked kinase, PINCH, and parvin
JNK	c-Jun amino-terminal kinase
LB	Luria Broth
LT	Leukotriene
MAPK	Mitogen-activated protein kinase
MCC	Mucociliary clearance
MCP	Monocyte chemotactic peptide
MMP	Matrix metalloproteinase
NE	Neutrophil elastase
NF	Nuclear factor
NK	Natural killer
OD	Optical density
PDGF	Platelet-derived growth factor
PI3	Phosphoinositide 3

PMSF	Phenylmethanesulfonylfluoride
PP1α	Protein phosphatase 1α
PRRs	Pattern recognition patterns
PTB	Phosphotyrosine-binding
PTEN	Phosphatase and tensin
PVDF	Polyvinylidene
RFLP	Restriction fragment length polymorphism
RIPA	Radio-Immuno-Precipitation-Assay
ROS	Reactive oxygen species
SDS-PAGE	Sodium dodecyl sulphate polyacrylamide gel electrophoresis
SH2	Src homology 2
SNP	Single nucleotide polymorphism
TAE	Tris-Acetate-EDTA
TBS	Tris Buffer Saline
TGF	Transforming growth factor
TGS	Tris-Glycine-SDS
Th	T helper
TLRs	Toll-like receptors
TNF	Tumor necrosis factor
TNS1	Tensin1
TSLP	Thymic stromal lymphopoietin
VEGF	Vascular endothelial growth factor

Chapter 1: Introduction

1.1 Chronic Obstructive Pulmonary Disease (COPD)

COPD is a chronic inflammatory disease of the airways (Rovina, Koutsoukou and Koulouris 2013). It is characterised by four pathologic features: chronic obstructive bronchitis, small airway fibrosis, emphysema and mucus overproduction. These conditions contribute in varying amounts to the development of small airway obstruction, the key characteristic of the disease (Marin et al. 2011). Spirometry is the main tool used for the diagnosis of COPD and in particular for identifying airflow obstruction, the hallmark of COPD (Brusasco, Barisione and Crimi 2015, Siafakas et al. 1995). FEV_1 (Forced expiratory volume in second 1) to FVC (Forced vital capacity) ratio of <0.70 indicates the presence of airflow limitation. Severity of airway obstruction can be classified into four groups (GOLD1, GOLD 2, GOLD 3 and GOLD 4) based on post-bronchodilator FEV_1 value (From the Global Strategy for the Diagnosis, Management and Prevention of COPD, Global Initiative for Chronic Obstructive Lung Disease (GOLD) 2017) (**Table 1.1**). Available at: http://goldcopd.org). COPD is often overlooked in at risk groups as 50-90% of the disease burden remains undiagnosed (Haroon et al. 2015).

Mild COPD	$FEV_1/FVC < 0.7$ FEV_1 > or = 80% predicted	Asymptomatic. Patient probably unaware of lung function decline
Moderate COPD	$FEV_1/FVC < 0.7$ FEV_1 50% TO 79% predicted	Symptoms develop with evident shortness of breath.
Severe COPD	$FEV_1/FVC < 0.7$ FEV_1 30% TO 49 % predicted	Worsening shortness of breath. COPD exacerbations are common
Very Severe COPD	$FEV_1/FVC < 0.7$ FEV_1 < 30% predicted	Impaired quality of life. COPD exacerbations can be life threatening.

Table 1.1: GOLD spirometric criteria for COPD severity.

1.1.1 COPD epidemiology

COPD constitutes a major cause of morbidity and mortality in developed countries (Yang et al. 2012). It is expected to be the 3rd leading cause of death worldwide by 2020 and the UK is among the top 20 countries for COPD mortality (Marin et al. 2011). More than 200 million people are affected worldwide (Shaykhiev and Crystal 2013). In the UK, a 9% increase in the prevalence of COPD was recorded between 2008 and 2012; currently 1.2 million people are diagnosed with COPD (British Lung Foundation - Respiratory Health of the Nation project). Although, the prevalence of COPD has increased dramatically (Adeloye et al.), relatively very little is known about the mechanisms involved in disease pathogenesis.

1.1.2 COPD aetiology and risk factors

The development of COPD is multifactorial and risk factors for COPD include genetic and environmental factors.

1.1.2.1 Environmental factors

Tobacco smoking is by far the largest risk factor for COPD. Although it is widely accepted that smoking is the main causative factor, only 15-20% of smokers develop COPD (Rovina et al. 2013). It is therefore likely that an abnormal response to cigarette smoking leads to the development of COPD in a susceptible individual, likely due to genetic and/or developmental factors.

Air pollution, oxides, carbon dioxide and biological allergens are all environment factors associated with COPD. A community-based study showed that increased traffic density was significantly associated with lower FEV_1 and FVC in women (Kan et al. 2007).

1.1.2.2 Genetic factors

Evidence suggests that gene-environment interactions constitute a critical factor for the development of COPD (Agusti, Sobradillo and Celli 2011). The influence of each gene in isolation is probably weak, but it has been suggested that multiple genes can act synergistically towards the development of COPD (Caramori, Casolari and Adcock 2013). A well-established genetic factor for the development of COPD is severe α_1–antitrypsin (AAT) deficiency, which is responsible for 1-2% of cases of COPD. A mutation in the SERPINA 1 gene can cause severe AAT-deficiency (Foreman, Campos and Celedon 2012). Another gene significantly associated with the development of COPD, and in particular emphysema, is BICD1. A single nucleotide polymorphism in this gene affects telomere length. This supports the principle that accelerated aging contributes to the development of emphysema (Agusti et al. 2011). Moreover, there are several on-going Genome Wide Association Studies (GWAS) that suggest the role of many genes in determining pulmonary function and the development of COPD, such as TNS1, GSTCD and HTR4 (Soler Artigas et al. 2011). However, more research needs to be performed to establish their role in COPD.

1.1.2.3 Infections

Enhanced responsiveness to respiratory infections is another characteristic of COPD. Colonisation of the airways, and particularly the small airways, with various bacteria, such as *Streptococcus pneumoniae* and *Haemophilus Influenzae*, results in exacerbations of the disease and strongly correlates with severity of disease (Shaykhiev and Crystal 2013). Infections have been previously recorded in 30% of patients with stable disease and 50% of patients during exacerbation episodes (Sethi and Murphy 2008).

1.1.2.4 Other risk factors

Exposure to dusts and fumes, previous tuberculosis, childhood respiratory infections and low birth weight, asthma and maternal smoking are other risk factors associated with the development of airflow obstruction and reduced FEV_1 (Decramer, Janssens and Miravitlles 2012, Barker et al. 1991).

1.1.3 COPD pathogenesis

Altered immunity, activation of the nuclear factor (NF)-κB pathway, and inflammation are some of the features involved in COPD pathogenesis and they will be discussed in further detail.

1.1.3.1 Innate immunity in COPD

The lung innate immune system includes the airway epithelial barrier and innate leukocytes including alveolar macrophages, dendritic cells, neutrophils, mast cells and natural killer cells. These cells constitute the first responders to tissue injury that direct the subsequent immune and inflammatory responses seen in COPD (Holtzman et al. 1983).

Airway epithelial barrier removes microbes via the mucociliary clearance mechanism involving airway host defence proteins and epithelial cell-derived cytokines (Shaykhiev et al. 2011). Airway epithelial cells, and in general epithelial cells, express various pattern recognition receptors (PRRs) and an example is the Toll-like receptors (TLRs). TLR3 and TLR4 respond to viral and bacterial products respectively leading to cell activation and the triggering of acute inflammatory responses (Wang et al. 2011, Trompette et al. 2009). Both receptors result in the activation of a number of cytokines, such as anti-viral type I and type III interferons for TLR3, and pro-inflammatory cytokines, such as tumor necrosis factor (TNF) –α, interleukin (IL) -1β and Il-6 for TRL4 (Ioannidis et al. 2013, Miller et al. 2005). Clara cells, a cell population mostly found in the distal airways, protect the lining of the bronchiolar epithelium by detoxifying harmful substances and producing host defence proteins, such as secretoglobin and uteroglobin. However, smoking and other irritants result in the loss of Clara cells and this has as a consequence the inefficiency of the epithelium to eliminate microbes (Fernandez-Valdivia et al. 2006, Lumsden, McLean and Lamb 1984).

Macrophages, a heterogeneous population of cells, can be activated either directly via the PRRs or indirectly via damage-associated molecular patterns

(DAMPs). DAMPs are proteins found on the surface of the cell following tissue injury (Grashoff et al. 1997). Impaired inflammation and tissue injury, but also wound repair and control of inflammation can be the result of activated macrophages as macrophages are responsible for the production of pro- and anti-inflammatory mediators, cytokines, reactive oxygen and nitrogen intermediates (ROIs) (RNIs) (Hiemstra 2013). Increased numbers of macrophages and macrophages chemoattractants have been found in COPD subjects and these are correlated with the degree of airway obstruction and severity of COPD (Barnes 2004).

Dendritic cells constitute another component of the innate immune system and their activity is impaired in COPD. Dendritic cells migrate to lymphoid tissues to present antigens to lymphocytes. This results in the activation of T cells and primary immune responses. However, these cells are extremely responsive to pollutants and DAMPs produced by irritants resulting in sending altered signals to T cells and in general inability to activate an immune response (Upham and Xi 2016). Decreased numbers of mature dendritic cells have been found in COPD subjects suggesting further inefficiency to accomplish their purpose (Van Pottelberge et al. 2010).

Mast cells, important immune effector and modulatory cells, also participate in the early recognition of pathogens. Within seconds of stimulation, they undergo degranulation resulting in the release of bioactive agents found in their cytoplasmic granules. Pro-fibrotic, pro-angiogenic such as vascular endothelial growth factor (VEGF), and anti-angiogenic factors are some of the bioactive agents released during mast cell degranulation (Abraham and St John 2010,

Norrby 2002). Increased number of mast cells has been reported in the epithelium of current and ex smokers with COPD, when compared to controls (Grashoff et al. 1997). Furthermore, positive correlation between ASM and epithelial mast cell density and FEV_1 predicted and FEV_1/FVC ratio respectively has been reported (Gosman et al. 2008). These data suggest a role for mast cells in COPD, and potentially in preserving airway function.

Neutrophils are immune cells that migrate to the site of tissue injury or damage, only when particular pro-inflammatory cytokines and chemoattractants have already been released. Once, they arrive at the site of injury, they release anti-microbial and highly reactive oxidants, such as lytic granules and neutrophil elastase to inactivate the pathogen and then phagocytose it. However, this process is impaired in COPD resulting in inevitable damage to the host tissue (Hoenderdos and Condliffe 2013). Increased number of neutrophils has been observed in the airways of COPD subjects, which results in the production of several inflammatory cytokines such as interleukin (IL) -1β, IL-6 and tumor necrosis factor (TNF) -α (Lugade et al. 2014).

Finally, natural killer (NK) cells are also involved in the immunity in the lungs. Exposure to irritants and cigarette smoke promotes the expression of ligands activating NK cells by airway epithelial cells. NKG2D is an example of a ligand that results in the activation of NK cells (Borchers et al. 2009). Upon their activation, IFN-γ, TNF-α and IL-12 are released to activate other immune cells for assistance in order to destroy the stressed and infected cells. It is believed that tobacco smoke causes inhibition of production of TNF-α and IFN-γ resulting in decreased NK cell activity in smokers (Mian et al. 2008).

1.1.3.2 Adaptive immune responses in COPD

The innate immune response constitutes the first line of defence, however an adaptive immune response is extremely important for the prolonged protection of the airways from irritants, pathogens and regulation of inflammation and other processes. Infiltration of cluster of differentiation (CD) 8+ T, T helper (Th) 1 and Th17 CD4+ and B cells indicates the presence of activated adaptive immune responses in COPD (Pouwels et al. 2014). Positive correlation between the number of CD8+ T cells and severity of airway obstruction and emphysema in COPD has been reported. Apoptosis and necrosis of structural cells can occur from the release of proteolytic enzymes by the activated CD8+ T cells (Saetta et al. 1998). Another type of T cells, CD4+, is also upregulated in the lungs of COPD subjects. There are several types of CD4+ cells, including the Th1, Th2 and Th17. Th1 cells predominantly secrete IFN-γ, Th2 cells secrete IL-4, IL-5 and IL-13, whereas Th17 cells produce IL-17A and F and regulate inflammation (Miossec, Korn and Kuchroo 2009). Furthermore, a decrease in the number of T-regulatory cells has been reported in smokers with COPD, these cells regulate the action of the other T cells and generally suppress inflammation and prevent autoimmunity (Pouwels et al. 2014).

B cells express CD20 (MS4A1) and constitute a population of lymphocytes that develops into antibody-secreting plasma cells (Cooper 2015). Increased numbers of B cells have also been observed in the small and large airways of COPD patients. It has been reported that B cells produce IL-10 that contributes to macrophage activation and the release of matrix metalloproteinases (MMPs) with an effect on airspace enlargement. MMPs have an important role in the

regulation of cytokine and chemokine production, apoptosis and proliferation (Polverino et al. 2016). An ongoing recruitment of activated antigen presenting cells occurs in COPD. An example is the constant production of mediators activating B cells resulting in further tissue injury and inflammation. Increased amount of autoantibodies have been found in COPD patients' serum supporting the hypothesis that COPD may also be an autoimmune disease (Nunez et al. 2011).

1.1.3.3 The nuclear factor (NF)-κB pathway in COPD

NF-κB, a protein complex, is ubiquitously expressed in eukaryotic cells, including alveolar macrophages. Irritants, including cigarette smoke, result also in the activation of a kinase known as IκB kinase. IκB kinase (IKK) then causes degradation and phosphorylation of IκB component, a component bound to the NF-κB protein complex. NF-κB migrates into the nucleus and activation of several cytokines and inflammatory mediators occurs, such as TNF-α and IL-1β (Marin et al. 2011). This eventually results in the recruitment of other inflammatory cells, which in turn results in the expression of several cytokines and growth factors (**Figure 1.1**). It is proposed that this leads to airway damage and emphysema (Caramori et al. 2013).

1.1.3.4 Inflammation in COPD

COPD is a chronic inflammatory disease and perpetuates a state of chronic inflammation. Defective innate immunity in the lungs, as discussed above, leads to an increased frequency of infections and aggravation of the airway inflammation (Shaykhiev and Crystal 2013). Several cells, including epithelial cells, macrophages and neutrophils, are contributing in the orchestration of inflammation by releasing pro-inflammatory cytokines. Epithelial cells, once activated, can produce a number of inflammatory cytokines including TNF-α, IL-1β, granulocyte macrophage colony stimulating factor (GM-CSF) and IL-8. In small airways, epithelial cells also secrete transforming growth factor (TGF) β, which can then induce fibrosis (Barnes, Shapiro and Pauwels 2003). TGFβ1 increases the endothelial and epithelial permeability resulting in disruption of the adherens junctions (Leikauf et al. 2012). Neutrophils recurrent infiltration results in the secretion of reactive oxygen species (ROS) and MMP8 and MMP9 that in turn result in tissue destruction and in prolonged inflammation (Barnes et al. 2003). Macrophages are also involved in the development of airway inflammation and appear to have a crucial role in the pathogenesis of COPD, as they are associated with many characteristics of the disease. Macrophages secrete a number of inflammatory mediators including IL-8, TNF-α, leukotriene (LT) B4, CXC chemokines and monocyte chemotactic peptide (MCP) 1 (Rovina et al. 2013).

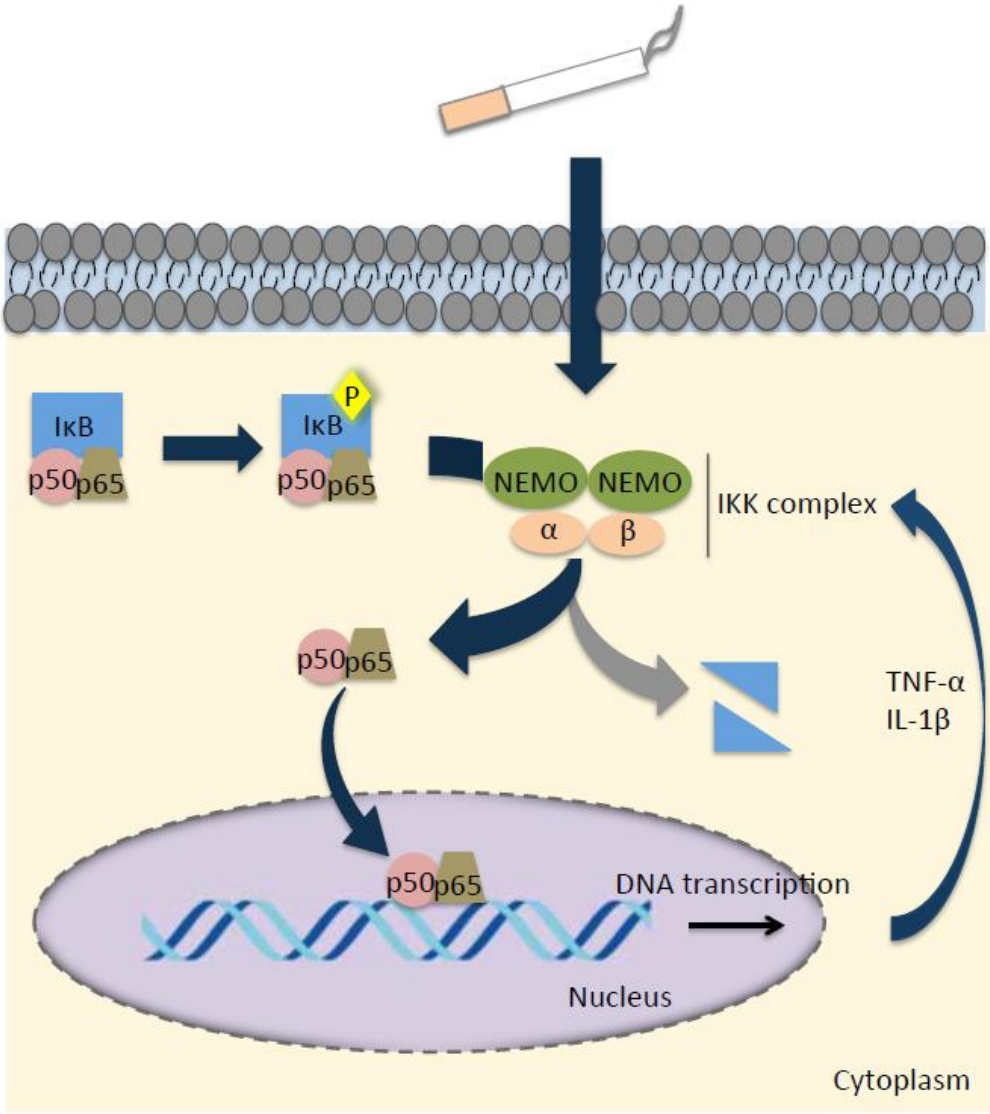

Figure 1.1: The NF-κB pathway. Cigarette smoking triggers this pathway and its activation leads to the expression of several cytokines and chemokines. This causes infiltration of several inflammatory cells resulting in initiation of the inflammatory cascade seen in COPD pathophysiology.

1.1.3.5 Apoptosis and eferocytosis

Apoptosis is another mechanism that is dysregulated in COPD like immune system and inflammation. Increased numbers of apoptotic structural cells, epithelial and endothelial cells, in the lungs of COPD patients has been reported (Segura-Valdez et al. 2000). Another study indicates impaired apoptosis in neutrophils. Altered expression of bak, bcl-xl and mcl-1 apoptotic genes in unstimulated neutrophils from COPD patients has been reported when compared to healthy controls, suggesting delayed neutrophil apoptosis in COPD. This is independent of the smoking habit of the individual (Zhang et al. 2012).

Eferocytosis is the process of removal of apoptotic immune and structural cells by phagocytosis. This process can be carried out by dendritic, epithelial and mesenchymal cells, but the cell type primarily responsible for this is airway macrophages (Grabiec and Hussell 2016). Accumulation of apoptotic cells in the lungs of individuals with COPD occurs and indicates inefficiency of the cells to carry out eferocytosis. This deficiency in alveolar macrophages might be the consequence of altered expression of cluster of differentiation (CD) 31, 44 and 91, proteins involved in apoptotic recognition and binding (Hodge et al. 2007). Uncontrolled eferocytosis promotes the release of DAMPs which results in aberrant inflammation (Grabiec and Hussell 2016).

1.1.4 COPD and pathophysiology

As described above, a characteristic of COPD is chronic airway inflammation(Han and Criner 2013). Exposure to tobacco smoking and/or inhaled pollutants can

enhance this via the activation of structural and inflammatory cells, which in turn result in the release of chemotactic mediators. Chemotactic mediators then cause infiltration of further inflammatory cells. These changes cause a perpetuated state of chronic inflammation which is thought to result in structural changes in the airways, destruction of alveoli leading to emphysema and subsequent airway obstruction (Stockley, Mannino and Barnes 2009). Airway obstruction is the major pathophysiological feature of COPD (Siafakas et al. 1995). It occurs due to both emphysema and airway wall pathology. The presence of emphysema leads to a reduction in the elastic recoil of the lung which leads to airway collapse. Airway obstruction also results from changes in the airway wall, including deposition of matrix proteins, hyperplasia and hypertrophy of airway smooth muscle, and mucus gland hyperplasia with associated mucus hypersecretion (Chung 2005).

1.1.4.1 Emphysema

Pulmonary emphysema is defined pathologically as a permanent abnormal enlargement of air spaces distal to the terminal bronchioles with destruction of the alveolar septa with little or no fibrosis (1985). As a consequence, both ventilation and perfusion in emphysematous regions are reduced (Brusasco et al. 2015). The development of emphysema in COPD is proposed to occur due a protease-antiprotease imbalance, a hypothesis arising from two different studies. The first study showed that rodents develop emphysema following instillation of proteases in the lungs (Gross et al. 1965). The second study revealed that three out of five subjects with severe α_1–antitrypsin (AAT)

deficiency, a well-established genetic factor for the development of COPD, have developed emphysema (Larsson 1978). Smoking and other irritants, as discussed above, evoke a recurrent infiltration of inflammatory cells, such as macrophages and neutrophils, resulting in the release of proteolytic enzymes. The amount of proteolytic enzymes released exceeds the natural capacity of the lungs protease inhibitors resulting in tissue injury and airspace enlargement (Abboud and Vimalanathan 2008). These proteolytic enzymes subsequently cause activation of other proteinases and elimination of chemotactic mediators contributing to the recurrent protease-antiprotease imbalance (Houghton 2015).

Emphysema involves the degradation of elastin and collagen lung matrix components. Elastin degradation can be the result of action of several proteases found in the neutrophils' granules and of extreme importance are neutrophil elastase (NE), proteinase 3 and cathepsin G (Guyot et al. 2014). Elastin is the protein responsible in maintaining lung tissues' elasticity and tensile strength. Subjects with AAT deficiency lack the inhibitor for neutrophil elastase and as a consequence it can perform its catalytic activity against elastin unchecked. Although NE alone can trigger tissue destruction (Shapiro et al. 2003), more severe lung damage has been observed when neutrophil serine proteases (cathepsin G, NE and proteinase 3) act synergistically (Guyot et al. 2014). MMPs can also cause elastin degradation, and in particular macrophage elastase (MMP12). Decreased lung macrophage infiltration has been reported in MMP12-deficient smoke-exposed mice (Houghton et al. 2006). There is evidence that NE and MMP12 support the action of each other as NE causes degradation of

inhibitors of MMPs and MMPs in turn degrade AAT during smoke-induced emphysema (Shapiro et al. 2003).

Collagen degradation is also evident in emphysema (Michaeli and Fudenberg 1974). It has a role in both emphysema development and severity (Pins et al. 1997). MMP1 (collagenase 1) appears to have a role in the development of emphysema in COPD subjects. Increased MMP1 expression has been reported and expression was positively correlated with severity of disease by GOLD stage (Gosselink et al. 2010). Other MMPs that exhibit collagenase catalytic activity are MMP8 and MMP13. However, their role in development of emphysema in COPD subjects remains unclear and evidence is sparse (Houghton 2015).

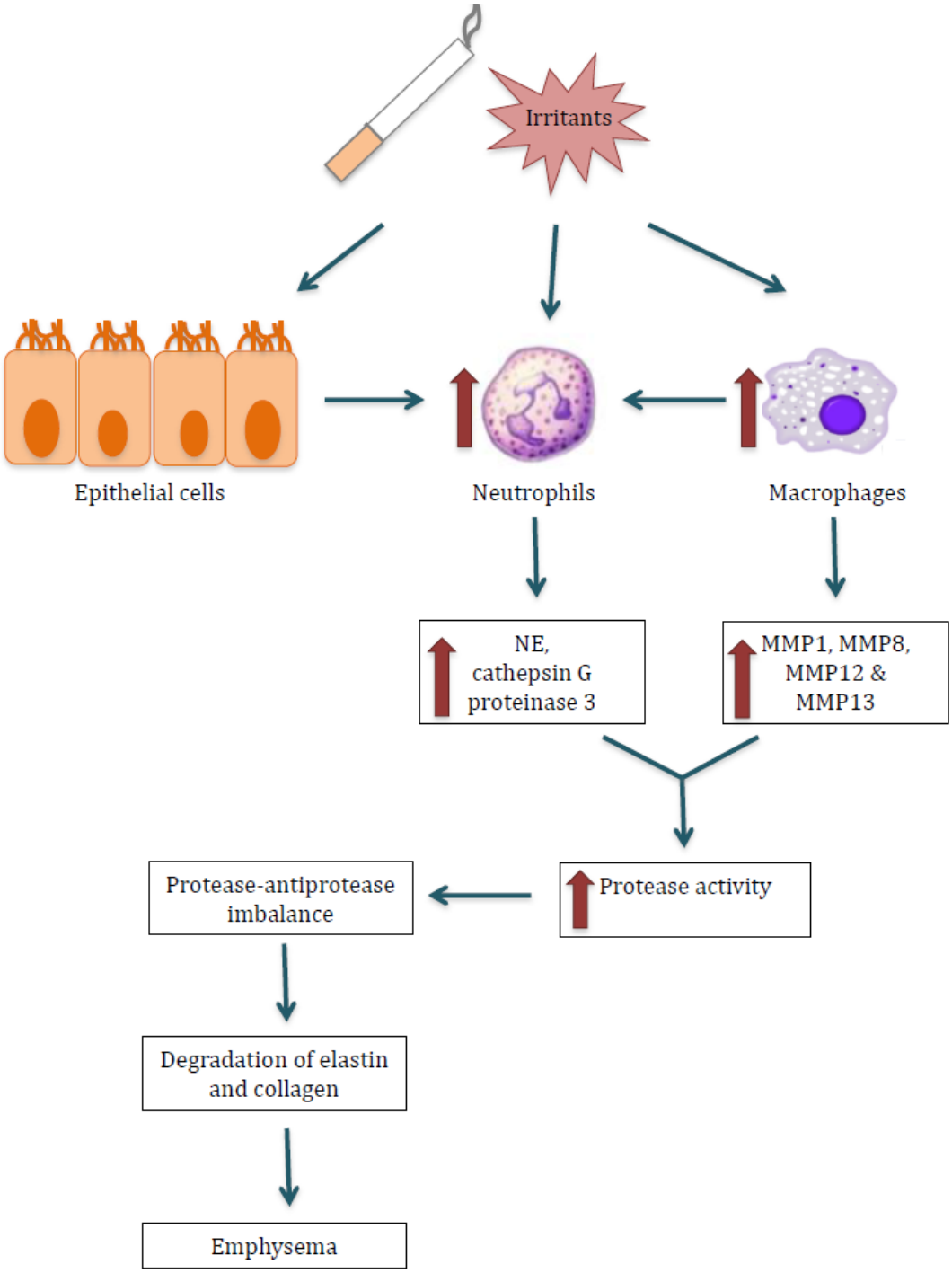

Figure 1.2: Schematic of emphysema pathogenesis. A diagram illustrating the role of inflammation infiltration, activated by tobacco smoking and irritants, in protease-antiprotease imbalance and subsequently in the development of emphysema.

1.1.4.2 Airway wall pathology

Pathological abnormalities occur in both the small and large airways in COPD. These abnormalities are associated with the degree of airway obstruction. An ongoing inflammatory response, changes of normal airway structure, such as thickening of the airway wall and airway smooth muscle, mucus hypersecretion and emphysema are features contributing to the development of airway obstruction (Barnes et al. 2003, Smaldone et al. 1993, Chung 2005). In these processes, interactions between cells, between cells and the environment and mechanical forces of breathing are of extreme importance for the excessive narrowing of conducting airways seen in COPD (Prakash 2016).

1.1.4.2.1 The airway mucus

In healthy airways, mucus lines the intrapulmonary airways and is composed of a number of antimicrobial enzymes (defensins), immunomodulatory molecules (cytokines) and glycoproteins (mucins) generated by specialised secretory cells (Evans et al. 2010). Mucins are large glycoproteins binding to water and as a result mucus contains 97% water. In a healthy individual, ciliary beating prevents mucus accumulation and adhesion of the glycoproteins to the apical epithelial membrane (Fahy and Dickey 2010). Cilia are hair-like structures lining the respiratory tract and beat in a synchronised manner propelling mucus and the substances it traps towards the glottis (Wanner, Salathe and O'Riordan 1996).

Irritants, tobacco smoking and inhaled pollutants can cause changes in epithelial structure leading to increased numbers of mucus secreting goblet cells. Squamous metaplasia, the replacement of differentiated ciliated and secretory cells with squamous cells, is associated with basal and goblet cell hyperplasia. Increased number of goblet cells results in increased mucin secretion leading to excessive amounts of mucus (Schamberger et al. 2015). Mucin can also make the mucus layer more viscous making it difficult to be removed by beating cilia. Th17 inflammation, triggered by irritants as discussed above, has a crucial role in the development of mucus metaplasia as IL-17 can induce production of IL-6 by airway epithelial cells and both can then in turn cause production of Muc5AC and Muc5B, mucins found in the airways mucus (Chen et al. 2003). IL-13 also induces mucus production, and particularly Muc5AC, and goblet cell hyperplasia (Kanoh, Tanabe and Rubin 2011). Another factor contributing to mucus production is excess of Na^+ and fluid absorption by surfaces expressing hyperactive epithelial Na^+ channels causing airway surface liquid deletion. Epithelial Na^+ channels have a key role in mediating airway volume and facilitate mucociliary clearance (MCC) mechanism. Enhanced proteolysis of these channels result in increased viscosity of airway fluids (Gentzsch et al. 2010, Barnes 1998).

Mucus metaplasia and hyperplasia are followed by formation of mucus plugs and impaired MCC mechanisms (Munkholm and Mortensen 2014). MCC is an important primary innate defense mechanism enabling clearance of inhaled particles, including microorganisms, from the respiratory tract (Wanner et al. 1996). Chronic airway infections with *Haemophilus influenzae* and *Staphylococcus aureus* may be promoted in the presence of mucus plugs and

impaired MCC. Chronic mucus hypersecretion has been associated with increased mortality rate as a result of recurrent pulmonary infections in hospitalised COPD patients *(Wanner et al. 1996, Prescott, Lange and Vestbo 1995)*. Impaired MCC in disease and increased mucus secretion results in airway mucus obstruction with substantial effects on lung function and homeostasis as lung function is inversely correlated with MCC in chronic bronchitis patients (Mall et al. 2008, Smaldone et al. 1993, Anderson et al. 2015).

1.1.4.2.2 The extracellular matrix in COPD

The extracellular matrix (ECM) is primarily made of elastic and collagen fibres, proteoglycans, such as decorin, versican, and glycoproteins, such as fibronectin and tenascin. A single change in the type or amount of ECM can be detrimental for the stability and function of the respiratory system (Parameswaran et al. 2006). Maintenance of structural integrity, cellular migration and adhesion, release of growth factors and cytokines and fluid balance are features totally dependent on the extracellular matrix and the proteins composing it (Bonnans, Chou and Werb 2014).

Elastic fibres are insoluble ECM macromolecules consist of mainly elastin. They are localised throughout the respiratory tree and regulate alveolar expansion and recoil during breathing. Cleavage of these molecules can occur in the presence of specific enzymes, such as matrix protein metalloproteinases and serine proteases (Kielty, Sherratt and Shuttleworth 2002). These enzymes are released during inflammatory and immunity responses in COPD (Barnes et al.

2003, Polverino et al. 2016). A reduction in the volume of elastic fibres occurs in COPD subjects and this is associated with FEV_1% predicted (Black et al. 2008). An effect in the structure of elastic fibres occurs in severe COPD patients. Although, elastin mRNA expression is increased in those patients, elastic fibres appear to be loose and less dense (Deslee et al. 2009).

Collagens are the most abundant proteins of ECM and are extremely important for lung architecture. Collagen I, III and IV are the types of collagen mostly found in the airways. Expression of total collagen is increased in COPD subjects when compared to healthy controls (Eurlings et al. 2014). However, discrepancies between studies do not allow any conclusion to be made on the expression of each collagen type in healthy and disease state (Kranenburg et al. 2006, Annoni et al. 2012). Collagens are mostly localised in sites of epithelial injury in COPD subjects and their deposition is negatively correlated with FEV_1% predicted (Kranenburg et al. 2006). Furthermore, disorganised and immature collagen fibrils are present in the airways of COPD subjects (Tjin et al. 2014). The mechanism causing increased expression of collagens is unknown, however their deposition in ECM contributes to reduction of lung function and development of remodelling seen in COPD. There is evidence that increased expression of TGFβ1, a multifunctional cytokine secreted by epithelial cells in the presence of injury, causes increased production of collagen protein and reduces matrix degradation by impairing the collagenase-collagenase inhibitor balance in COPD subjects (Takizawa et al. 2001).

Finally, expression of proteoglycans and glycoproteins is also altered in COPD patients, and specifically in patients with severe COPD. Reduction in the

expression of biglycan and decorin proteoglycans occurs in the parenchyma in subjects with severe COPD (Zandvoort et al. 2006, van Straaten et al. 1999). Expression of another proteoglycan, versican, is increased in COPD patients. Versican has a role in inhibiting regeneration and synthesis of elastic fibres and its high expression levels may help explain the loss of expression and structure of elastic fibres in COPD (Merrilees et al. 2008). Increased expression of tenascin and fibronectin occurs in obstructed COPD patients when compared to non-obstructed COPD and healthy subjects and their expression is inversely correlated with lung function (Lofdahl et al. 2011, Annoni et al. 2012). Another component that appears to be increased in the airways, and in particular in the airway smooth muscle, is laminin β2 in COPD patients (Kranenburg et al. 2006). All these structural changes contribute to increased wall thickness and stiffness and airway remodelling, features seen in COPD.

1.1.4.2.3 The airway smooth muscle

The airway smooth muscle (ASM) under normal conditions has a critical role in regulating the tone of the airways and distribution of airflow by maintaining a balance between contractile and dilatory processes (James and Carroll 2000). These processes can be affected by a number of local and circulating factors. Circulating inflammatory factors can impair the dilatory mechanisms and enhance bronchoconstriction, which can both result in increased airway tone (Kistemaker and Gosens 2015). External factors can also affect proliferation or size of ASM cells. Furthermore, ASM constitutes a source of mediators and ECM proteins that can contribute to the induction of inflammatory responses and the

alteration of airway structure and function (Burgess et al. 2009, Xia et al. 2013). As a consequence, structural and functional responses of the airways can be both modulated and induced by the ASM. In this regard, ASM can be considered an active participant in processes contributing to disease development, but also a passive recipient of extrinsic factors resulting in ASM cell hyperplasia and/or hypertrophy (Chang et al. 2012, Ma et al. 2011).

In COPD, changes in ASM occur notably in the small airways, rather than in the large airways. This has been illustrated from studies examining ASM structure in proximal airway biopsies obtained by fiberoptic bronchoscopy. In these biopsies, no change in ASM mass and smooth muscle protein isoforms or correlation of ASM amount with airflow limitation was observed (Benayoun et al. 2003, Tiddens et al. 1995). In contrast, increases in ASM mass and an inverse correlation between ASM amount and lung function, and in particular FEV_1 % predicted, has been reported in several studies studying ASM structure and function in small airways (Bosken et al. 1990, Saetta et al. 1998). An increase in the ASM amount by almost 50% occurs in subjects with severe COPD (Gold stages 3 and 4) (Hogg et al. 2004). Another observation is the increased ability of the ASM to generate force in COPD (Opazo Saez, Seow and Pare 2000). It is therefore plausible to suggest that ASM contributes to airway narrowing in COPD. Although, it is not yet evaluated as to what exactly causes the increased ASM mass in COPD, there is information available on ASM function enabling understanding of its method of action.

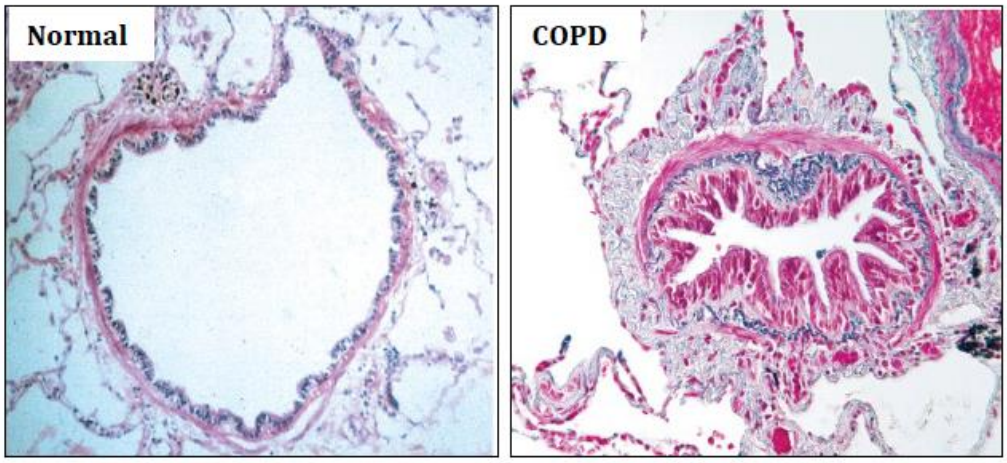

Figure 1.3: Haematoxylin & eosin immunostaining of healthy and COPD small airway. A small airway from a patient with severe COPD and healthy are shown. Infiltration with inflammatory cells, slightly thickened ASM layer, collagen deposition mainly around the airway (peribronchiolar fibrosis) and disrupted alveolar attachments (emphysema) in COPD can be seen, when compared to normal (Hogg 2004).

1.1.4.2.3.1 ASM-derived factors and their role in airway obstruction

ASM produces cytokines and chemokines that can induce and modulate inflammatory responses (Xia et al. 2013). IL-1β, IL-6, IL-8, IL-17, platelet-derived growth factor (PDGF) and TNF-α are cytokines that can be released from ASM cells (Koziol-White and Panettieri 2011). Release of pro-inflammatory cytokines, such as IL-1β and TNF-α, can in turn induce release of IL-8. IL-8 is considered a chemoattractant and activator of neutrophils, which in turn produce further inflammatory components and proteases (John et al. 1998, Lugade et al. 2014). TNF-α is also responsible for the release of CXCL10, a chemoattractant for immune cells, monocytes, neutrophils, mast cells, natural killer cells and T cells. Increased levels of CXCL10 have been reported in the airway smooth muscle of COPD subjects (Hardaker et al. 2004). Other chemokines that can be produced by ASM cells and result in recruitment of monocytes are CCL2, CCL7 and CCL8 (Pype et al. 1999).

TGFβ, a multifunctional cytokine, is upregulated in the airways of COPD subjects and is considered a primary cause of airway remodeling. TGFβ is found in its latent form in ECM and upon cleavage it becomes activated and induces inflammatory and structural responses (Konigshoff, Kneidinger and Eickelberg 2009, Takizawa et al. 2001). TGFβ causes activation and production of β-catenin, a protein localised at adherens junctions and important in cell-cell contacts, by ASM cells (Baarsma et al. 2011). β-catenin production results in stabilisation of cell-cell contacts allowing the transmission of contractile forces between cells (Jansen et al. 2010). β-catenin activation via TGFβ signaling is sufficient to stimulate increased expression of fibronectin by human ASM cells in COPD

subjects (Baarsma et al. 2011). Increased expression of smooth muscle contractile proteins, such as alpha smooth muscle actin (αSMA) and calponin, can also be induced by TGFβ. αSMA is abundant in ASM cells and it is mostly localised in the stress fibers, contractile organelles responsible for actin polymerisation and modulation of tension (Skalli et al. 1986, Katoh et al. 1998). Finally, a further role for TGFβ1 in particular, is the induction of perlecan deposition by ASM cells from subjects with COPD, an ECM glycoprotein localised mainly at the basement membranes. SMAD and JNK (c-Jun amino-terminal kinase) pathways mediate TGFβ1-induced perlecan deposition. However, perlecan deposition does not have any effect on proliferation or the rate of wound healing in human ASM cells (Ichimaru et al. 2012).

Deposition of ECM components in the airways can also be the result of ASM cell secretion. ASM cells are responsible for the production of a wide range of ECM proteins. In particular, collagens, fibronectin and laminin deposition in ECM is partially mediated by ASM cells in COPD (Johnson 2001, Aoshiba and Nagai 2004). ASM can cause ECM deposition not only by direct production of ECM proteins, but also by the production of growth factors, such as vascular-endothelial growth factor and CXCL8, which in turn enhance ECM production (Deacon and Knox 2015). Conversely, ASM also produces MMPs, and in particular MMP9 and MMP12, which can cause degradation of collagen, elastin and other ECM components (Liang et al. 2007). MMPs can also cause degradation of insulin-like growth factor binding proteins resulting in the release of insulin-like growth factor, which is known for its role in inducing airway smooth muscle proliferation and consequently hyperplasia (Fowlkes et al. 1994, Noveral et al.

1994). There is evidence of increased levels of active MPP12 in ASM cells of small airways of COPD subjects, however whether it acts in this manner still remains unknown (Xie et al. 2005). ECM matrix is extremely important for maintaining ASM structure and growth and promoting cytokine synthesis, differentiation, migration and contraction of human ASM cells. Increased ECM deposition, a feature of COPD pathophysiology, can have serious implications in these processes (Parameswaran et al. 2006).

1.1.4.2.3.2 ASM, a passive recipient of extrinsic signals

Inflammation in COPD results in the release of cytokines and growth factors, factors that can affect normal ASM function and structure. TNF-α, TGFβ, bFGF and PDGF are components usually released during inflammatory responses in COPD. Stimulation of human ASM cells with these factors results in increased proliferation. The effect of these components on proliferation of human ASM cells is mediated via PI3 kinase, p38 and MAPK (mitogen-activated protein kinase) signaling pathways (Stamatiou et al. 2012). This suggests that these factors are able to cause ASM hyperplasia in COPD. Enhanced ASM cell proliferation can also be caused by IL-4, IL-5, IL-13 and thymic stromal lymphopoietin (TSLP) in asthmatic patients, but their role in COPD pathogenesis has not been established (Perkins et al. 2011, Redhu et al. 2011, Khan 2013). Increased $CD8^+$ T cells, cells induced during inflammatory responses in COPD, and increased ASM area have been reported in the peripheral airways of smokers with COPD and these were correlated with reduction in expiratory airflow, suggesting a role of these cells in the development of chronic airflow

limitation in smokers with COPD. However, whether this causes the increase in ASM mass still needs further investigation (Saetta et al. 1998).

The increased ASM mass seen in COPD may also be the result of ASM hypertrophy. Mechanical stretch can increase the size of ASM cells, which can then in turn induce a number of signaling pathways, including Wnt and GSK3β, and transcription factors, including Klf5, TGFβ and Akt1 (Kwak et al. 2015, Li et al. 2016, Tang et al. 2015, Goldsmith et al. 2006). Mechanical stretch can further induce release of endothelial growth factor (EGF) from epithelial cells resulting in further airway remodeling (Shiomi et al. 2011). However, there is no evidence yet that these factors can execute these functions in the airways of COPD subjects.

Airway smooth muscle contraction can be induced by acetylcholine, the primary parasympathetic neurotransmitter in the airways. Airway inflammation causes increased parasympathetic activity and hence increased contractility of the airways. This is the principle behind the use of anticholinergic drugs in asthma and COPD (Gross and Skorodin 1984). Acetylcholine constitutes the natural ligand of muscarinic receptors. There are five subtypes of muscarinic receptors, M_1 to M_5 (Caulfield and Birdsall 1998). Expression of these receptors occurs by tissue-forming cells in the airways, including human airway smooth muscle and epithelial cells and fibroblasts. Distribution of muscarinic receptors in the human airway is restricted to M_1, M_2 and M_3 receptors (Mak, Baraniuk and Barnes 1992, Gosens et al. 2006). M_3 receptor is the receptor mainly involved in mediation of bronchial and tracheal smooth muscle contraction. Bronchoconstriction and mucus secretion in human lung and human central and peripheral airway

smooth muscle can be caused following stimulation with M_3 receptor (Roffel, Elzinga and Zaagsma 1990). Exposure to tobacco smoking and inflammation results in afferent airway neural responses (Fediuk et al. 2014, Allen et al. 2006). Elevated expression levels of M_3 receptor have been reported in COPD patients with bronchial hyperresponsiveness, when compared to patients without bronchial hyperresponsiveness (Selivanova et al. 2012). Muscarinic receptor inhibitors are important bronchodilatory components (Aalbers et al. 2002). Various muscarinic receptor inhibitors, such as tiotropium, also result in downregulation of pathways involved in inflammatory responses including LTB_4 and NF-κB (Profita et al. 2011). Furthermore, the muscarinic receptor inhibitor tiotropium inhibits the accelerated lung function decline seen in COPD patients (Anzueto et al. 2005).

Recurrent inflammation results in the release of reactive oxygen species (ROS), which can be induced by NOX4, a nicotinamide adenine dinucleotide phosphate oxidase. Elevated expression of NOX4 has been reported in the ASM in the small airways of COPD subjects. The level of NOX4 is inversely correlated with lung function and positively correlated with the ECM matrix component laminin and TGFβ, suggesting a role in ECM deposition (Liu et al. 2016). A role for NOX4 in ASM contraction in small airways in COPD has also been reported (Wiegman et al. 2015). Thromboxane is a well-known bronchoconstrictor and increased platelet biosynthesis of this has been found in the airways of COPD subjects (Davi et al. 1997). Furthermore, thromboxane can also induce Ca^{2+} release and actin polymerisation, factors that contribute to bronchoconstriction and airway stiffness, via acetylcholine receptor neural stimulation. It has been previously

demonstrated that calcium homeostasis is essential for maintenance of airway tone (Fediuk et al. 2014, Allen et al. 2006).

During some inflammatory responses Th17 cells release a number of cytokines, and some of these appear to have an effect in inducing ASM cell apoptosis. Among these cytokines, the most well-known are IL-8 and CCL11 (Halwani et al. 2011). Other factors that also stimulate apoptosis of ASM cells are extracellular laminin and TRPV1 agonists (Zhao et al. 2013, Tran et al. 2013). Conversely, proteases released by neutrophils, such as NE and cathepsin G, can cause collagen degradation that results in disruption of integrin binding. Disruption of integrin binding eventually results in the release of apoptotic signals for ASM cells (Oltmanns et al. 2005).

To sum up, there are a plethora of mechanisms that act on and are modulated by ASM cells contributing to COPD pathogenesis, and in particular bronchoconstriction and airflow limitation. ECM deposition, induction of inflammatory responses and the response of ASM to factors stimulating its contraction and hyperplasia are likely very important for small airway dysfunction in COPD. However, a lot still need to be elucidated to unmask the mechanism that ASM acts through in COPD.

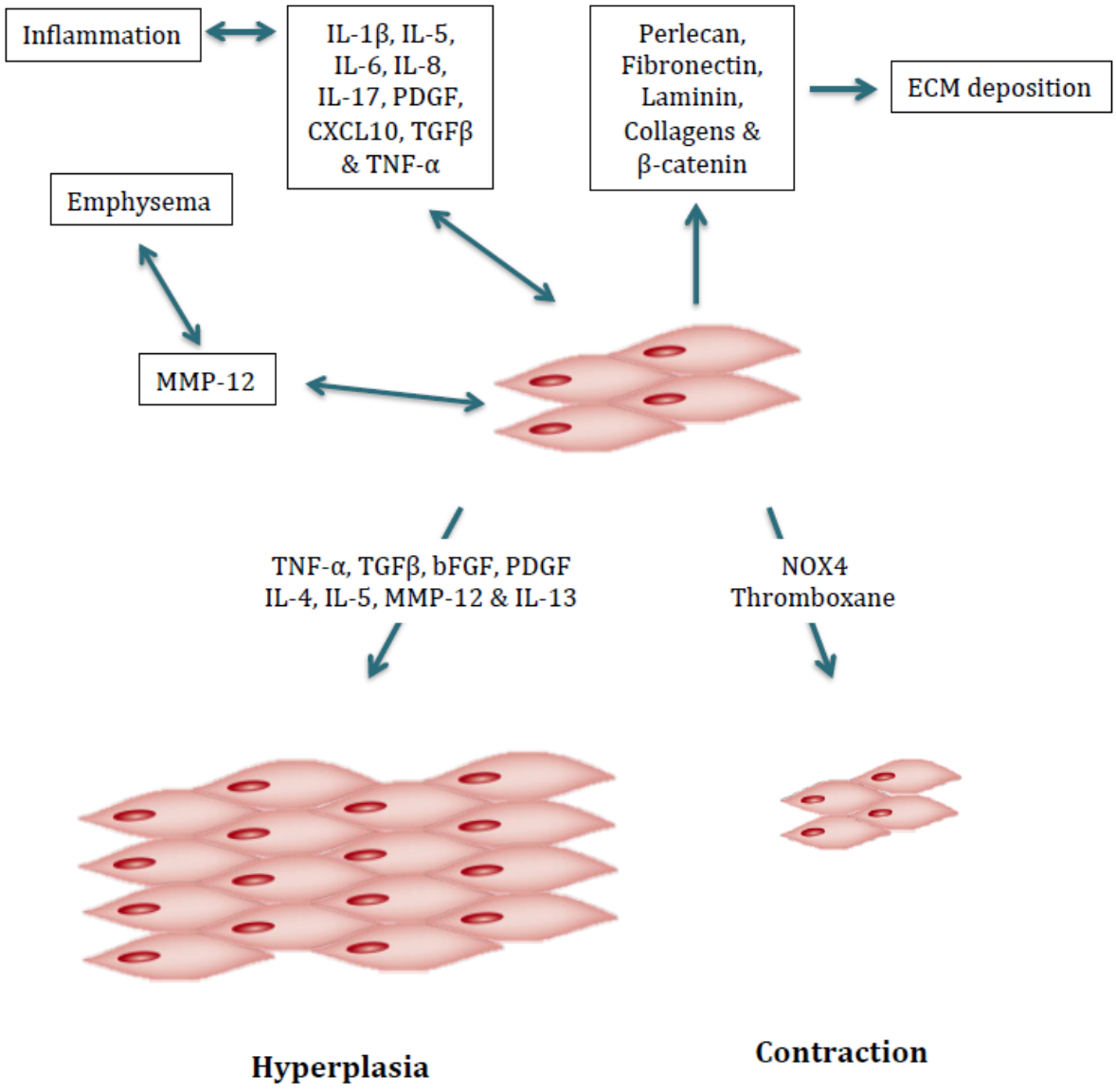

Figure 1.4: The airway smooth muscle in airway obstruction in COPD. ASM role in ECM deposition, inflammation and bronchoconstriction in COPD and the involvement of cytokines, growth factors and ECM proteins.

1.1.5 Comorbidities

Cardiovascular disorders, skeletal muscle dysfunction, lung cancer and depressive symptoms are important comorbidities associated with COPD. Oxidative stress and systemic inflammation result in increased risk of heart disease in COPD patients. Furthermore, advancing age, tobacco smoking and other irritants, risk factors for the development of COPD, are also associated with the development of heart disease, including arrhythmias and ischaemic heart disease (Tkac, Man and Sin 2007). It is then not surprising that COPD patients are 1.76 times more prone to arrhythmias and 3.84 times more prone to develop congestive heart failure (Curkendall et al. 2006).

Skeletal muscle dysfunction is another comorbidity associated with COPD. Skeletal muscle dysfunction development likely follows from the use of corticosteroids, immobility due to breathlessness, poor nutrition and hormonal changes. Dyspnoea and fatigue, two common symptoms that COPD patients develop, arise from reduced exercise endurance due to skeletal muscle loss (Casaburi 2000). Another important comorbidity is lung cancer, and its incidence is inversely correlated with disease severity and the degree of airway obstruction. The most common type of lung cancer found in COPD patients is squamous cell carcinoma (de Torres et al. 2011). Finally, depressive symptoms are common in COPD patients with some patients developing cognitive decline. Females and current smokers are more likely to develop depression and depressive symptoms are more common in patients with severe disease (Hanania et al. 2011).

1.1.6 Exacerbations

Exacerbations are very important in COPD, increasing both morbidity and mortality. An exacerbation is an acute event characterised by increased severity, signs and symptoms of the disease. This exceeds day-day variations and the individual needs a different type of medication (Celli and Vestbo 2011). Aetiologies of exacerbations are bacterial, viral, eosinophilic and pauci-inflammatory (Bafadhel et al. 2011). The most common causes are bacterial and viral respiratory tract infections, which account for 85% of cases. *Haemophilus influenzae* and *Streptococcus pneumoniae* are two common bacterial pathogens associated with COPD exacerbations (Bafadhel et al. 2011). Diagnosis of an exacerbation episode is based on the change of symptoms and assessment of its severity can be achieved by pulse oxymetry, arterial blood gases and chest X-rays. COPD patients experiencing exacerbations have greater changes in the computed tomography (CT) scan measurements from COPD patients not experiencing exacerbations indicating a role for exacerbations in accelerating emphysema progression (Tanabe et al. 2011). Reduction in the frequency of exacerbations can be achieved by long-term use of antibiotics in COPD patients, although long-term use of antibiotics can be associated with some adverse effects and emergence of antibiotics resistance (Santos et al. 2016).

1.1.7 Current management of COPD

Current treatments for COPD are focused on improving the quality of life by symptom management, and reductions in the frequency of exacerbations and rate of decline of FEV_1. Smoking cessation constitutes the most effective strategy

for the prevention of further lung function decline. However, there is evidence that even after smoking cessation, the inflammatory response fails to fully resolve (Bozinovski et al. 2016, Au et al. 2009).

Inhaled bronchodilators and corticosteroids are the two most efficient pharmacological strategies for symptom management and prevention of exacerbations. Inhaled bronchodilators constitute either β_2-adrenergic receptor agonists or cholinergic receptor antagonists and can be either short-acting or long-acting. These pharmacological agents are mainly successful in resolving bronchoconstriction, but also reduce the rate of severe exacerbations through mechanisms that are not really understood. Bronchodilation with these drugs is limited to about a 10% increase in FEV_1 in COPD. Better quality of life and improved symptoms, in particular dyspnoea have been reported following their use in COPD (Aalbers et al. 2002). Sinus tachycardia, somatic tremor and prostatic symptoms are some of the adverse effects that inhaled bronchodilators can have (Vijayan 2013). Many COPD treatments involve the combination of long-acting β_2-adrenergic receptor agonists and long-acting cholinergic receptor antagonists as primary medications. The beneficial effects that combinational therapy has are reduction of the annual rate of exacerbations, and improved health status and spirometric values. However, this combined regime does not have a significant effect in the COPD mortality rate (Calverley et al. 2007).

Inhaled corticosteroids constitute another pharmacological treatment option for COPD patients. Although, steroids improved the degree of inflammation in chronic asthma, there is not such evidence in COPD. However, improved symptoms, better quality of life and reduced frequency of exacerbations have

been reported with the use of inhaled corticosteroids in COPD patients (Calverley et al. 2003). Adverse effects associated with the use of inhaled corticosteroids are oral candidiasis and skin bruising, and an approximately 60% increased risk of pneumonia (Singh, Amin and Loke 2009). Adverse effects and inefficiency of the current methods to prevent further FEV_1 decline marks the urgency for novel therapeutic approaches.

1.1.8 GWAS and COPD

Genome-wide association studies have been used recently to identify genes that might be involved in COPD susceptibility and progression. These studies aim to determine whether small variations called single nucleotide polymorphisms (SNP) that occur in the human genome are associated with disease. A genome wide association study showed a significant association of the gene tensin1 (TNS1) with airflow obstruction (Repapi et al. 2010), and a subsequent GWAS demonstrated a significant association with COPD (Soler Artigas et al. 2011). In both studies, the link with TNS1 involved a non-synonymous (leading to an amino acid change) SNP rs2571445 located at the 2q35 locus in the *TNS1* gene with a minor allele frequency of 0.40 (standardised to 1) in European populations. This base pair change replaces arginine with tryptophan at amino acid 1197 (R1197W, -1197C>T) in the tensin1 protein. This SNP is adversely correlated with FEV_1 as a 1% increase in tensin1 expression can result in a 0.035% decrease in FEV_1 value (Repapi et al. 2010).

1.2 Tensin1

Tensin1 is a 220kDa cytoplasmic phosphoprotein, which localizes to integrin-mediated focal and fibrillar adhesions, specialised regions where cells attach to the ECM (McCleverty, Lin and Liddington 2007). Tensin1 belongs to the tensin family proteins, which includes tensin1, tensin2, tensin3 and c-ten. Tensin proteins constitute multi-domain scaffold proteins providing a link between the ECM, actin cytoskeleton and signal transduction (Nishino et al. 2012). They are highly conserved proteins at their N- and C-terminal regions. However, the centre regions of all four family members have no sequence homology (Lo 2004). The structure of the tensin1 molecule can be divided into three regions that promote protein-protein interactions. The N-terminus contains an actin-binding domain (ABD) I a and b that enables tensin1 interaction with actin filaments. This region also contains a focal adhesion-binding (FAB) domain, important for the biological activity of tensin1 and for the phosphatase and tensin (PTEN) homologous sequence. PTEN is a lipid phosphatase and a regulator of the phosphoinositide 3 (PI3) kinase, a kinase involved in cell survival, growth and proliferation (Haynie 2014). As a consequence, PTEN is considered as a tumor suppressor gene and it has been reported that loss of PTEN function results in tumorigenesis and genomic instability (Dillon and Miller 2014). An ABD II domain is localised in the central region of tensin1 that retards polymerisation of the actin filaments. The C-terminus contains a Src homology 2 (SH2) domain, phosphotyrosine-binding (PTB) domain and another FAB site. The SH2 domain allows tensin1 to interact with tyrosine-phosphorylated proteins including PI3 kinase, p130Cas and focal adhesion kinase (FAK). At first, it was believed that the PTB domain found in the

tensin1 molecule was responsible for tensin1 interaction with phosphotyrosine proteins. However, it was then reported that the PTB domain of tensin1 only binds to the NPxY motifs of the cytoplasmic integrin tails of β1, 3, 5 and 7 (Auger et al. 1996).

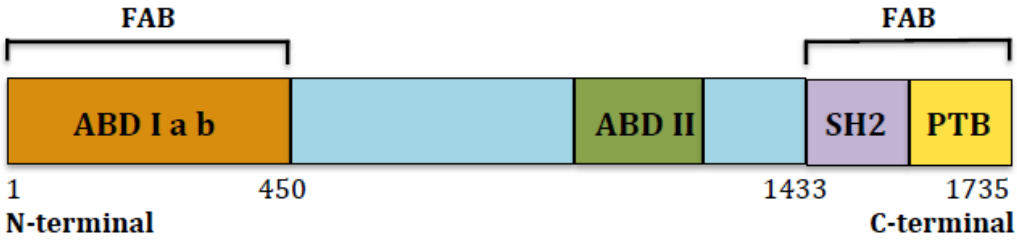

Figure 1.5: Structural and functional domains of tensin1. A schematic diagram illustrating the ABD, SH2, PTB and FAB domains of tensin1 and their location in human tensin1. ABD: Actin binding domain; SH2: Src homology 2; PTB: phosphotyrosine (Lo 2004).

1.2.1 Tensin1 recruitment to focal and fibrillar adhesions

Tensin1 is an adhesion protein localised to both focal and fibrillar adhesions. Adhesions, in general, constitute regions where cells attach to the extracellular matrix via a core of αβ integrin heterodimers. The extracellular portions of an integrin, are directly bound to the ECM, whereas the intracellular portion, the cytoplasmic tails, are indirectly bound to the actin cytoskeleton, and in particular F-actin, via a number of different proteins, such as talin, vinculin, paxillin, tensins, Src kinase and FAK (Jockusch et al. 1995) (**Figure 1.5**). These complexes enable the involvement of different signaling enzymes that have a role in cell behaviour, such as cell attachment, growth, death and differentiation (Giancotti and Ruoslahti 1999). There are three different stages of cell-ECM adhesions, focal contacts, focal adhesions and fibrillar adhesions. These matrix adhesions differ in shape, molecular composition and function. Their recruitment depends on the properties of the ECM, integrin activation, contraction state of the cytoskeleton and expression of several proteins (Romer, Birukov and Garcia 2006).

1.2.1.1 Focal contacts

Focal contacts are short-lived structures of approximately 1 μm diameter localised at the cell periphery (McCleverty et al. 2007). They are nascent adhesive structures and Rho family members Rac and cdc42 are responsible for their recruitment. They are mainly involved in regulating tight cell-substrate adhesions (Ren et al. 2000, Pylayeva and Giancotti 2007). Focal contacts contain

high levels of talin, vinculin, paxillin and $\alpha_V\beta_3$ integrin. Tensins, in general, are absent from the focal contacts (Zamir et al. 2000). During the maturation of focal contacts, Src causes phosphorylation of the integrin tails resulting in reduced affinity for talin. Src can be activated by autophosphorylation on specific tyrosine residues and their activation is of extreme importance for the generation of adhesion signals (McCleverty et al. 2007).

1.2.1.2 Focal adhesions

Oval shaped focal adhesions evolved from focal contacts. Formation of focal adhesions and production of FAK results from Rho activation and Rho-mediated tension (Ren et al. 2000). As discussed above, phosphorylation of integrin tails occurs in mature focal contacts, resulting in integrin availability due to talin release (McCleverty et al. 2007). As a consequence, focal adhesion proteins can bind to the integrins. Focal adhesions comprise vinculin, paxillin, tensins, α-actinin, $\alpha_V\beta_3$ and $\alpha_5\beta_1$ integrins and they are localised again in the cell periphery, but moving towards the centre of the cell (Chen et al. 2000, Pylayeva and Giancotti 2007) (**Figure 1.5**). High-tension development due to the Rho-mediated actomyosin pulling does not allow these adhesions to migrate far from the cell periphery (Zamir et al. 2000). Tensins has identical affinity for both $\alpha_V\beta_3$ and $\alpha_5\beta_1$ integrins (Pankov et al. 2000, Chen et al. 2000). They can probe the stiffness of the environment and promote migration. FAK regulates focal adhesions turnover by down-regulating expression of Rho (Ren et al. 2000).

1.2.1.3 Fibrillar adhesions

FAK and Rho-mediated actomyosin tension cause transformation of focal into fibrillar adhesions (Ren et al. 2000). Fibrillar adhesions are elongated structures, mainly composed of actin cables. They arise from the median ends of focal adhesions and localise centrally in the cell (Zamir et al. 2000). They are enriched in tensin proteins and $\alpha_5\beta_1$ integrin as a result of $\alpha_5\beta_1$-actin, and in particular F-actin, linkage reinforcement by integrin linked kinase and the adaptor proteins, PINCH1 and parvin, (IPP) complex. The IPP complex constitutes also a platform for tensins recruitment (Stanchi et al. 2009). Tyrosine kinases, and in particular Src, is another component promoting recruitment of tensin proteins to these kind of adhesions (Volberg et al. 2001). $\alpha_5\beta_1$ integrin is bound to the moveable extracellular matrix component fibronectin and recruitment of only tensins occurs due to low tension. Vinculin, paxillin and other proteins typical to focal contacts are not present in fibrillar adhesions as their recruitment requires high-tension development (Zamir et al. 2000, Katz et al. 2000a).

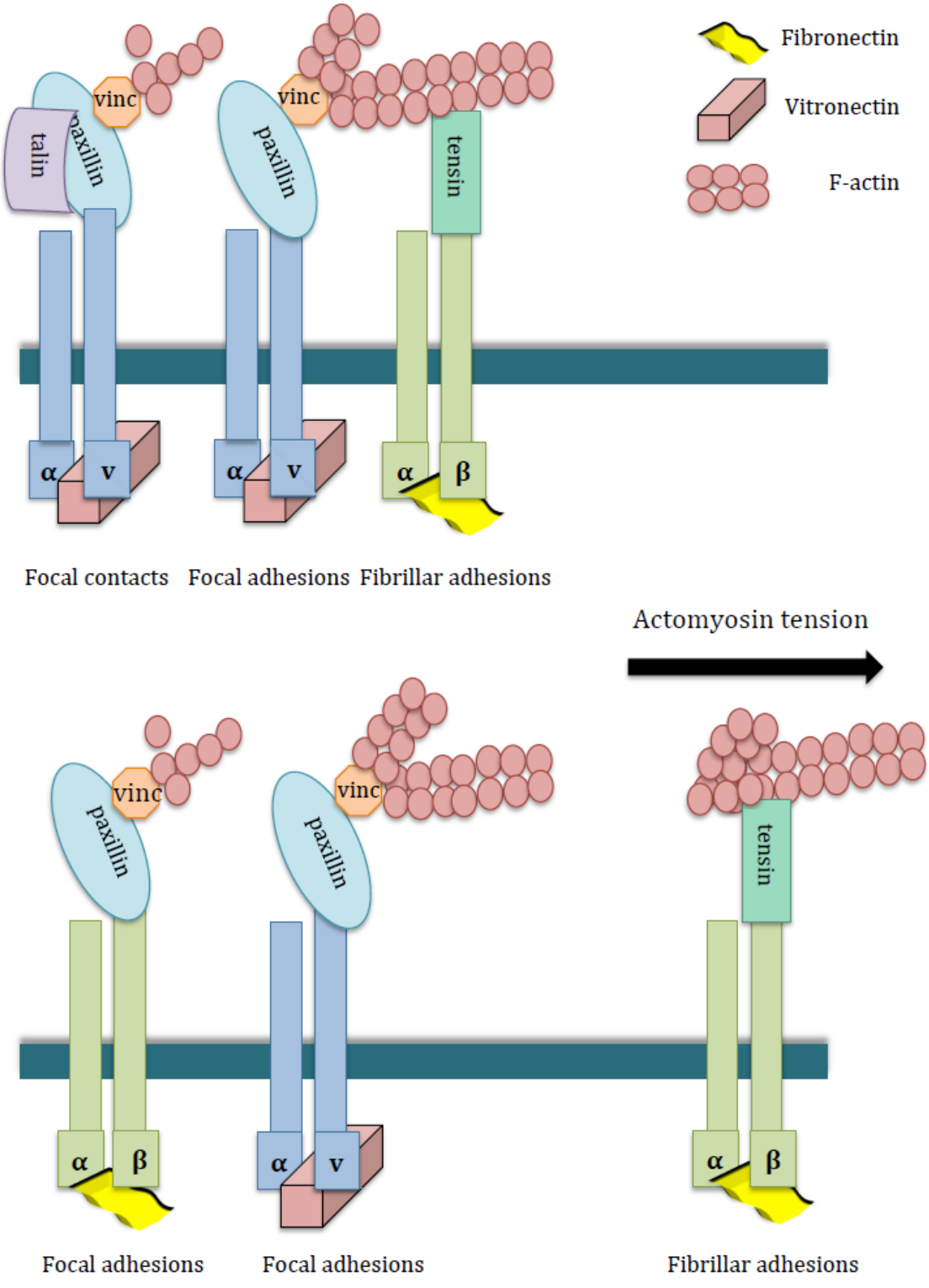

Figure 1.6: Focal contacts, focal adhesions and fibrillar adhesions. A figure illustrating the components make up the different type of cell-ECM adhesions, focal contacts, focal adhesions and fibrillar adhesions and tensin1 localisation (Zamir et al. 2000).

1.2.2 Tensin1 phosphorylation

Tensin1 phosphorylation is cardinal for the function of tensin1. Tensin1 phosphorylation enables its involvement in a number of signaling pathways via signal transduction. It can be phosphorylated on tyrosine and serine/threonine residues. 10 tyrosine and 62 serine/threonine phosphorylation sites have been previously reported. Phosphorylation of these residues can be achieved with the function of several growth factors and ECM substrates (Hall et al. 2010).

Tyrosine phosphorylation of tensin proteins, in general, is particularly important for embryonic development and cell transformation. Endothelial growth factor (EGF), PDGF, thrombin, angiotensin and oncogenes, such as Src and BCR/ABL can induce tensins tyrosine phosphorylation (Bockholt and Burridge 1993, Jiang et al. 1996, Szabo et al. 2002). It can only be induced when cells are attached to ECM substrates. Fibronectin, vitronectin and laminin constitute some of the ECM substrates that can cause tyrosine phosphorylation of tensins. This also indicates that this phosphorylation is dependent on integrin-mediated signaling (Jiang et al. 1996). Cell spreading is also required for the occurrence of tyrosine phosphorylation in tensins, as inhibition of tyrosine phosphorylation has been observed when cell spreading on ECM substrates was restricted (Pelletier, Bodary and Levinson 1992). Cytoskeletal turnover occurs during cell spreading and activity of Src is essential for this process. Tyrosine phosphorylation of tensin1, as expected, and cell spreading on collagen matrices was significantly decreased in kinase-inactive Src into vascular smooth muscle cells (Ishida et al. 1999).

Although, serine/threonine phosphorylation of tensin1 occurs, evidence confirming this has been limited. Evidence supports that serine/threonine phosphorylation enables tensin1 to act as a scaffold protein and recruit enzymes to focal adhesions. Serine/threonine phosphorylation is mediated by p38 MAPK (mitogen-activated protein kinase), which in turn regulates binding of tyrosine-phosphorylated proteins, such as p130Cas, FAK and DLC-1 (deleted in liver cancer-1), to SH2 domain. Staurosporine is a negative regulator of tensin1 phosphorylation as it can inhibit serine/threonine phosphorylation (Hall et al. 2010).

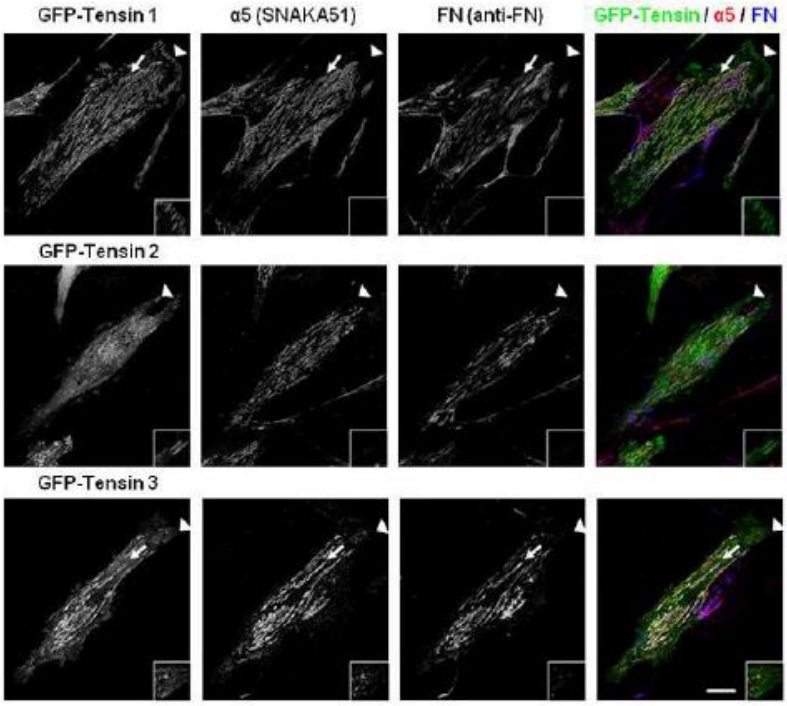

Figure 1.7: Localisation of tensin1 in focal and fibrillar adhesions. Human foreskin fibroblasts were transfected with GFP-tensin cDNAs. Cells were stained with anti-α5 integrin (SNAKA51), which detects the ligated α5β1 receptor, and anti-fibronectin (anti-FN) to identify fibrillar adhesions (arrows). Arrowheads indicate focal adhesions (Clark, Howe et al. 2010).

1.2.3 Tensin1 function

Tensin1 is broadly expressed in human tissues, such as heart, skeletal muscle, lung, kidney, liver and colon. Human tensin1 expression in brain, thymus and circulating leukocytes was low, or even not detectable (Chen et al. 2000). Tensin1 location and tyrosine and serine/threonine phosphorylation enable its involvement in a number of signaling pathways and processes including migration, cytoskeletal organisation, apoptosis and remodelling.

1.2.3.1 Tensin1 role in signal transduction and cytoskeletal organisation

Tensin1 induces the activation of two pathways, the c-Jun amino-terminal kinase (JNK) and p38 pathways independently of Rac and cdc42 GTP binding proteins (Katz et al. 2000b). These pathways do not only require cell-ECM attachment to be activated, but also association of the cells with fibronectin fibrils. This suggests that tensin1 localised in fibrillar adhesions induces their activation (Bourdoulous et al. 1998). JNK and p38 pathways are involved in a number of different cellular processes, including proliferation, cytokine production, apoptosis and cytoskeletal reorganisation. This indicates a role of tensin1 in signal transduction.

Tensin1 constitutes a substrate for calpain II, a calcium-dependent cysteine protease, which cleaves tensin1 upon its activation. Inhibition of tensin1 cleavage by calpain results in morphological changes and abnormal reorganization of the cytoskeleton and focal adhesion complexes (Chen et al. 2000). Tensin1 also indirectly associates with PP1α (protein phosphatase 1α), a

phosphatase regulating the serine/threonine phosphorylation of tensin1, and deleted in liver cancer-1 (DLC-1) RhoGAP protein, a tumour suppressor gene (Hall et al. 2010). Inhibition of the association of tensin1 with PP1α and DLC-1 results in significantly longer adhesions, and alterations in cell morphology with a rounder cell shape, and an absence of a leading edge or extended tail in fibroblasts. Changes in cellular adhesions indicate the disruption of cell-ECM interactions and suggests an effect of tensin1 in cytoskeletal organisation and contractility (Hall et al. 2009). Tensin1 and tensin2-silenced fibroblasts exhibited a strongly reduced ability to contract that was dependent on Rho activity (Clark et al. 2010, Saintigny et al. 2008).

1.2.3.2 Tensin1 and cell migration

The role of tensin1 in promoting cell migration has been widely studied. Ectopic expression of tensin1 promotes cell migration as cells expressing GFP-tensin1 migrated significantly faster than GFP-control in stably transfected 293 cell line (Chen et al. 2002). Mutations in the tensin1 gene resulted in impaired association with phosphotyrosine proteins and disrupted tensin1 localisation in focal adhesions, which in turn caused suppressed cell migratory properties (Chen and Lo 2003). Therefore, localisation of tensin1 in focal and fibrillar adhesions and interactions with phosphotyrosine proteins enable its involvement in cell migration. DLC-1 interactions with tensin1 seem critical for the regulation of migration as well. Inhibiting this association induces persistent directionality and significantly slower cell migration (Hall et al. 2009). Finally, altered migratory properties of the cells evolve from a weakened

association of β_1 integrin with the actin cytoskeleton in focal adhesions induced by EGF (Irie et al. 2005). However, tensin1 expression is barely detectable following stimulation with EGF, suggesting disruption of the adhesions, although this was not further examined (Katz et al. 2007).

1.2.3.3 Tensin1 and apoptosis

Apoptosis is characterised by morphological changes, including cell shrinkage, detachment from the ECM and nuclear condensation. Caspases are protease enzymes that can promote apoptosis by inactivating regulators of apoptosis (Thornberry and Lazebnik 1998). A role for tensin1 in the disruption of the actin cytoskeleton during apoptosis has been previously reported (Kook et al. 2003). In this study, it was revealed that tensin1 cleavage occurs in etoposide-induced apoptosis in chicken embryonic fibroblasts and it is primarily coordinated by caspase-3. Kook, et al. showed that tensin1 and PI3 kinase interaction is significantly reduced during apoptosis resulting in disrupted survival signals derived from PI3 kinase, as PI3 kinase-dependent survival signals are normally sent due to its interaction with the ECM (Kook et al. 2003). Tensin1 also constitutes a substrate for calpain II. Inhibiting the action of calpain II in bovine aortic endothelial cells evolved un-cleaved tensin1, inactivation of calpain II and changes in the cellular morphology. Cleavage of tensins and other focal adhesion molecules by calpain II is of extreme importance for the maintenance of cell morphology. As a consequence, cells were rounded up and started detaching from the dish indicating a role of tensin1 in cell survival (Chen et al. 2000).

1.2.3.4 Effects of tensin knockdown in mice

Two knockout mouse studies have been reported illustrating the effects of tensin inactivation on mice. Although tensin is expressed in several tissues during embryogenesis, tensin knockout mice developed normally and were healthy for several months. However, inactivation of the TNS gene over time resulted in multiple cyst formation and renal failure. Cell-matrix junctions appeared normally in non-cystic areas, but this was not the case in cystic areas. Disrupted cell-matrix junctions and loss of cell polarisation were observed in the areas with multiple cysts development (Lo et al. 1997). The role of tensin in skeletal muscle regeneration was also examined. Regeneration in the anterior tibial muscles process was examined using cardiotoxin in tensin knockout and wild-type mice. The knockout mice exhibited a significantly longer regeneration process, with delayed expression of myosin and paxillin, fewer myogenic cells and reduced fusion capacity (Ishii and Lo 2001).

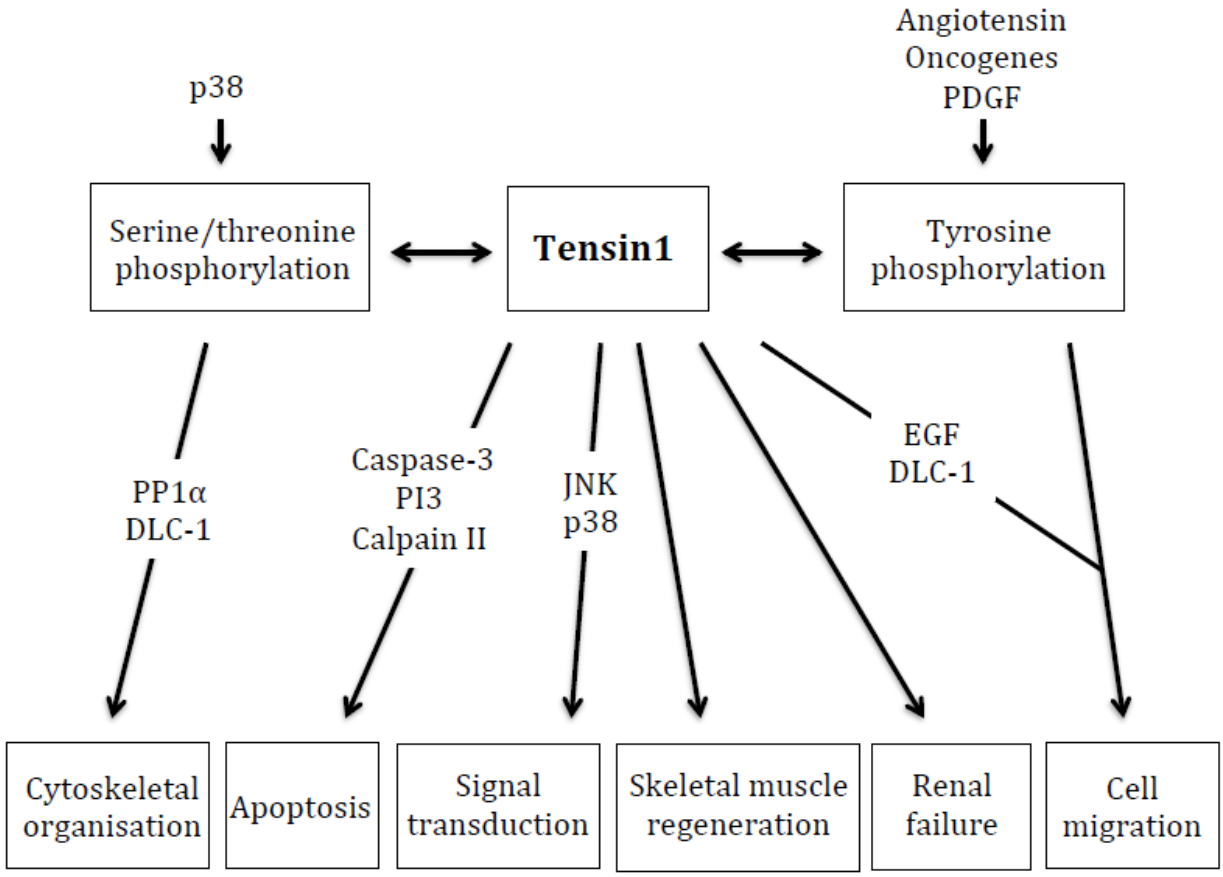

Figure 1.8: A diagram summarising tensin1 function. Tensin1 can regulate a number of processes, including cytoskeletal organisation, apoptosis, signal transduction, skeletal muscle regeneration, renal failure and cell migration via the action of several proteins and growth factors.

1.2.4 Tensin1 in cancer

Cell-matrix adhesions, actin dynamics and cell-cell communications are of extreme importance for cancer development (Mouneimne and Brugge 2007). Tensins expression is largely absent or not detectable in human cancer cell lines, in particular brain, bone, lymph node, colorectal adenocarcinoma, renal carcinoma and breast cancer cell line (Hall et al. 2009, Martuszewska et al. 2009, Webber, Bello and Quader 1997). Association of tensin1 with a RhoGAP protein, DLC-1 indicates a role in tumor formation. DLC-1 is a tumor suppressor gene and several studies showed downregulation of its expression in several cancers. Its tumor suppressive function is totally dependent on its focal adhesion localisation as it is recruited by the SH2 domain of tensin1 (Liao and Lo 2008). Studies have also reported a role of tensin1 in mediating tumor invasion (Hall et al. 2009). A mutation in the TNS1 gene causing inhibition of the PP1α association with tensin1 resulted in significantly more invasive breast cancer cells (Hall et al. 2009). Finally, an inverse correlation between tensin1 and tumor grade has been reported as high tensin1 expression correlated with low tumor grade in renal cell carcinoma (Martuszewska et al. 2009).

1.3 Summary

In summary, COPD is characterised by irreversible airway narrowing which limits airflow to and from the lungs resulting in shortness of breath (Zhang et al. 2012). Genome wide association studies showed significant associations between the gene, tensin1 (TNS1) and COPD (Soler Artigas et al. 2011). Tensin1 is a 220kDa cytoplasmic phosphoprotein, which localizes to integrin-mediated fibrillar adhesions (McCleverty et al. 2007). Tensin1 appears to have several functions. Inhibition of tensin1 cleavage by calpain resulted in morphological changes and abnormal reorganization of the cytoskeleton (Chen et al. 2000, Kook et al. 2003). Another important function of tensin1 is association with deleted in liver cancer-1 (DLC-1), a RhoGAP protein (Qian et al. 2007). This interaction enables tensin1-dependent control of cell migration and invasion in metastatic breast cancer cells (Hall et al. 2009). Finally, tensins, and tensin1 in particular, have a very important role in cell-matrix interactions as tensin-silenced fibroblasts exhibited a strongly reduced capacity to contract (Saintigny et al. 2008, Clark et al. 2010). These points are indicatives that tensin1, for which GWAS implicated relevance in COPD, is a molecule of interest to characterise further in COPD.

1.4 Hypothesis

Tensin1 is involved in the pathogenesis of COPD, and in particular airway dysfunction, which is an important component of the COPD pathophysiology.

1.5 Aims and Objectives

The overall aim of the project is to examine the potential role of tensin1 in the airway pathophysiology of COPD. The specific aims and objectives of my study are to examine:

1. The expression of tensin1 protein in human airway tissue, and mRNA and protein expression in human airway smooth muscle cells (HASMCs), human bronchial epithelial cells (HBECs) and human lung myofibroblasts (HLMF) from health versus COPD.
2. The effects of tensin1 knockdown on cell function.
3. The effects on cell function of overexpression of tensin1 containing the R1197W SNP, identified in GWAS studies.
4. The functional responses of cells obtained from patients with wild-type versus the R1197W SNP.

Chapter 2: Methods and Materials

2.1 Subjects and Ethics

To study tissue by immunohistochemistry, airway tissue was collected at the time of lung resection from lung cancer patients who also met the GOLD criteria for COPD (GOLD Strategy G, 2016). Control tissue was also collected from patients with lung cancer without evidence of COPD undergoing lung resection. Lung resections constitute representative samples of small airway tissue. Healthy volunteers and asthmatic patients were also recruited and underwent fiberoptic bronchoscopy conducted according to the British Thoracic Society guidelines (BTS, 2001). Control subjects included those with and without a smoking history without airflow obstruction. Bronchial mucosal biopsies were taken from the right middle lobe and lower lobe carinae located in the large airways. These specimens were used for immunohistochemistry studies and gave rise to the data described and analysed in Section 3.1 Clinical characteristics of subjects are stated on **Table 3.1**. Both lung resections and endobronchial biopsies were not genotyped and thus tensin1 genotype is not known in these data.

For the study of primary human airway cells (HASMCs and HBECs) in culture, healthy control subjects and patients with COPD or asthma were recruited from respiratory clinics. COPD subjects were all ex or current smokers with spirometric evidence of airflow obstruction according to the Global Obstructive Lung Disease (GOLD) criteria for COPD (GOLD Strategy G, 2016). Again, asthma severity was defined by the 'British guideline on the management of asthma' (BTS, 2001). Subjects with a history of asthma had a <10 pack year smoking history. Control subjects included those with and without a smoking history without airflow obstruction. Primary airway cells were grown from tissue

collected from subjects, healthy controls and patients, undergoing fiberoptic bronchoscopy (samples of large airways). These specimens were used for all the experiments in the thesis, except for experiments that gave rise to data reported in Section 3.1. Clinical characteristics of subjects are stated on **Table 3.2**. Tensin1 genotype is only known for the data shown in Section 3.5 and nomenclature is shown in **Figure 3.40**.

All subjects and patients gave written informed consent, and the collection of tissue was approved by the National Research Ethics Service (reference numbers: 07/MRE08/42, 04/Q2502/74, 08/H0406/189).

2.2 Immunohistochemistry on Airway Tissue

Immunohistochemistry involves the immunostaining and detection of proteins in tissue and was performed to examine the expression and localisation of tensin1 in human lung tissue. Tissue was processed into glycol methacrylate resin and then immunostained as described previously (Bradding et al. 1992), or stained with the Dako EnVision FLEX+ staining technique.

2.2.1 Glycolmethacrylate (GMA) resin embedding

Firstly, tissue was fixed in ice-cold acetone containing 20mM iodoacetamide and 2mM phenylmethylsulfonyl fluoride overnight at -20^{o}C. The fixative was then replaced with acetone at room temperature for 15 minutes and transferred to methyl benzoate at room temperature for 15 minutes. Tissue was immersed in GMA monomer consisting of 5% methyl benzoate for 6 hours. Over the 6 hour

incubation, the GMA solution was changed 3 times. The tissue was then placed in polythene capsules with lids containing GMA embedding resin (70mg Benzoyl peroxide dissolved in 10mL GMA solution A and 250 µl GMA solution B) at 4^{o}C for 16 h. The biopsies were finally stored at -20^{o}C in an airtight container.

2.2.2 Avidin-biotin system staining technique

2 µm GMA biopsy sections were cut using the LEICA RM2255 microtome and placed into a water path containing 0.2% ammonia for 60 seconds. The slides were then dried at room temperature for 1-4 hours. Once air-dried, sections were incubated for 30 minutes with 0.1% sodium azide in order to inhibit endogenous peroxidise activity. Slides were washed 3 times for 5 minutes with Tris Buffer Saline (TBS) and then blocking medium (Dulbecco's Modified Eagle medium (DMEM) containing fetal calf serum and BSA) was added to sections for 30 minutes. The sections were incubated with primary antibody overnight at room temperature, washed, and then the appropriate secondary biotinylated antibody was added for 2 hours. After further washing, avidin-biotin peroxidase complexes were then added for 2 hours, following by washing and then the addition of the 3-Amino-9-EthylCarbazole (AEC) chromogen for 7 minutes. The sections were counterstained with Mayer's Haematoxylin for ~20 minutes. The primary antibodies along with the secondary antibodies used with this particular technique are shown in **Table 2.1**.

Primary Antibody	Clone or catalogue number	Working Concentration	Company	Isotype Control	Company	Secondary Antibody	Company
Tensin1	SAB4200283	5 µg/ml	Sigma-Aldrich	Rabbit IgG	Dako, UK	Polyclonal Swine Anti-Rabbit	Dako, UK
Tensin1	sc-28542	4 µg/ml	Santa-Cruz	Rabbit IgG	Dako, UK	Polyclonal Swine Anti-Rabbit	Dako, UK
Mast Cell Tryptase	AA1	0.1 µg/ml	Dako, UK	mIgG1	Dako, UK	Polyclonal Rabbit Anti-Mouse	Dako, UK

Table 2.1: Antibodies used in immunostaining. Table showing the tensin1 antibodies along with the isotype controls and the secondary antibodies.

2.2.3 Dako EnVsion FLEX+ staining technique

2 µm GMA biopsy sections were cut and air-dried as described above. Once air-dried, sections were incubated for 10 minutes with the Peroxidase Blocking Reagent. Slides were washed 3 times for 5 minutes with the EnVision FLEX wash buffer. The primary antibody was then added to the sections for 1 hour. Primary antibody was then washed away and the EnVision Flex Linker was added to the sections for 15 minutes to enhance the staining. Sections were again washed and the EnVision Flex/HRP was added to each section for 30 minutes. The secondary antibody HRP was then washed away and the DAP (3,3'-diaminobenzidine) chromogen was added to the slides for 10 minutes. The sections were then counterstained with Mayer's Haematoxylin. The primary antibodies along with the secondary antibodies used with this technique are shown in **Table 2.2**.

Primary Antibody	Clone or catalogue number	Working Concentration	Company	Isotype Control	Company	Secondary Antibody	Company
Tensin1	SAB4200283	2.5 µg/ml	Sigma-Aldrich	Rabbit IgG	Dako, UK	Polyclonal Swine Anti-Rabbit	Dako, UK
Tensin1	sc-28542	1 µg/ml	Santa-Cruz	Rabbit IgG	Dako, UK	Polyclonal Swine Anti-Rabbit	Dako, UK
Mast Cell Tryptase	AA1	0.1 µg/ml	Dako, UK	mIgG1	Dako, UK	Polyclonal Rabbit Anti-Mouse	Dako, UK

Table 2.2: Antibodies used in immunostaining with the Dako EnVision FLEX+ staining technique. Table showing the antibodies and the antibody concentrations used for this particular staining technique.

2.2.4 Quantification of immunohistochemical staining

For quantitative assessment of tensin1 immunostaining in the epithelium, airway smooth muscle and lamina propria, a thresholding technique was used that had been established previously in the lab (Siddiqui et al. 2008b, Shikotra et al. 2012). Briefly, two non-contiguous sections were thresholded for each patient. The median lower and upper limit of hue intensity saturation (HIS) were then defined from 6 validation subjects. The lower value of hue, maximum saturation and median intensity were then selected as the final threshold to quantify the tensin1 staining. This final threshold was also applied to the isotype control slides of the 6 validation patients. Then, the mean percentage of isotype staining was calculated. Finally, the image noise was calculated as the mean percentage of staining + 2SD (Standard Deviation).

2.3 Primary Cell Isolation and Culture

For all the experiments primary human lung myofibroblasts, airway smooth muscle cells and bronchial epithelial cells were used.

2.3.1 Human myofibroblasts

Myofibroblasts were extracted from explanted lung tissue as described previously (Roach et al. 2013). Small fragments (1-2 mm^3) of lung tissue were placed into 6 well plates. Plates were then left for 1 hour for the tissue to adhere in an incubator at 37°C in humidified chamber (5% CO_2/95% air). Once adherent, 2 ml of Myofibroblast growth medium (DMEM with glucose and GlutaMAX™ supplemented with 10% Fetal Bovine Serum, Antibiotic/Antimycotic solution and non-essential amino acids) was added gently to each well, and then the plate was incubated again at 37°C. The plates were monitored for cell growth and the myofibroblast growth medium was changed every two days. When there was substantial cell growth, ~day 7, the tissue was discarded and medium was washed away with Hank's Balanced Salt Solution. Cells were then detached using 0.25% Trypsin EDTA. Cells were then centrifuged for 7 minutes at 1300 rpm and the cell pellet was then resuspended in 1 ml of medium. Cell counting and viability was then assessed using the Trypan Blue method and the cells were then seeded into T75cm^2 flasks (15 x10^4 cells in each flask). This was deemed passage 1 and cells were washed and fed every 3 days. Immunofluorescent staining and flow cytometry was performed as previously (Roach et al. 2013). The myofibroblast identity of the cells was confirmed as they demonstrated the typical stellate morphology, and were

positive for αSMA, Thy-1 and Fibroblast Surface Protein (FSP) and negative for CD34 and CD68. The procedure described above was followed until the cells were 80%-90% confluent and in the required passage for experiments.

2.3.2 Human airway smooth muscle cells

Bronchial biopsies were obtained from healthy controls and patients during bronchoscopy as described previously (Brightling et al. 2005). Airway smooth muscle bundles were dissected free from the surrounding tissue using a dissecting microscope, and the pieces of muscle were then placed into 6 well plates and the same culture procedure used for myofibroblasts was followed. Confirmation of the identity of the cultured cells as being smooth muscle cells was investigated by labelling monolayers of cells for αSMA and myosin as described previously (Brightling et al. 2005). Once the cells reached the appropriate passage and confluence they were used for experiments.

2.3.3 Human bronchial epithelial cells

Bronchial brushings were obtained during bronchoscopy and were put directly in Bronchial Epithelial Growth medium (BEGM). BEGM was consisted of 500 ml BEBM (Bronchial Epithelial Basal medium) (Clonetics) SingleQuot bullet kit (SingleQuots), 1.5 ml fungizone (GIBCO) and 5 ml of Antibiotic/Antimycotic solution). The cells were dispersed by vigorously shaking the tubes containing the brushes. The brushes were then removed and cells centrifuged at 227 x g for 8 minutes. The cell pellet was then resuspended in 1 ml of BEGM and the cells

were transferred into 6-well plates pre-coated with 1% PureCol collagen (Inamed Biomaterials). Each well was then topped up in order to contain 1 ml of medium. Plates were then incubated at 37°C in 5% CO_2/95% air for 24 hours when the cells were adherent. Cells were then detached using 0.1% Trypsin EDTA, counted and reseeded in T75cm^2 flasks. Immunofluorescence staining with Cytokeratins 5 and 14 (markers specific for epithelial basal cells) was performed to confirm that the cells isolated were in fact human airway epithelial basal cells. Cells were fed every 2 days until they reached the required confluence and passage for experiments.

2.4 Tensin1 Expression in Human Airway Structural Cells

2.4.1RNA isolation and qRT-PCR

2.4.1.1 RNA isolation

To examine tensin1 mRNA expression, confluent cells were recovered using trypsin-EDTA and centrifuged at 1300 rpm for 8 minutes. RNA was isolated using the RNeasy Plus kit (QIAGEN, UK) and QIAShredder spin columns (QIAGEN, UK) according to the manufacturer's instructions. RNA was measured using the NanoDrop (Thermofisher) bioanalyser. To study the effect of transforming growth factor (TGF) β1 (10 ng/ml, R&D systems, Abingdon, UK) on TNS1 expression, cells were grown to confluence and then serum-starved for 24 h prior to stimulation for 24 hours.

2.4.1.2 qRT-PCR primers

The normaliser gene used for analysis was β-actin and the primers used were gene-specific Hs_ACTB_1_SG QuantiTect® Primer Assay primers (QT00095431, Qiagen). These are specific to ACTB, detecting the NM_001101 transcript, spanning exons 3/4 and producing a final product length of 146 base pairs (bp). Tensin1 mRNA expression was analysed using primers designed by myself (TNS1 (forward primer: 5'- AGCGGAGACCTGACATCAC-3', reverse primers: 5'-CGGTTTCCCTTGTTGTGTAGAAC-3') using NCBI primer designing tool. These primers are specific to tensin1 mRNA detecting the NM_022648 transcript and giving a product of 166 bp.

2.4.1.3 qRT-PCR

Gene expression quantification was performed using the 1-step method Brilliant SYBR® Green qRT-PCR. 12.5µl of 2 x SYBR® QRT-PCR mastermix, 7µl of RNA-free water, 2.5µl of the appropriate primers, 1µl of Reference dye and 1µl of Reverse Transcriptase were added per reaction per well in a 96-well qRT-PCR plate. 1 µl of 100ng/µl RNA concentration was added per reaction. All reactions were performed in triplicate. No-template and no-Reverse Transcriptase control were also performed.

The plate was then centrifuged at 302 x g for 1 minute and then analysed in the Mx3000P™ quantitative PCR machine (Agilent) which was set to read both ROX, the reference dye, and SYBR Green. The cycling conditions used for the protocol were as follows:

Cycles	**Step**	**Duration of cycle**	**Temperature**
1	Initial Reverse Transcription (RT)	30 minutes	50°C
1	RT Inactivation	10 minutes	95°C
50	Denaturation	30seconds	95°C
	Annealing	1 minute	60°C

	Extension	30 seconds	72°C
1	Melting curve	30 seconds 30 seconds 30 seconds 30 seconds	90°C 60°C 90°C 60°C

2.4.1.4 Agarose gel

An agarose gel was run to confirm that the required product was amplified in the qRT-PCR reaction. 0.75 g of agarose (Sigma) was added into 50 ml of Tris-Acetate-EDTA (TAE) buffer in order to prepare 1.5% agarose gel. The mixture was then placed into a microwave until the agarose was completely dissolved. 2 µl of Ethidium Bromide was then added once the mixture was cooled. The mixture was then poured in a gel mould with comb. Once set, the comb was removed and the gel mould was placed into a tank containing ~1 L of TAE buffer. 2 µl of loading dye was then added to 10 µl PCR product and to 10 µl of a 100 bp DNA ladder (G2101, Promega). Samples were then loaded into the agarose and the gel was left to run for 1 hour at 80V. The gel was then visualised on an IllumoVision camera and pictures were acquired. PCR products were also sequenced by PNACL (University of Leicester) to confirm that tensin1 was the product amplified.

2.4.1.5 Quantification of gene expression

Firstly, validation of the primers used in qPCR needed to be done to ensure that the amount of PCR product doubles every cycle and that the amount of fluorescence signal produced is proportional to the starting material. Efficiency of the primers was assessed using the standard curve method in which each primer pair amplified samples of known concentrations. Threshold cycle (C_T) value was plotted against input amount to generate an amplification plot of each reaction. An amplification efficiency of ~100% indicated the applicability of primers for the method.

Quantification of gene expression was performed using the 2^-(ΔCt) method. The Ct values are determined from a log-linear plot of the PCR signal versus the cycle number and these values were used to perform the quantification. The mean Ct values for both the target and the internal control genes were calculated from triplicate reactions. The equation used to quantify the fold change on the target gene normalised to β-actin is $\Delta Ct = Ct_{target} - Ct_{actin.}$ Normalising to an endogenous reference provides a method for correcting results for differing amounts of input RNA (Livak and Schmittgen 2001). The results were then illustrated in bar charts to show relative tensin1 expression in different donors.

2.4.2 Protein extraction and western blot

2.4.2.1 Protein extraction

To examine the expression of tensin1 protein in human airway smooth muscle cells (HASMCs), cells were grown to confluence, detached using trypsin-EDTA, centrifuged at 227 x g for 7 minutes, the supernatant removed and the cells then washed using PBS. Cells were centrifuged again in order to wash away any excess of PBS. Cells were then lysed in RIPA lysis buffer (sc-24948, Santa-Cruz) consisting of Radio-Immuno-Precipitation Assay (RIPA) buffer, protease inhibitor, phenylmethanesulfonylfluoride (PMSF) and sodium orthovanadate. Cells were carefully resuspended in the cell lysis buffer and left on ice for 30 minutes. If the mix was still viscous, cells were disrupted further using a gauge needle. The mix was then centrifuged for 15 minutes at 13,000 x g. The supernatant was saved and cell pellet was discarded.

2.4.2.2 Protein assay, determining the concentration of the protein

The Bio-Rad DC Protein Assay was used to determine the concentration of the protein. Six protein standards using BSA were prepared with the concentration ranging from 0.0mg/ml to 1.5 mg/ml. Samples were prepared with a 1:1 dilution in RIPA buffer. The AS' solution was then prepared according to manufacturer's instructions. 25 µl of AS' solution, 200 µl of Solution B and 5 µl of protein standard/sample were added per reaction per well in a 96-well plate. All reactions were performed in duplicate. The plate was then incubated for 20 minutes on the rocker and then measured using a spectrophotometer set at an

absorbance of 750 nm. Protein concentration was then determined from the linear equation acquired from the protein standards and the particular sample absorbance.

2.4.2.3 Protein electrophoresis and membrane blotting

Firstly, it was necessary to perform sodium dodecyl sulphate polyacrylamide gel electrophoresis (SDS-PAGE). 7.5% SDS-polyacrylamide gels (4561024, Bio-Rad) were used and they were placed in gel running units and the Tris-Glycine-SDS (TGS) running buffer was added. Protein samples were then prepared. Protein samples were diluted in RIPA buffer until the required concentration (30 μg) was acquired and 4x loading dye was added in the protein sample to allow visualisation of the proteins. The MagicMark XP western standard (LC5602, Invitrogen) was prepared as well to allow visualisation of protein standard bands. Western standard and protein samples were then loaded in the gel and the gel was run at 150V for ~90 minutes.

Following electrophoresis, the gels were removed from the units. The glass plates were detached and the gel was transferred into transfer buffer. Using a semi-dry transfer technique, the proteins were transferred from the gel to a polyvinylidene (PVDF) membrane. After the transfer, the membrane was placed in 0.1% TBS Tween20 to disassemble.

2.4.2.4 Detection of the proteins

The membrane was blocked for 1 hour in 5% Milk (w/v) and 0.1% TBS (v/v) Tween20 at room temperature. The membrane was then placed into a container with the primary antibody diluted in 5% Milk +0.1% TBS Tween20 and left overnight at 4°C. The membrane was then washed for 10 minutes in 0.1% TBS Tween20 for 3 times. After the washing, the membranes were incubated for 1 hour with the secondary antibody diluted again in 0.1% TBS Tween20. Therefore, the membranes were again washed for 5 minutes in 0.1% TBS Tween20 for three times. The membranes were then developed using the Amersham Enhanced ChemiLuminescence (ECL) western blot detection system. Pictures of the membranes were acquired using the Image Quant LAS 4000. The Antibodies used in Western blot analysis are sown in **Table 2.3**.

Primary Antibody	**Working Concentration**	**Company**	**Secondary Antibody**	**Company**
Tensin1	1µg/ml	Sigma-Aldrich	Polyclonal Goat Anti-Rabbit	Santa-Cruz
Tensin1	4µg/ml	Santa-Cruz	Polyclonal Goat Anti-Rabbit	Santa-Cruz
B-actin Clone C4	10ng/ml	Santa-Cruz	Polyclonal Goat Anti-Mouse	Dako, UK

Table 2.3: Antibodies used in western blot analysis. Table showing the primary and secondary antibodies used for the detection of tensin1 protein.

2.4.3 Immunoprecipitation

2.4.3.1 Preparation of whole cell lysates

Whole cell lysates from HASMCs were prepared for immunoprecipitation. Cells were grown to confluence, detached using trypsin-EDTA, centrifuged at 227 x g for 7 minutes, the supernatant removed and the cells then washed using PBS. Cells were centrifuged again in order to wash away any excess of PBS. Cells were then lysed in RIPA lysis buffer consisting of RIPA buffer, protease inhibitor, PMSF and sodium orthovanadate. Cells were carefully resuspended in the cell lysis buffer and left on ice for 30 minutes. If the mix was still viscous, cells were disrupted further using a gauge needle. The mix was then centrifuged for 15 minutes at 13,000 x g. The supernatant was saved and cell pellet was discarded.

2.4.3.2 Preparation of protein A/G beads

Protein A/G PLUS Agarose beads (sc-2003, Santa-Cruz) were resuspended. 50 µl of beads were washed three times with PBS and resuspended in 50 µl RIPA buffer.

2.4.3.3 Pre-clearing lysate and antibody binding

Protein concentration was determined using the Bio-Rad DC Protein Assay (as described before) and 300 µg of protein were used for this particular experiment. Cell lysate was incubated with 20 µl washed bead slurry for 30

minutes rotating at 4°C to pre-clear the lysate of any proteins that non-specifically bind to beads.

Whilst the cell lysate was pre-clearing, tensin1 antibodies (SAB4200283, 4 µg/ml, Sigma-Aldrich or sc-28542, 2 µg/ml, Santa-Cruz) were added at the appropriate dilution to the remaining washed beads. The bead-antibody complex was then incubated for 30 minutes on ice.

2.4.3.4 Antibody-lysate-beads complex

The pre-cleared cell lysate was then transferred into a new tube and it was then incubated with the bead-antibody complexes overnight at 4°C to allow the antigen to bind to the bead-antibody complex with rotating agitation. The complex was then washed three times with lysis buffer and boiled in Laemmli Buffer for SDS-page and western blot analysis (as described before).

2.4.4 Confocal immunofluorescence microscopy

2.4.4.1 Direct confocal immunofluorescence microscopy

HASMCs were cultured on 8 well chamber slide (Thermofisher). Once the cells reached confluence, culture media was aspirated and they were washed with PBS. Cells were fixed using iced cold methanol for 20 minutes on ice. The fixative was removed and the slides were air-dried. A blocking solution of 3% BSA/PBS was added to each well for 30 minutes to eliminate non-specific binding. The blocking solution was then removed and primary antibodies were added for 90 minutes. The cells were washed again with PBS/0.05 Tween20. They were then counterstained with 4',6-diamidino-2-phenylindole (DAPI) (32670, Sigma-Aldrich). Finally, cells were washed six times with PBS, mounted with Fluoroshield (F6182, Sigma-Aldrich) and cover-slipped. Images were captured on a confocal laser scanning microscope (Leica TCS SP5, Leica UK Ltd) and staining was quantified using the Cell F Imaging software (Olympus UK Ltd). Matched exposures were used for isotype controls.

Primary Antibody	**Clone**	**Working Concentration**	**Company**	**Isotype Control**	**Company**
αSMA FITC	H-300	10 µg/ml	Sigma-Aldrich	Mouse IgG2a-FITC	Dako, UK

Table 2.4: Antibodies used for direct immunofluorescence staining. Table showing the alpha smooth muscle actin (αSMA) FITC positive control antibody along with the isotype control and secondary used as positive control for the staining.

2.4.4.2 Indirect confocal immunofluorescence microscopy

The same procedure was followed up the addition of the primary antibody. After 90 minutes of primary incubation, the cells were washed three times with PBS/0.05% Tween20 and then secondary antibodies indirectly labelled with fluorescein conjugates (FITC) and/or Alexa 594 were applied for a further 90 minutes. The cells were washed again with PBS/0.05 Tween20. They were then counterstained with DAPI. Finally, cells were washed six times with PBS, mounted with Fluoroshield and cover-slipped. Images were captured on a confocal laser scanning microscope (Leica TCS SP5, Leica UK Ltd) and staining was quantified using the Cell F Imaging software (Olympus UK Ltd). Matched exposures were used for isotype controls.

To study the effect of the extracellular matrix protein fibronectin and TGFβ1 on tensin1 expression and localisation, slides were coated with human recombinant fibronectin (F0895, Sigma-Aldrich) for 1 hour prior to seeding and stimulated with TGFβ1 (10ng/ml) for 24 hours when 50% confluent. Quantification of fibrillar adhesion length was measured by Cell F imaging software (Olympus UK Ltd).

Primary Antibody	**Clone**	**Working Concentration**	**Company**	**Isotype Control**	**Company**	**Secondary Antibody**	**Company**
Tensin1	-	4.5 µg/ml	Sigma-Aldrich	Rabbit IgG	Dako, UK	Goat Anti-rabbit FITC	Sigma-Aldrich

Table 2.5: Antibodies and working dilutions used for indirect immunofluorescence staining. Table showing the tensin1 antibody along with the isotype control and secondary antibody.

2.5 Tensin1 and αSMA Co-localisation on Human Airway Smooth Muscle Cells

2.5.1 Indirect confocal immunofluorescence co-staining

Tensin1 and alpha smooth muscle actin (αSMA) co-staining was performed to examine co-localisation of the two proteins. The indirect confocal immunofluorescence protocol was followed as described above (Section 2.4.4.2). Cells were incubated with both tensin1 and αSMA along with the isotype controls and secondary antibodies relevant for both primary antibodies (**Table 2.6**). Images were captured on a confocal laser scanning microscope (Leica TCS SP5, Leica UK Ltd). Matched exposures were used for isotype controls.

Primary Antibody	Clone or catalogue number	Working Concentration	Company	Isotype Control	Company	Secondary Antibody	Company
Tensin1	SAB4200283	4.5 µg/ml	Sigma-Aldrich	Rabbit IgG	Dako, UK	Goat Anti-rabbit FITC	Sigma-Aldrich
αSMA	1A4	0.7 µg/ml	Dako, UK	Mouse IgG2a-FITC	Dako, UK	Goat Anti-mouse Alexa Fluor 594	Thermofisher

Table 2.6: Antibodies used for indirect immunofluorescence co-staining. Table showing the tensin1 antibody and αSMA antibody along with the isotype controls and secondary antibodies.

2.5.1.1 Quantification of tensin1 and αSMA co-staining

Tensin1 and αSMA co-staining was performed to examine co-localisation of the two proteins. A co-localisation plugin in ImageJ, JaCoP, implements and performs the pixel intensity correlation over space methods of Mander's and Pearson's correlation. Both the coefficients are used to quantify the degree of co-localisation between fluorophores. Mander's overlap coefficient reports the fraction of the total intensity that co-occur. However, Pearson's coefficient measures the degree to which the intensity variation of the first fluorophore follows variation in the second fluorophore. Thus, taking into consideration both correlations is important to eliminate the possibility of a random co-localisation as both proteins are located on the cytoskeleton (Adler and Parmryd 2010).

2.5.2 Tensin1- αSMA co-immunoprecipitation

Tensin1 immunoprecipitates (SAB4200283, 4 µg/ml, Sigma-Aldrich) were acquired using the conventional immunoprecipitation protocol described in Section 2.4.3. Immunoprecipitates were then washed three times with lysis buffer and boiled in Laemmli Buffer for SDS-page and western blot analysis (Section 2.4.2.3). The membrane was probed against αSMA (M0851, 1µg/ml, Dako) to examine tensin1-αSMA interaction respectively.

2.6 Effect of Tensin1 Silencing on Human Airway Smooth Muscle Cell Function

2.6.1 Tensin1 downregulation using small interfering RNA (siRNA)

These experiments were performed on both cells from healthy and diseased donors. One day prior to transfection, HASMCs were seeded into 6-well plates at a density of 300 000 cells/well in antibiotic-free medium. 24 hours later, 10 µl of 20 µM siRNA were diluted in 100 µl antibiotic and serum-free medium and mixed by pipetting. Separately, 6 µl Lipofectamine 2000 (11668, Life Technologies) was mixed with 100 µl antibiotic and serum-free medium and incubated for 5 minutes at room temperature. The two solutions were then mixed together and incubated for 20 minutes at room temperature to allow the formation of transfection complexes. During this incubation, medium from the cells was replaced with 1.78 ml antibiotic and serum-free medium. Finally, transfection complexes were added drop-wise to the cells to give a total volume of 2 ml and cells were cultured at 37°C. After 6 hours, medium was replaced with antibiotic-free medium for 48 hours. siGLO, a fluorescently tagged, non-functional, non-targeting siRNA was used in order to determine the transfection efficiency. A siCON functional control, designed to not target any gene in the cell, was used in all experiments to distinguish sequence-specific silencing from non-specific effects. Knockdown efficiency was defined by qRT-PCR and western blot analysis.

siRNA	Sequence 5'-3' (Sense Strand)	Company
siGLO RISC-Free siRNA	Proprietary Sequence (Catalogue No. D-001600-01)	GE Life Sciences Dharmacon
TNS1 (human tensin1) siGENOME SMARTpool sihT1	GAAGGUACGUGCAUUACUU (sihT1.1) GCAACUACCUGCUGUUCAA (sihT1.2) GCAAUGUGCUCUUCAUCAA (sihT1.3) GAAGCUCCAUGCCAAGGUA (sihT1.4)	GE Life Sciences Dharmacon

Table 2.7: siRNA sequences. Table showing the sequence of siGLO RISC FREE and sihT1 siRNA.

2.6.2 Cell survival/proliferation assay

The MTS assay (G3582, Promega) was used to assess viability and proliferation of the cells after tensin1 silencing. 48 hours after transfection, cells were collected and 2 x 10^3 cells were plated into 96-well plates in culture media in the absence of antibiotics overnight. Cells were stimulated with TGFβ1 for 24 hours. 20 µl of CellTiter 96 Aqueous one solution containing the tetrazolium compound MTS, [3-(4,5-dimethylthiazol-2-yl)-5-(3-carboxymethoxyphenyl)-2-(4-sulfophenyl)-2H- tetrazolium] (Promega) solution was added to each well. The

optical density (OD) at 490nm was determined with a spectrophotometer. Each experimental condition was run in triplicate.

Cell survival was assessed also using the trypan blue method. Tensin1 downregulation was performed and cells were centrifuged to form a cell pellet. The pellet was then resuspended in 1 ml of growth medium and the cells counted using the trypan blue method (Tennant 1964). This assesses cell viability by exclusion of the trypan blue dye. Both, the MTS and trypan blue assay were performed on n=4 healthy and COPD subjects.

2.6.3 Assessing αSMA expression after tensin1 knockdown

Tensin1 depletion was performed and RNA was isolated from HASMCs to assess their ability to express αSMA at the mRNA level by qRT-PCR. Isolation of RNA and qRT-PCR were performed as described in Section 2.4.1. The primers used were gene-specific, ACTA2 detecting the NM_001141945 (forward primer: 5'-GAAGGAATAGCCACGCTCAG-3', reverse primers: 5'-TTCAATGTCCCAGCCATGTA-3').

Effect of tensin1 knockdown on αSMA protein expression was examined using immunofluorescence staining. Cells were seeded on coverslips into-6-well plates at a density of 300 000 cells/well. Tensin1 knockdown was performed as described in the previous section. 48 hours post transfection, coverslips were rinsed once in 1x PBS and fixed with iced cold methanol for 20 minutes on ice. The fixative was removed and the coverslips were air-dried. Immunofluorescence staining and confocal imaging were undertaken as

described in Section 2.5. Primary and secondary antibodies used are listed in **Table 2.6**. Western blotting analysis was also used to analyse αSMA expression after tensin1 knockdown. Protein extraction and western blotting was performed as described in Section 2.4.2. Band intensity was measured using the ImageJ software. αSMA antibody was used at a concentration of 1μg/ml (M0851, Dako). Both immunofluorescence staining and western blotting analysis were performed on n=4 healthy and COPD subjects.

2.6.4 Collagen gel contraction assay

This technique was used to examine the effect of tensin1 in the contractility of HASMCs as described previously (Woodman et al. 2008). Knockdown of tensin1 protein was performed as described in 2.6.1. The cells were then washed and harvested using trypsin-EDTA and resuspended in 600 μl serum-free medium. Collagen gels were made on ice and consisted of 299 μl of PureCol type 1 collagen (Inamed Biomaterials), 37 μl of 10X MEM (Invitrogen), 20 μl of sodium bicarbonate (Invitrogen) and impregnated with 144 μl cell suspension (150 000 per collagen gel). Gels were added to 24 well plates coated with PBS/0.5% BSA and left to polymerise at 37°C for 1.5 hours. The gels were then detached from the plate and resuspended in 1ml of serum-free medium or serum-free medium containing TGFβ1 (10 ng/ml) where appropriate. Pictures were taken at 0, 4, 18, 24 and 48 hours. The percentage of contraction was quantified using the ImageJ software. The experiment was performed in n=4 healthy and disease donors.

2.7 Generating the pEGFP C1 Construct with Mutant Tensin1

The aim of this experiment was to generate a pEGFP C1 Tensin1 construct containing the mutant tensin1 (homozygous –TT-), so it could be used for transfection experiments along with the pEGFP C1 Tensin1 construct with the wild-type tensin1 (homozygous –CC-) kindly provided by Dr Katherine Clark. Furthermore, both constructs were used as controls for the restriction fragment length polymorphism (RFLP) method, method discussed below. To generate plasmid DNA containing full length SNP Tensin1, a cloning procedure was followed involving site-directed mutagenesis to correct the sequence from the pBs Tensin1 containing the wild-type, purification of PCR products, bacterial transformation, digestion of Tensin1 from the pBluescript vector, ligation of the corrected Tensin1 into the pEGFP C1 vector.

2.7.1. Oligonucleotide design

Primers for site-directed mutagenesis were approximately 24 nucleotides in length. The forward and reverse primers contained the desired mutation in the middle of the sequence with 10-15 bases of correct sequence on both sides Primers were designed by myself (TNS1 (forward primer: 5'-CTAGTCCTGGCTTCGGC**T**GGCGG-3', reverse primers: 5'-GGGATTGATGGCCCGCC**A**GCCG-3') using NCBI primer designing tool.

2.7.2 Small scale site-directed mutagenesis

A smaller construct, the pBluescript Tensin1 containing the wild-type, was used to introduce the site-directed mutagenesis (again provided by Dr Katherine Clark). To induce nucleotide changes in plasmid DNA, 10 ng of target plasmid (pBluescript Tensin1) was amplified by PCR with the mutagenesis primers designed in a reaction mix containing 10 µM forward primers, 10 µM reverse primer, 23 µl of DNA polymerase master mix (kindly provided by Dr Xiaowen Yang). Two high fidelity DNA polymerases were tested, Phusion® (M0B30, NEB) and Platinum® pfx (11708, Life Technologies). The PCR parameters for each DNA polymerase are shown in **Table 2.8** and **Table 2.9**. Amplification was confirmed by agarose gel electrophoresis. Gel was run as described in Section 2.4.1.5. 1 kb DNA ladder was used for this set of experiments (G5711, Promega).

Cycles	**Step**	**Duration of cycle**	**Temperature**
1	Initial Denature	30 seconds	98°C
27	Denature Annealing Extension	10 seconds 30 seconds 150 seconds	98°C 59°C 72°C
1	Final Extension	5 minutes	72°C
	Hold	-	4°C

Table 2.8: Phusion® DNA polymerase. Table showing the PCR amplification cycle parameters.

Cycles	Step	Duration of cycle	Temperature
1	Initial Denature	2 minutes	94°C
27	Denature Annealing	15 seconds 30 seconds	94°C 59°C
1	Final Extension	5 minutes	68°C
1	Hold	-	4°C

Table 2.9: Platinum® pfx DNA polymerase. Table showing the PCR amplification cycle parameters.

2.7.3 Large scale site-directed mutagenesis

Large scale site-directed mutagenesis was then performed. The Platinum® pfx DNA polymerase was used as it gave a better fragment. The same principle was used as described in Section 2.7.2, but this time the reaction mix was four times bigger with a final volume of 104 µl. The amplification reaction was then treated with 10U Dpn1 (R0176S, New England BioLabs) restriction enzyme at 37°C for 1 hour. DpnI causes digestion of the parental methylated and hemimethylated plasmid DNA, leaving only the plasmid containing the mutation.

2.7.4 Gel purification of PCR products

After confirmation that the PCR reaction gave a product of sufficient yield and predicted size (6.2 kb), the band was visualised and excised from the gel. DNA was purified using a QIAquick Gel Extraction kit (QIAGEN, UK) according to the manufacturer's instructions. Purified DNA was eluted in 15 µl of distilled water. DNA concentration was measured using the NanoDrop (Thermofisher) bioanalyser. Product yield was confirmed by agarose gel electrophoresis.

2.7.5 Bacterial transformation

1 µl of the purified PCR product was added to competent DH5α E.coli cells, which had been thawed on ice. DNA and competent cells were incubated on ice for 30 minutes. Heat shock was then performed for 1min at 42°C to allow plasmid DNA uptake and then returned to ice for further 5 minutes. 250 µl of Luria Broth (LB) media (17 mM NaCl, 1% tryptone and 0.5% yeast extract) was added to cells and incubated for 30 minutes at 37°C with agitation. Following incubation 100 µl of cell suspension was spread on Luria Broth agar plates (17 mM NaCl, 1% tryptone, 0.5% yeast extract and 2% agar) containing antibiotic for selection (ampicillin at 100 µg/ml and kanamycin at 30 µg/ml). Plates were incubated for 16 hours at 37°C and colonies were then picked for growth in 5ml LB media with the appropriate antibiotic. 5 ml cultures were incubated for 16 hours at 37°C with agitation. Cells were then centrifuged at 4000 rpm for 10 minutes for plasmid preparation.

2.7.6 Miniprep purification for the isolation of plasmid DNA

DNA was isolated using the QIAprep Spin Miniprep kit according to manufacturer's instructions. DNA was measured using the NanoDrop (Thermofisher) bioanalyser. Product yield was confirmed using gel electrophoresis. The construct was also sequenced to confirm that tensin1 was correctly inserted in the plasmid and no PCR errors were introduced during the site-directed mutagenesis.

2.7.7 Restriction digest of the pBluescript and pEGFP C1 plasmid

After confirming that the plasmid isolated contained the SNP tensin1 (homozygous –TT-), the corrected tensin1 was digested from the pBluescript Tensin1 construct. But also, the pEGFP C1 vector was isolated from the pEGFP C1 Tensin1 construct. To achieve this, two restriction enzymes, EcoR1 and Sal1, were used to perform the digestion on both constructs. DNA plasmids were incubated with EcoR1 and Sal1 for 1 hour at 37°C. Products were run on a 1.5% agarose gel and the predicted bands of 3.2 kb (corrected SNP tensin1) and 2.961 kb (pBluescript) and 6.5 kb (wild-type tensin1) and 4.7 kb (pEGFP C1) on pBluescript and pEGFP C1 constructs' digestion, respectively, were visualised. Non-restricted digested products were run along the digested constructs to confirm specificity of the reaction. The corrected tensin1 and the pEGFP C1 vector were excised from the gel and purified using the QIAquick Gel Extraction kit (QIAGEN, UK) according to the manufacturer's instructions. Purified DNA was eluted in 15 µl of distilled water. DNA concentration was measured using the

NanoDrop (Thermofisher) bioanalyser. Product yield was confirmed by agarose gel electrophoresis.

2.7.8 Ligation of the pEGFP C1 vector and corrected SNP tensin1

The corrected SNP tensin1 was ligated into the pEGFP C1 vector (Promega) according to manufacturer's instructions. A standard reaction mix of 50 ng vector DNA was used. T4 DNA ligase (M1801, Promega) was diluted in the appropriate ligation buffer. A negative control with no insert was used. Reactions were incubated for 1 hour at room temperature. Ligation was confirmed using gel electrophoresis and DNA concentration was measured using the NanoDrop (Thermofisher) bioanalyser. Bacterial transformation and purification of the plasmid DNA was followed (Section 2.8.1.5 & Section 2.8.1.6) to isolate the product of interest. To confirm ligation, the purified plasmid DNA was again restricted digested with EcoR1 and Sal1 and predicted bands were visualised using gel electrophoresis. Product was sequenced to confirm in-frame ligation.

2.7.9 Maxiprep purification for the isolation of plasmid DNA

Maxiprep was performed to obtain stocks of the construct for the use in transfections. Individual colony was picked to inoculate 5ml LB media with the appropriate antibiotic. The cultures were incubated for 8 hours at 37°C with agitation. 100 µl of this was then used to inoculate 50ml LB containing antibiotic which was subsequently incubated for 16 hours at 37°C with agitation. Cells were then centrifuged at 6000 rpm for 15 minutes for plasmid preparation using the

QIAfilter Plasmid Maxi kit (QIAGEN) according to manufacturer's instructions. Isolated plasmid DNA was resuspended in 150 µl dH_2O and DNA concentration was measured using the Nanodrop (Thermofisher) bioanalyser.

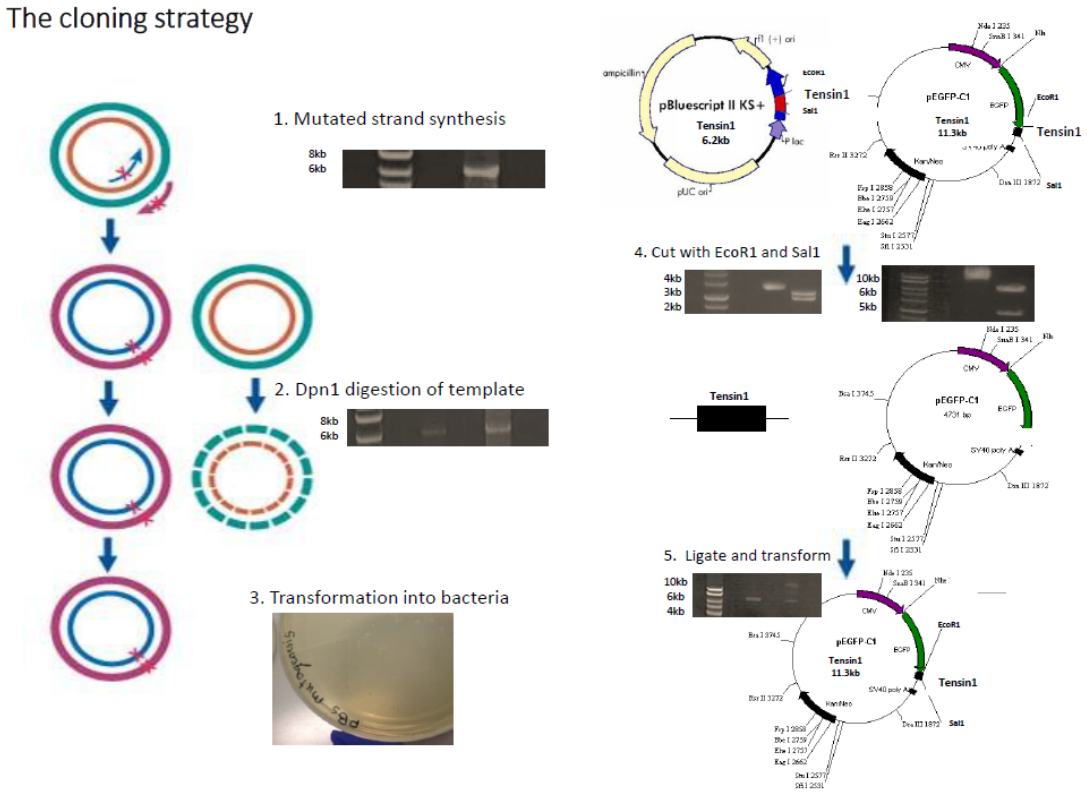

Figure 2.1: A schematic diagram illustrating the cloning strategy used.

2.8 Effect on Functional Responses of Cells Obtained from Subjects with Wild-Type Versus the R1197W SNP

2.8.1 Restriction Fragment Length Polymorphism (RFLP) mapping

RFLP is a difference in homologous DNA sequences. This can be detected by a process called restriction digestion. Therefore, restriction endonucleases are used to digest DNA samples. Gel electrophoresis is performed to separate by length the digested DNA samples. Therefore, it is important, the fragments generated to be of a different size. Molecular markers are used to estimate the fragment size.

In this study, the SNP is located at the 2q35 locus in TNS1 gene and has a missense amino acid change, specifically the amino acid arginine is replaced with tryptophan at position 1197, written as R1197W. This suggests that the sequence acquired when tryptophan is present is cttcggctggcgg. Eag1 can recognise C^GGCCG and can thus digest the DNA only when the wild-type tensin1, R1197 is present.

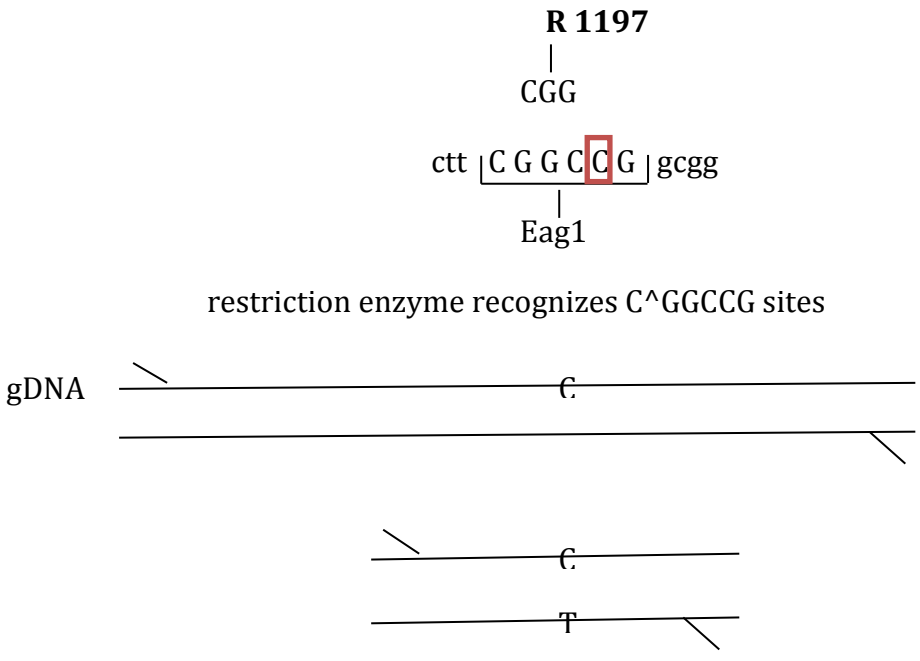

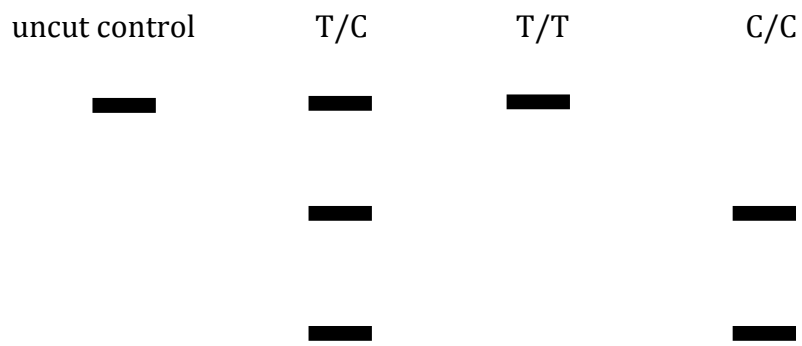

Figure 2.2 The restriction fragment length polymorphism method used on the R1197W site. A diagram illustrating the site of the mutation, the Eag1 restriction site formation in the presence of the wild-type tensin1 and the fragmented DNA bands expected to see upon restriction digest.

2.8.1.1 RNA isolation

To examine the prevalence of SNP among subjects, RFLP was used. Firstly, RNA was isolated using the RNeasy Plus kit and QIAShredder spin columns according to manufacturer's instructions. RNA was measured using the NanoDrop (Thermofisher) bioanalyser.

2.8.1.2 PCR primers

Tensin1 primers covering the region of interest were designed by myself. The polymorphic region was amplified using the following primer sequences: forward 5'-ATCTGCCCAGAGAAACTACCAGAGC-3' and reverse 5'-

ATCATCTGGTGATGGCTCAAACTG-3'. These primers are specific to tensin1 mRNA detecting the NM_022648 transcript and giving a product of 279 bp.

2.8.1.3 qRT-PCR for primer validation

To confirm single product amplification and specificity of the primers qRT-PCR was performed. qRT-PCR was performed using the 1-step method Brilliant III Ultra-Fast SYBR® Green qRT-PCR. 10 µl of 2 x SYBR® QRT-PCR mastermix, 7 µl of RNA-free water, 2.5 µl of the appropriate primers, 0.3 µl of Reference dye, 0.2 µl of 100 mM DTT and 1 µl of Reverse Transcriptase were added per reaction per well in a 96-well qRT-PCR plate. 1 µl of 100 ng/µl RNA concentration was added per reaction. All reactions were performed in triplicate. No-template and no-Reverse Transcriptase control were performed as well.

The plate was then centrifuged at 302 x g for 1 minute and then analysed in Mx3000P™ quantitative PCR machine which was set to read both ROX, the reference dye, and SYBR Green dye. The cycling conditions used for the protocol were:

Cycles	**Step**	**Duration of cycle**	**Temperature**
1	Initial Reverse Transcription (RT)	10 minutes	50°C
1	RT Inactivation	3 minutes	95°C

50	Denature	20 seconds	95°C
	Annealing	20 seconds	62°C
1	Melting curve	30 seconds 30 seconds 30 seconds 30 seconds	95°C 60°C 95°C 60°C

2.8.1.4 Restriction digest of PCR products

DNA was isolated from HASMCs and normal PCR process was followed. PCR products were analysed by restriction digestion with Eag1. The enzyme digested the PCR products containing the CGG codon, the mutation. 2 µl of 10x Reaction buffer (ER0331, Life Technologies), 2 µl of dH_2O, 15 µl of amplified DNA and 1 µl of EagI restriction enzyme (ER0331, Life Technologies) were added per reaction. The tubes were mixed thoroughly and incubated for one hour at 37°C.

2.8.1.5 Agarose gel

Firstly, an agarose gel was run in order to confirm that the required product was amplified in the qRT-PCR reaction. Then, non-digested and digested DNA products were run on an agarose gel to investigate whether the mutation is present or not. The -1197TT genotype produced one band (278bp), the -1197CC genotype produced two bands (214 and 64bp) and the heterozygotes displayed

all three bands (278, 214 and 64bp) (**Figure 2.2**). A pEGFP C1 Tensin1 construct containing the wild-type, kindly given by Dr Katherine Clark, and the pEGFP C1 Tensin1 containing the SNP, that has been generated (Section 2.7), were used to confirm validity of the RFLP protocol. ImageJ was used to further establish the presence of the different tensin1 phenotypes and assess efficient digestion by intensity measurement.

2.8.2 Collagen gel contraction assay

Collagen gel contraction assay was performed to investigate the effect of the R1197W SNP on the contractility of human airway smooth muscle cells. The assay was performed as described in Section 2.6.4.

2.9 Effect of Overexpression of Tensin1 Containing the Wild-Type and the SNP on Cell Function

2.9.1 Transfection of the pEGFP C1 constructs containing the wild-type and SNP tensin1

Lipofection was used to transfect cells with the pEGFP C1 constructs. This experiment was performed on HASMCs derived from healthy and COPD subjects. One day prior to transfection, HASMCs were seeded into 6-well plates at a density of 300 000 cells/well in antibiotic-free medium. 24 hours later, 5 µg of pEGFP C1 construct was diluted in 150 µl antibiotic and serum-free medium and mixed by pipetting. Separately, 5 µl Lipofectamine LTX and 5 µl of PLUS reagent (15338100, Life Technologies) were mixed with 150 µl antibiotic and serum-free medium and incubated for 5 minutes at room temperature. The two solutions were then mixed together and incubated for 25 minutes at room temperature to allow the formation of transfection complexes. During this incubation, medium from the cells was replaced with 1.70 ml antibiotic and serum-free medium. Finally, transfection complexes were added drop-wise to the cells to give a total volume of 2 ml and cells were cultured at 37°C. After 4 hours, medium was replaced with antibiotic-free medium for 24 hours. Transfection efficiency was confirmed by qRT-PCR and immunofluorescence. A non-transfected control was used along experiments.

2.9.2 Cell survival/proliferation assay

The MTS assay (G3582, Promega) was used to assess viability and proliferation of the cells following transfections. 24 hours after transfection, cells were collected and 2 x 10^3 cells were plated into 96-well plates in culture media in the absence of antibiotics overnight. 20 µl of CellTiter 96 Aqueous one solution containing the tetrazolium compound MTS, [3-(4,5-dimethylthiazol-2-yl)-5-(3-carboxymethoxyphenyl)-2-(4-sulfophenyl)-2H- tetrazolium] (Promega) was added to each well. The optical density (OD) at 490nm was determined with a spectrophotometer. Each experimental condition was run in triplicate. This experiment was performed on healthy (n=3) and COPD subjects (n=3).

2.9.3 Collagen gel assay

Following the transfection of HASMCs derived from healthy and COPD subjects with the pEGFP C1 containing the wild-type (homozygous –CC-) and SNP (homozygous –TT-) tensin1, the collagen gel assay was performed. Assays were performed as described in Section 2.6.4. After polymerisation, the gels were then detached from the plate and resuspended in 1ml of serum-free medium or serum-free medium containing bradykinin (1 nM, Sigma) where appropriate. Pictures were taken at 0, 1, 2, 3, 4, 18, 24 and 48 hours. The percentage of contraction was quantified using the ImageJ software. This experiment was performed on healthy (n=3) and COPD subjects (n=3).

2.10 Statistical Analysis

Statistical analysis was performed using GraphPad Prism 6 (GraphPad software, San Diego, CA, USA). Data are presented as mean±SEM. Parametric data were analysed by ANOVA across groups and t-tests between groups. Mann-Whitney and Kruskal Wallis tests were used to analyse non-parametric data. Between groups Tukey's and Dunnett's post tests were used for comparison to a control and multiple comparisons respectively. Correlations were assessed using the Spearman rank and Pearson's correlation tests.

Chapter 3: Results

3.1 Localisation of Tensin1 in Airway Tissue

3.1.1 Clinical characteristics

Tensin1 localisation was examined in n=9 healthy and n=10 asthmatic endobronchial biopsies, and n=11 healthy and n=13 COPD lung resection samples. The clinical characteristics of the healthy controls, COPD and asthma subjects used for immunohistochemistry are summarized in **Table 3.1**. The most noteworthy features are the reduced lung function, lower FEV_1 predicted % and FEV_1/FVC ratio, and the smoking status of the COPD subjects when compared to healthy controls.

	Lung resections		Biopsies	
	Healthy Lung resections (n=11)	COPD Lung resections (n=13)	Healthy Biopsies (n=9)	Asthmatic Biopsies (n=10)
Age (y), mean±SEM	66.9±2.5	74.3±2.6	31.6±5.3	37.7±4.6
Gender (M/F)	8/3	9/4	5/4	4/6
FEV_1(% predicted)	83.3±2.8	68.2±3.0	102.2±4.9	79.4±7.1
FEV_1/FVC ratio (%)	79.8±2.0	60.0±2.4	81.4±3.5	66.9±4.4
Pack Years (y)	15.5±4.6	34.7±4.6	0.4±0.4	0.9±0.8
PC20 methacholine (mg/ml), geometric mean (95% CI)	ND	ND	>16	6.8 (2.9-10.5)
Reversibility to β-agonist (%)	ND	ND	1.6±1.6	19.7±9.4
Serum IgE (KU/L), geometric mean (95% CI)	ND	ND	43.8 (16.2-71.4)	172.1 (97.5-246.6)
Inhaled Corticosteroid dose (µg)	0	0	0	192.9±56.0
Severity	NA	GOLD 1 (2) & GOLD (11)	NA	Mild (3), Moderate (2) & Severe (5)
Age of Onset	NA	ND	NA	20.3±5.4

Table 3.1: Clinical characteristics of healthy controls, COPD and asthmatic subjects used for immunohistochemistry.

3.1.2 Testing different tensin1 antibodies and staining techniques

Immunohistochemistry was performed first to examine whether tensin1 is expressed in human lung tissue. Firstly, titration of the tensin1 antibodies was performed to decide on the appropriate antibody concentration to be used, and then a decision was needed on which staining method and which antibody was the best to use to acquire specific immunostaining. Briefly, two different tensin1 antibodies were tested. The two tensin1 antibodies from Sigma-Aldrich (SAB4200283) and Santa-Cruz (sc-28542) revealed similar staining (**Figure 3.1** & **Figure 3.2**). Two different staining methods, the avidin-biotin and the Dako EnVision, were tested with both tensin1 antibodies. Tryptase immunostaining was undertaken as a positive control for the immunostaining process. Cellular staining appeared cleaner and more consistent with the tensin1 antibody from Sigma-Aldrich using the Dako EnVision staining technique (**Figure 3.3**).

Once preliminary immunostaining had been undertaken to identify cells that might express tensin1 in human airways, further antibody validation was undertaken using western blot, immunoprecipitation and siRNA knockdown as described in Section 3.2.3 and Section 3.4.2.

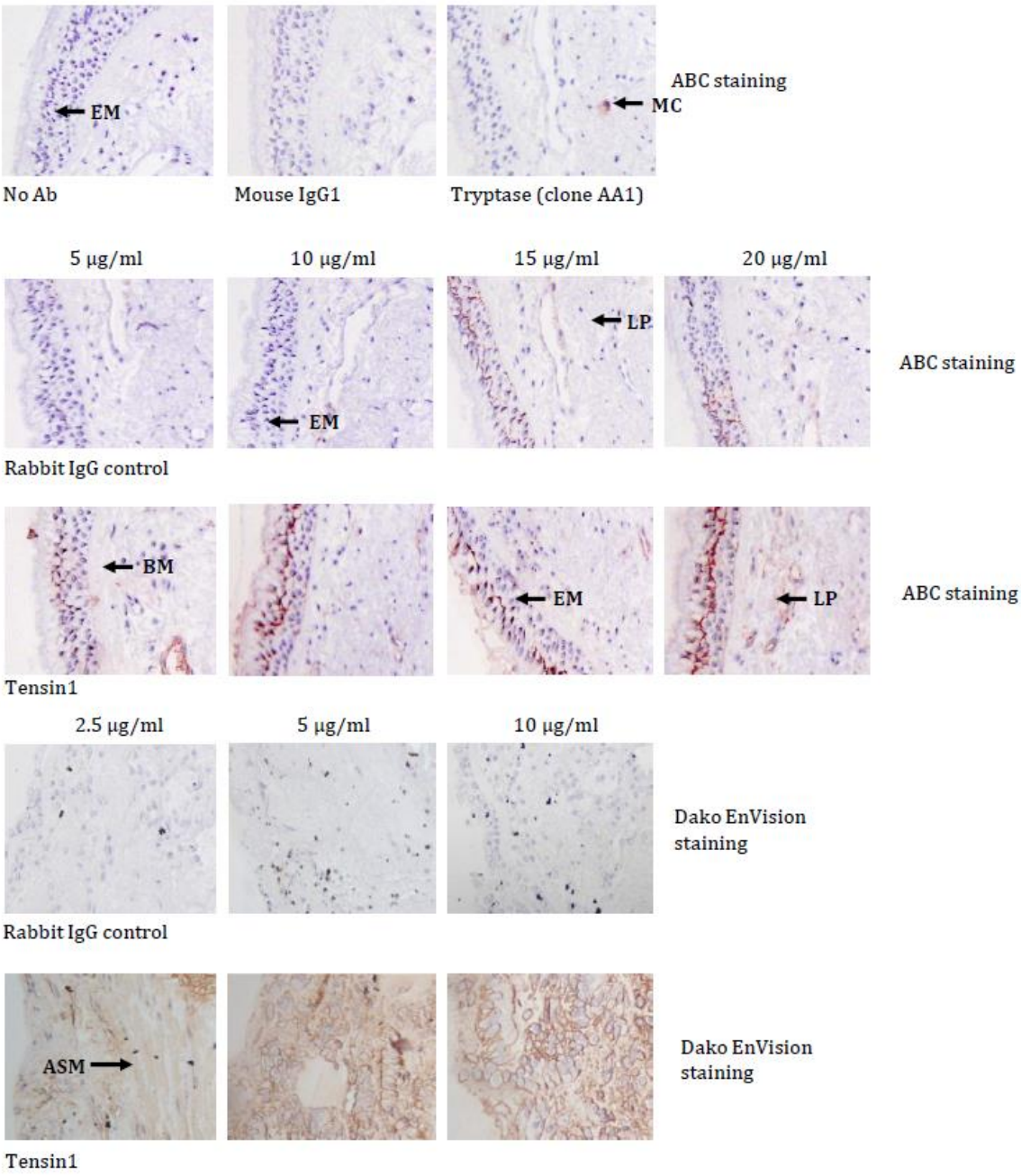

Figure 3.1: Titration of the tensin1 antibody (SAB4200283/Sigma-Aldrich) using both staining techniques. Staining was observed in the epithelium, lamina propria and connective tissue in both staining techniques. Different concentrations were used in order to titrate the antibody. The most appropriate concentrations were 5 µg/ml and 2.5 µg/ml for the avidin-biotin and Dako EnVision staining techniques respectively. ASM: airway smooth muscle; BM: basal membrane; EM: epithelial membrane; LP: lamina propria; MC: mast cell.

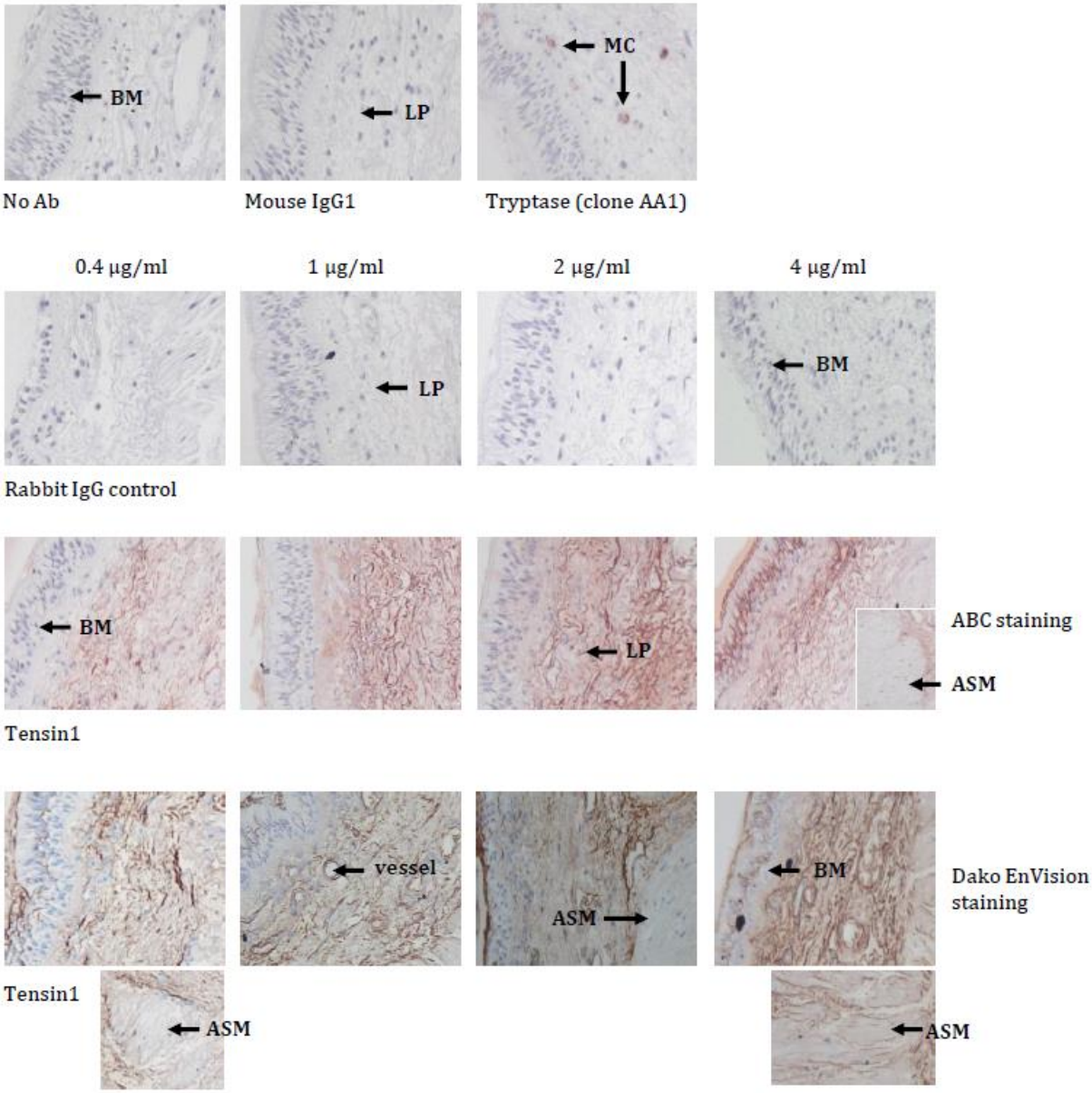

Figure 3.2: Titration of the tensin1 antibody (sc-28542/Santa-Cruz) using both staining techniques. Staining was observed in the epithelium, lamina propria and connective tissue in both staining techniques. Different concentrations were used in order to titrate the antibody. The most appropriate concentrations were 4 µg/ml and 1 µg/ml for the avidin-biotin and Dako EnVision staining techniques respectively. ASM: airway smooth muscle; EM: epithelial membrane; LP: lamina propria; MC: mast cell.

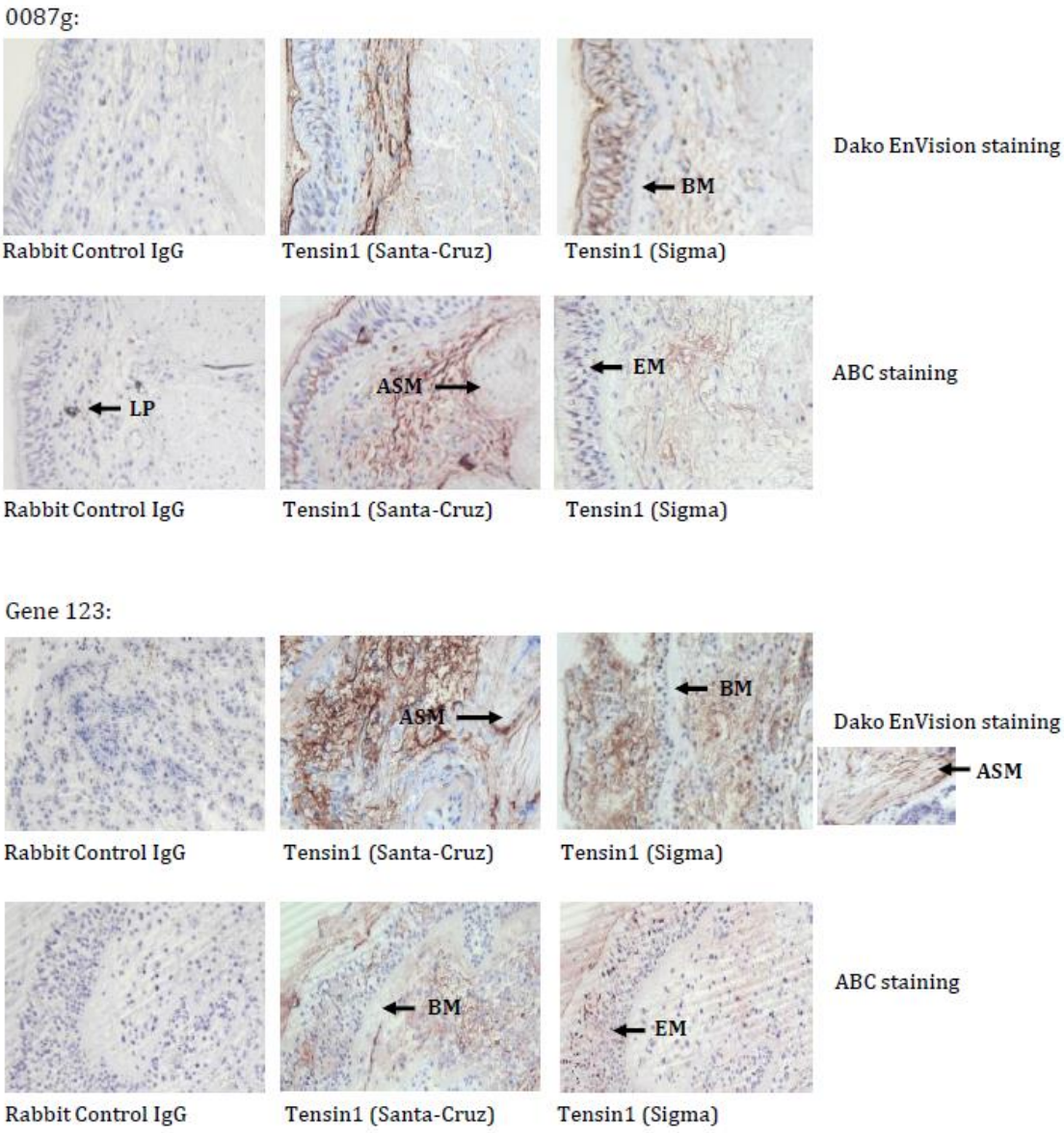

Figure 3.3: Comparison of the two staining techniques, avidin-biotin and Dako EnVision staining and also the two tensin1 antibodies (SAB4200283/Sigma-Aldrich and sc-28542/Santa-Cruz). Consistent and structural cell staining was observed best with the Dako EnVision staining method and therefore the Dako EnVision staining method was chosen for further experiments. The tensin1 antibody from Sigma showed consistent and specific staining for the epithelium and airway smooth muscle and therefore solely only this antibody was used for further immunohistochemical staining. ASM: airway smooth muscle; BM: basal membrane; EM: epithelial membrane; LP: lamina propria.

3.1.3 Tensin1 immunostaining in healthy and asthmatic bronchial biopsies and healthy and COPD lung resections

Immunostaining was performed using the tensin1 antibody from Sigma-Aldrich (SAB4200283) and the Dako EnVision staining technique. Representative images of the immunostaining are shown in **Figure 3.4** and **Figure 3.5**. The no-antibody and mouse IgG immunoglobulin control sections did not show any staining, whereas the positive control tryptase sections showed mast cell staining as expected. Immunostaining for tensin1 on bronchial biopsies and lung resections from asthmatic and COPD donors respectively and respective healthy controls was evident. Tensin1 immunoreactivity was detected in the apical bronchial epithelium, cells within the lamina propria and airway connective tissue, ASM cells and vessels.

Quantification of the tensin1 immunostaining was performed using the thresholding technique based on hue saturation and intensity (HSI), which has been previously validated (Shikotra et al. 2012, Siddiqui et al. 2008a). Tensin1 immunostaining was compared to healthy controls using the nonparametric Mann-Whitney U test. As shown in **Figure 3.6**, a significant increase in tensin1 immunostaining was detected in the ASM (**p=0.0073) and lamina propria (*p=0.0121) in COPD donors when compared to healthy controls. However, no difference in the tensin1 immunostaining was observed in healthy and asthmatic biopsies (**Figure 3.6**).

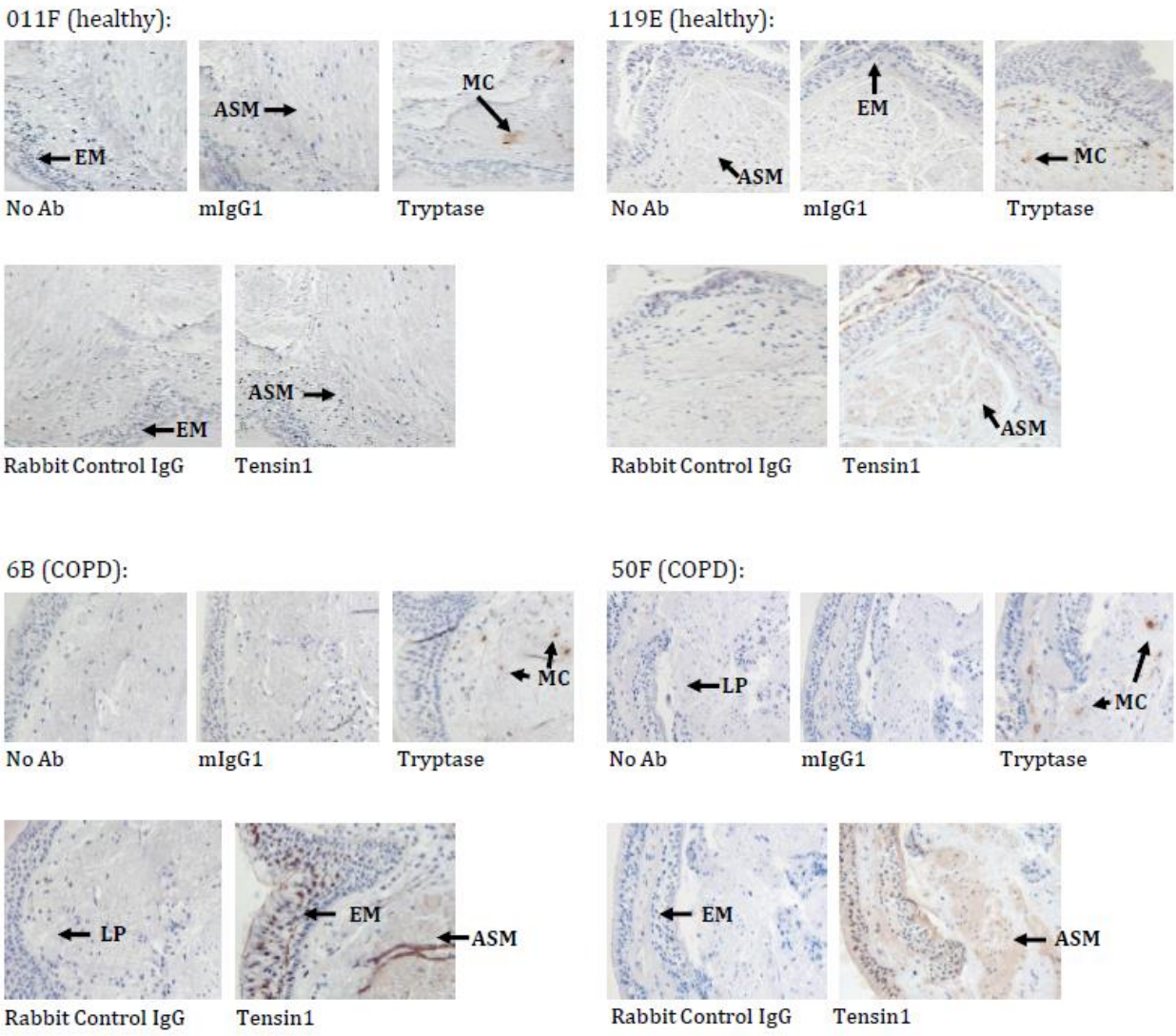

Figure 3.4: Tensin1 immunohistochemistry staining in healthy and COPD lung resections. Examples of tensin1, tryptase positive control, and isotype control immunostaining in lung resections from COPD and healthy controls. ASM: airway smooth muscle; EM: epithelial membrane; LP: lamina propria; MC: mast cell.

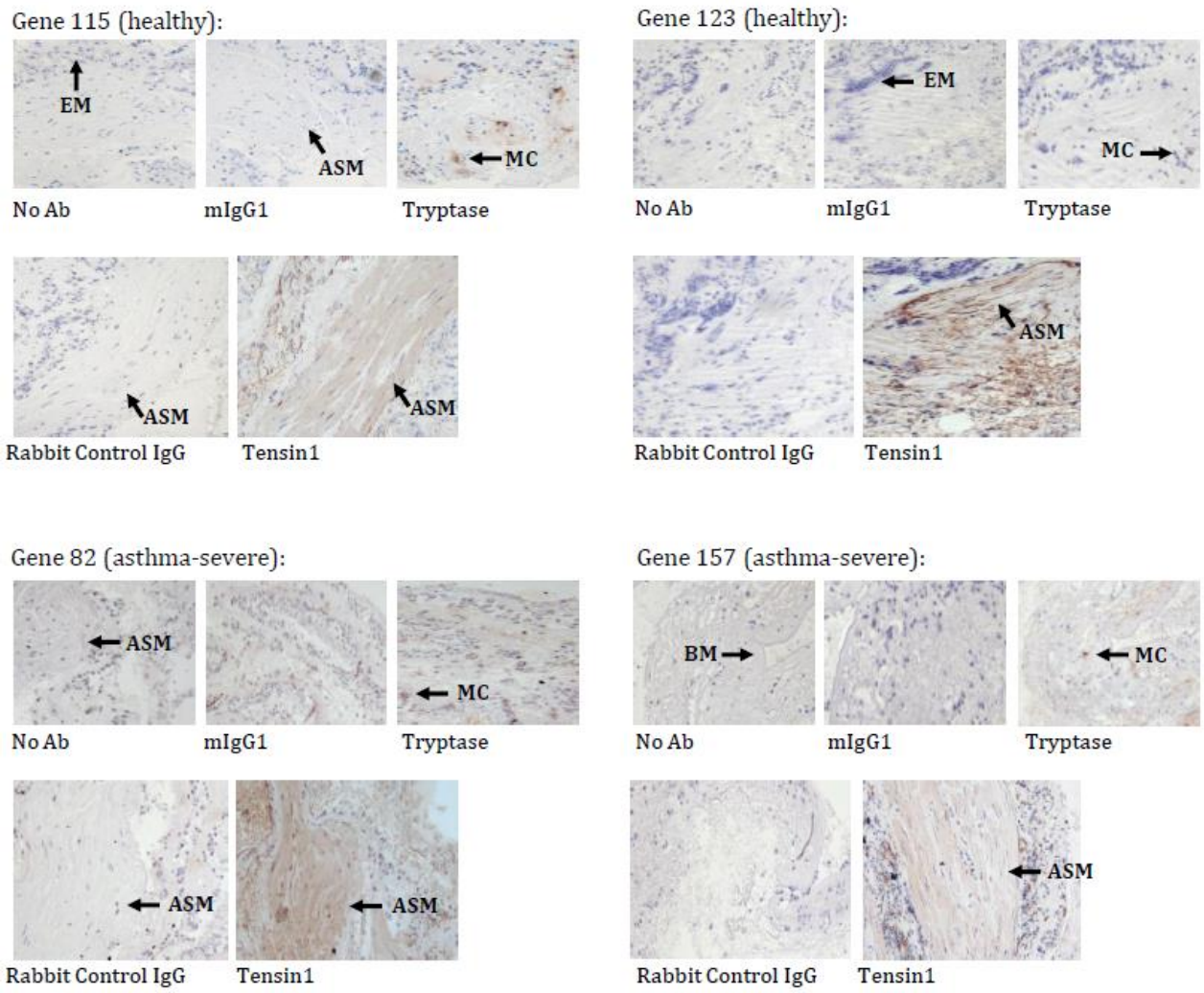

Figure 3.5: Tensin1 immunohistochemistry staining in healthy and asthmatic biopsies. Representative images of tensin1 immunostaining in healthy and asthmatic bronchial biopsies, along with the appropriate negative and positive controls. ASM: airway smooth muscle; BM: Basal membrane; EM: epithelial membrane; LP: lamina propria; MC: mast cell.

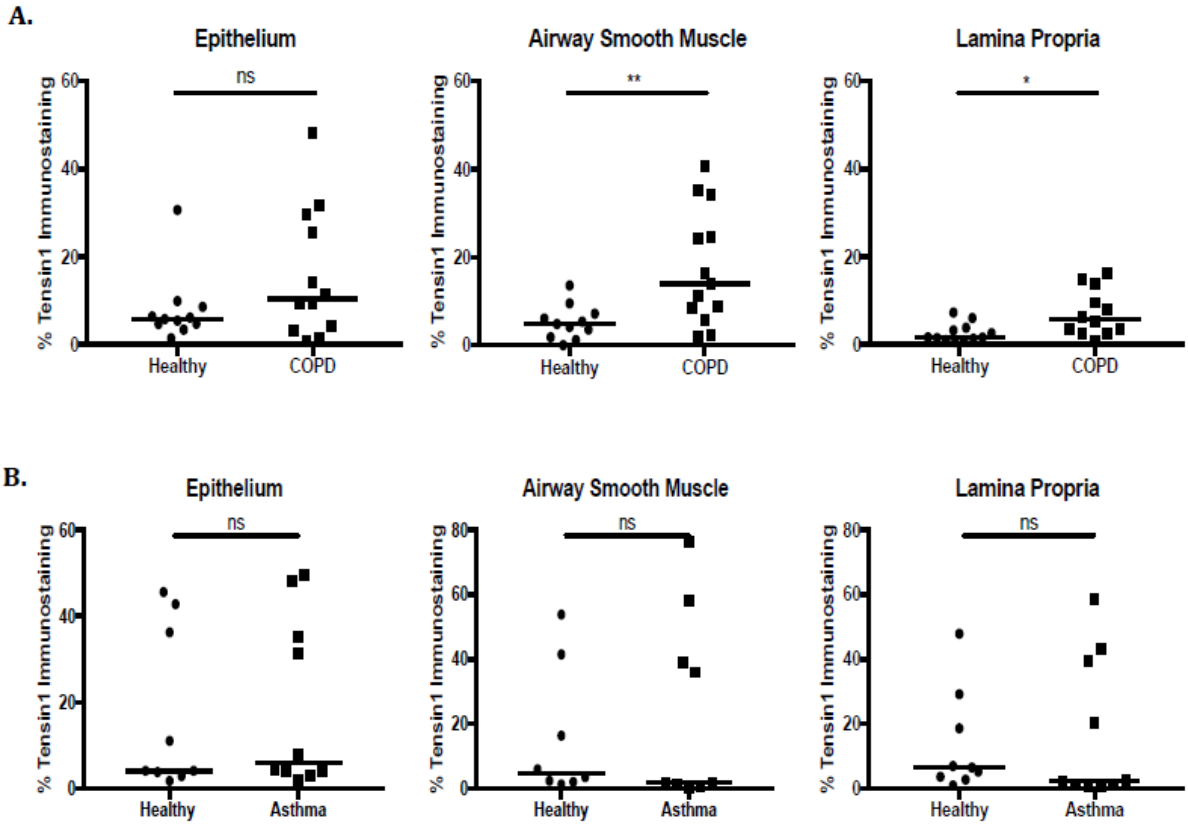

Figure 3.6: Quantification of tensin1 immunostaining in healthy and COPD lung resections and healthy and asthmatic biopsies. (A) Extent of tensin1 immunostaining in epithelium, airway smooth muscle and lamina propria was assessed based on threshold measurements. Increased tensin1 immunostaining was observed in the airway smooth muscle and lamina propria in COPD subjects when compared to healthy controls. **(B)** No difference in the tensin1 immunostaining was observed in any of the areas in asthmatic subjects when compared to healthy controls (*$p<0.05$, **$p<0.01$).

3.1.4 Tensin1 immunostaining is not correlated with FEV_1 and FEV_1/FVC

To help evaluate the role of tensin1 in COPD, correlation between tensin1 staining and FEV_1 % predicted and FEV_1/FVC ratio were examined using the Spearman rank correlation test. There was no significant correlation between the tensin1 immunostaining in epithelium, airway smooth muscle or lamina propria with the FEV_1 % predicted value or FEV_1/FVC ratio (**Figure 3.7** & **Figure 3.8**).

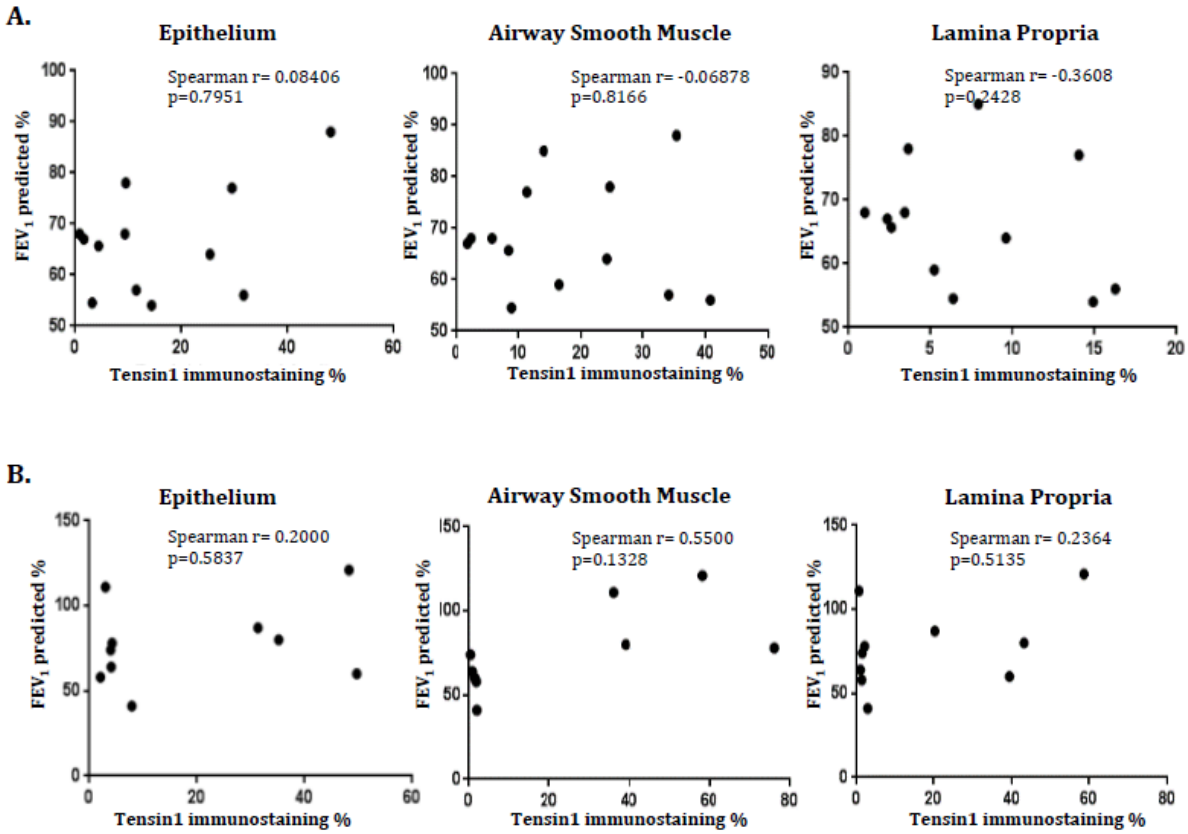

Figure 3.7: Tensin1 immunostaining did not correlate with FEV_1 predicted %. Correlation between the tensin1 immunostaining and FEV_1 predicted % was tested. The spearman rank correlation test was used. A p value <0.05 was considered as a statistical significance value. No correlation was detected between tensin1 immunostaining and FEV_1 predicted % in either COPD or asthmatic subjects.

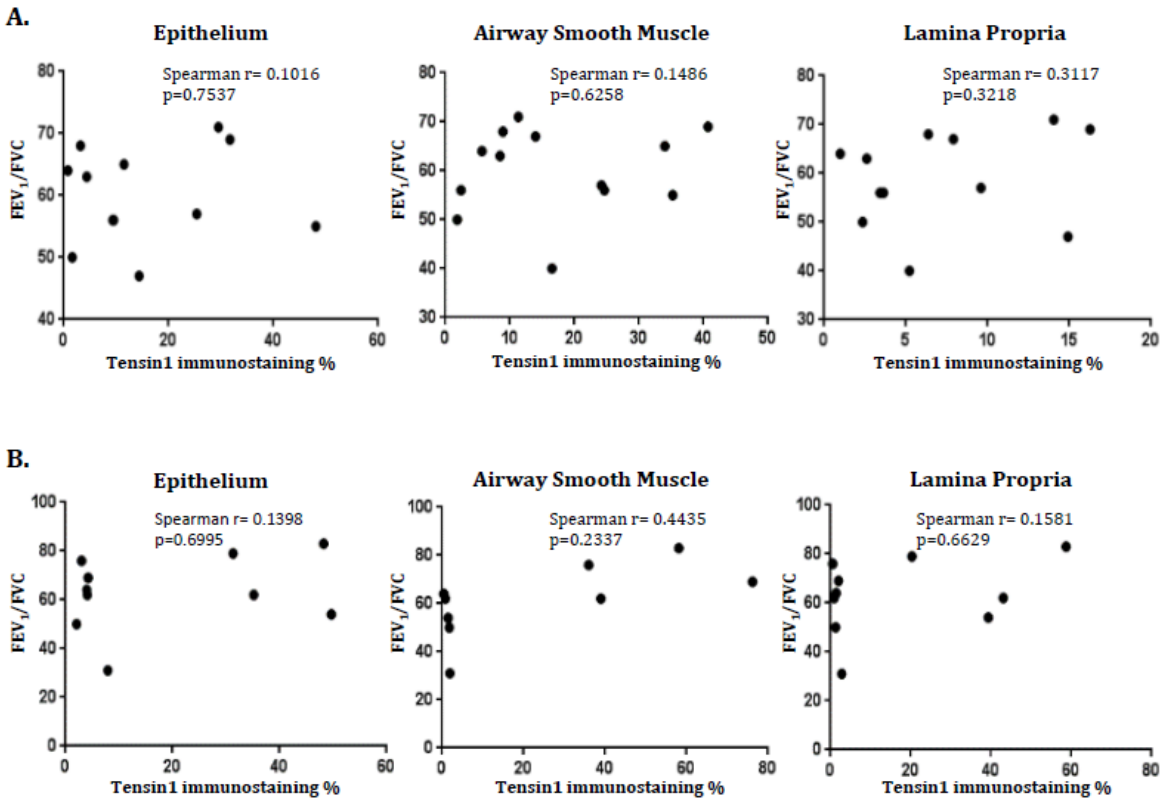

Figure 3.8: Tensin1 immunostaining did not correlate with FEV_1/FVC ratio. Correlation between the tensin1 immunostaining and FEV_1/FVC ratio was tested. The spearman rank correlation test was used. A p value <0.05 was considered as a statistical significance value. The extend of tensin1 immunostaining did not correlate with FEV_1/FVC ratio in either COPD or asthmatic subjects.

3.2 Tensin1 Expression in Human Airway Structural Cells

3.2.1 Clinical characteristics

The clinical characteristics of the subjects used for the cell culture experiments on HASMCs, HBECs and HLMFs are summarised in **Table 3.2**. As part of this study, material became available from patients suffering from interstitial pulmonary fibrosis (IPF) that could be used as clinical control samples to study fibrotic markers. These patients' clinical data can be found in **Table 1** (Appendix). The recorded data include age, gender, lung function (FEV_1 % predicted, FVC and FEV_1/FVC ratio), treatment, severity and age of onset. Again, the most noteworthy feature is the reduced lung function, lower FEV_1 % predicted/lower FEV_1 and FEV_1/FVC ratio in COPD, asthma and IPF subjects when compared to healthy controls.

	HASMCs			HBECs		
	Healthy	COPD	Asthma	Healthy	COPD	Asthma
Age (y), mean±SEM	42.5±4.7	69.7±1.5	44.5±5.2	45.3±7.9	68±2	55.3±1.1
Gender (M/F)	5/7	7/3	6/3	4/6	4/6	3/3
FEV_1(% predicted), mean±SEM	95.6±3.2	54.4±5.4	96.5±4.8	101.2±2.3	65.1±5.5	79.9±16.9
FEV_1/FVC ratio (%), mean±SEM	80.2±1.5	53.7±3.1	79.1±2.4	83.12±3.9	52.3±7.8	60.5±6.6
Pack Years (y), mean±SEM	1.7±0.9	41.7±4.5	6.1±5.4	5±5	37.8±10.3	0
PC20 methacholine (mg/ml), geometric mean (95% CI)	9.3 (3.9-14.6)	ND	4.3 (1.3-7.3)	17.9 (16.4-19.4)	ND	0.8 (-0.2-1.86)
Reversibility to β-agonist (%), mean±SEM	NA	ND	-1.3±2.4	NA	ND	ND
Serum IgE (KU/L), geometric mean (95% CI)	4.9 (4.2-5.5)	ND	498 (396.3-699.6)	52.3 (-5.7-110.4)	32.9 (5.2-60.6)	131.1 (41.9-220.3)
Inhaled Corticosteroid dose (µg), mean±SEM	0	500	633.3±190.5	0	291±295.6	1325±550
Severity	NA	GOLD 1 – GOLD 4	GINA 1 – GINA 5	NA	GOLD 1 – GOLD 3	GINA 1 – GINA 5
Age of Onset, mean±SEM	NA	57±2.3	31.5±3.6	NA	37±16.5	44±13.9

Table 3.2: Clinical characteristics of healthy controls, COPD and asthmatic subjects used for cell culture studies.

3.2.2 HASMCs, HBECs and HLMFs express tensin1 at the mRNA level

Tensin1 expression at the mRNA level was examined via qRT-PCR in the presence of SYBR green fluorescent dye. Primers specific to TNS1 and β-actin were used for this purpose. Fluorescence intensity directly correlates to the amount of dsDNA produced and therefore amplification efficiency of the primers was tested by plotting the threshold cycle (C_T) against RNA samples of known concentration. Amplification effiency of both primer pairs was ~100% suggesting that any difference in the C_T value correlates to the amount of the gene present in the sample and therefore that any difference in healthy and disease samples is reflecting the difference in abundance of tensin1 transcription (**Figure 3.9**).

3.2.2.1 Evidence for mRNA expression of tensin1

Based on the immunostaining results, three different cell types, HASMCs, HBECs and HLMFs, were tested for tensin1 gene expression. Tensin1 mRNA was expressed in all three cell types. Relatively low expression of tensin1 mRNA was detected in HBECs compared to HASMCs and HLMFs, which showed a similar level of expression. The PCR products were also run in a 1.5% agarose gel to confirm the size of the product and that only one product was amplified which was indeed the case. The PCR templates were also sequenced and confirmed that tensin1 mRNA was the product that had been amplified (**Figure 3.10**). β–actin was consistent in all the donors and therefore was used as a housekeeping gene.

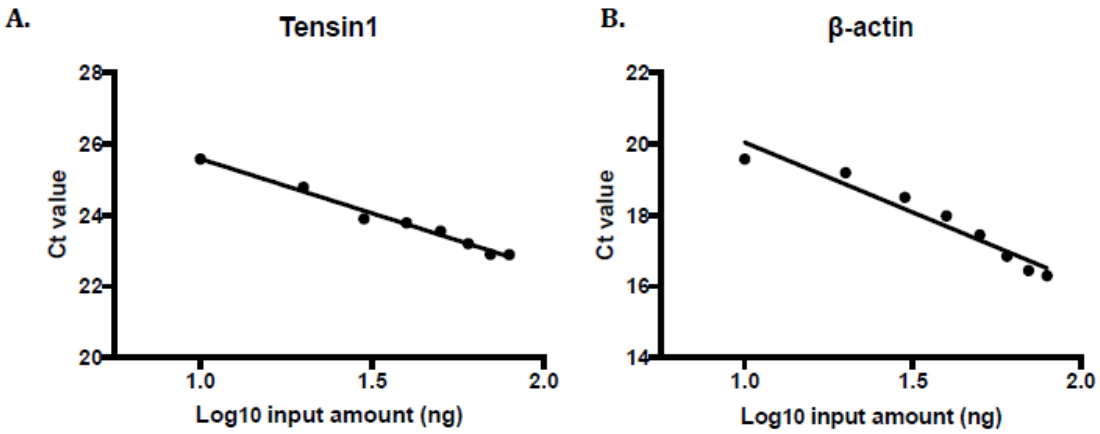

Figure 3.9: Validation of the amplification efficiency of the qPCR primers. The efficiency of TNS1 and housekeeping gene primer pairs were assessed using the standard curve method in which each primer pair was used to amplify RNA samples of known concentrations. Fluorescence intensity, Ct value, was plotted against Log_{10} input amount (ng). The two primer pairs amplified with similar efficiencies of approximately 100% suggesting their applicability in qPCR.

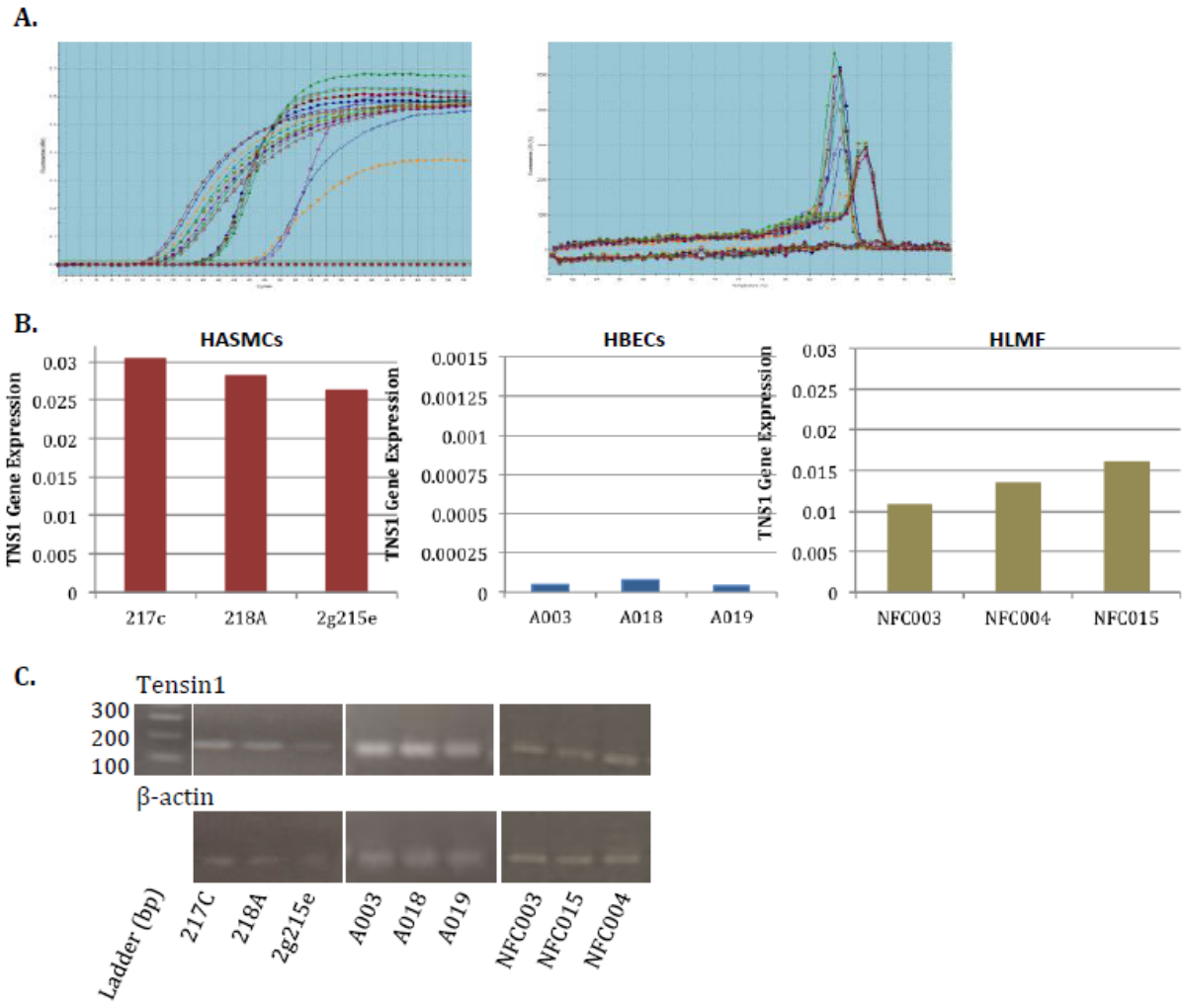

Figure 3.10: qRT-PCR showing expression of tensin1 in HASMCs, HBECs and human lung myofibroblasts (HLMF). (A) Tensin1 was detected in monolayers of primary HASMCs, HBECs and HLMF. qPCR was used to quantify tensin1 expression in health and disease. The amplification plot shows the fluorescence emission occurred during the qRT-PCR, which is proportional to the synthesised DNA. The dissociation curve illustrates a single peak suggesting specificity of the primers. **(B)** The relative amount of tensin1 expression was calculated using the 2^-(ΔCt) method. **(C)** Products from qRT-PCR for tensin1 were visualised on an agarose gel image to confirm size of the product amplified (TN1 PCR product size 166bp). β-actin (PCR product size 146bp) was used as the normalising control in all HASMCs, HBECs and HLMF.

3.2.2.2 Comparing tensin1 mRNA expression in health and disease subjects

Tensin1 mRNA expression was assessed in healthy and disease subjects in all three cell types. Tensin1 expression was compared to healthy controls using one-way ANOVA with Tukey's multiple comparison test. Firstly, expression was investigated in HASMCs, where seven donors were used from each phenotype (healthy, asthmatic and COPD). A similar level of tensin1 mRNA expression was detected in HASMCs obtained from COPD and asthmatic donors when compared to healthy controls (**Figure 3.11**). Tensin1 expression was also investigated in healthy (n=6), asthmatic (n=6) and COPD donors (n=6) in HBECs. Again, a very low level of tensin1 mRNA expression was observed in all the three subgroups (**Figure 3.12**). Additionally, expression was assessed in healthy (n=8) and IPF (n=8) donors in HLMFs. A significant decrease in tensin1 expression was observed in the IPF donors (*p=0.040) when compared to healthy controls (**Figure 1 (Appendix)**).

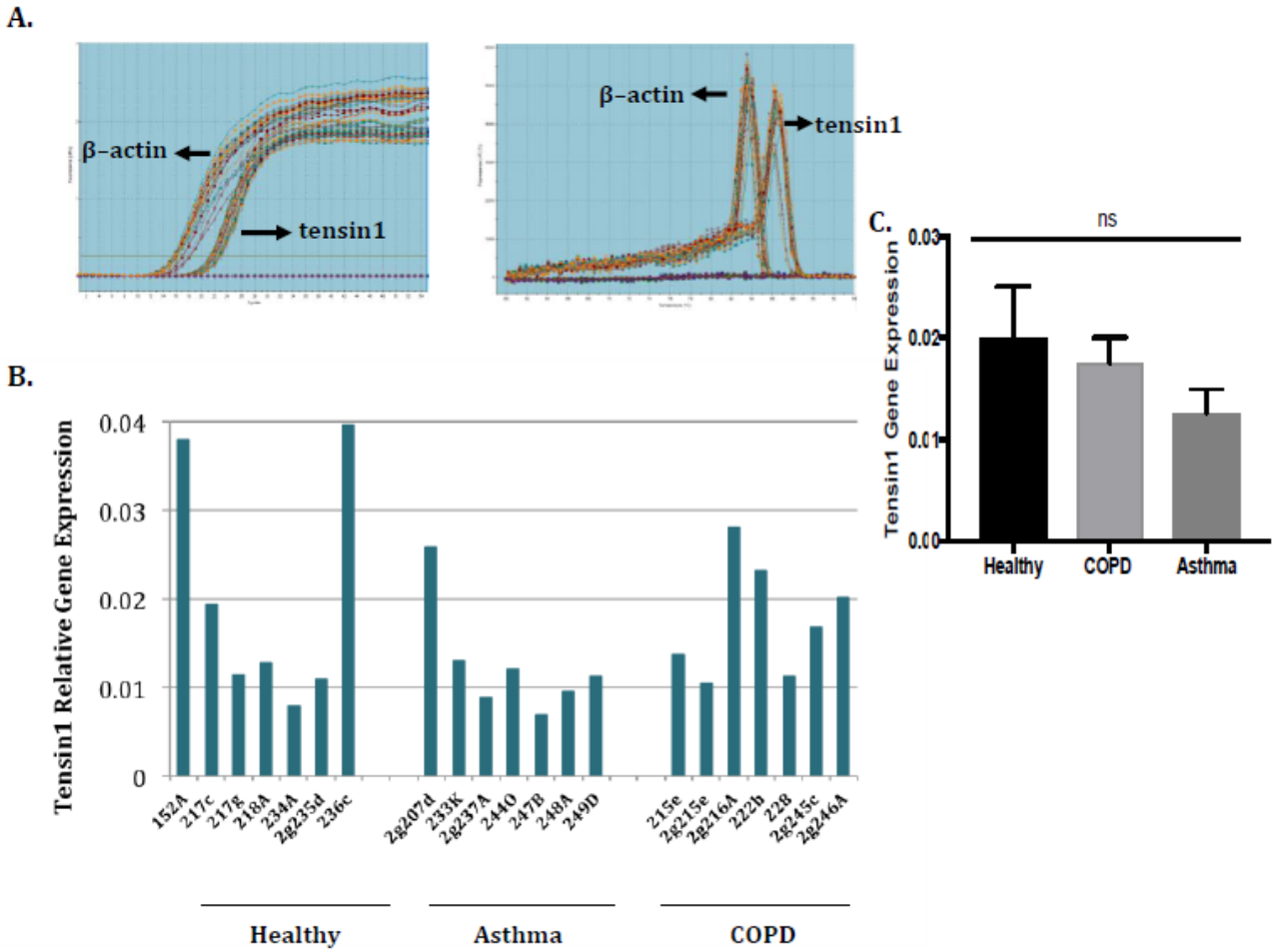

Figure 3.11: qRT-PCR showing expression of tensin1 in HASMCs. (A) Tensin1 was detected in monolayers of primary HASMCs isolated from both patients with COPD and asthma, and healthy controls, alongside the housekeeping gene β–actin. qPCR was used to quantify tensin1 expression in health and disease. Amplification curve shows the fluorescence emission occurred during the qRT-PCR, which is proportional to the synthesised DNA. Dissociation curve illustrates amplification of a single product during the reaction suggesting specificity of the primers. **(B)** The relative amount of tensin1 expression was calculated using the 2^-(ΔCt) method. **(C)** Graph shows the mean±sem relative tensin1 expression in healthy, asthmatic and COPD subjects in HASMCs.

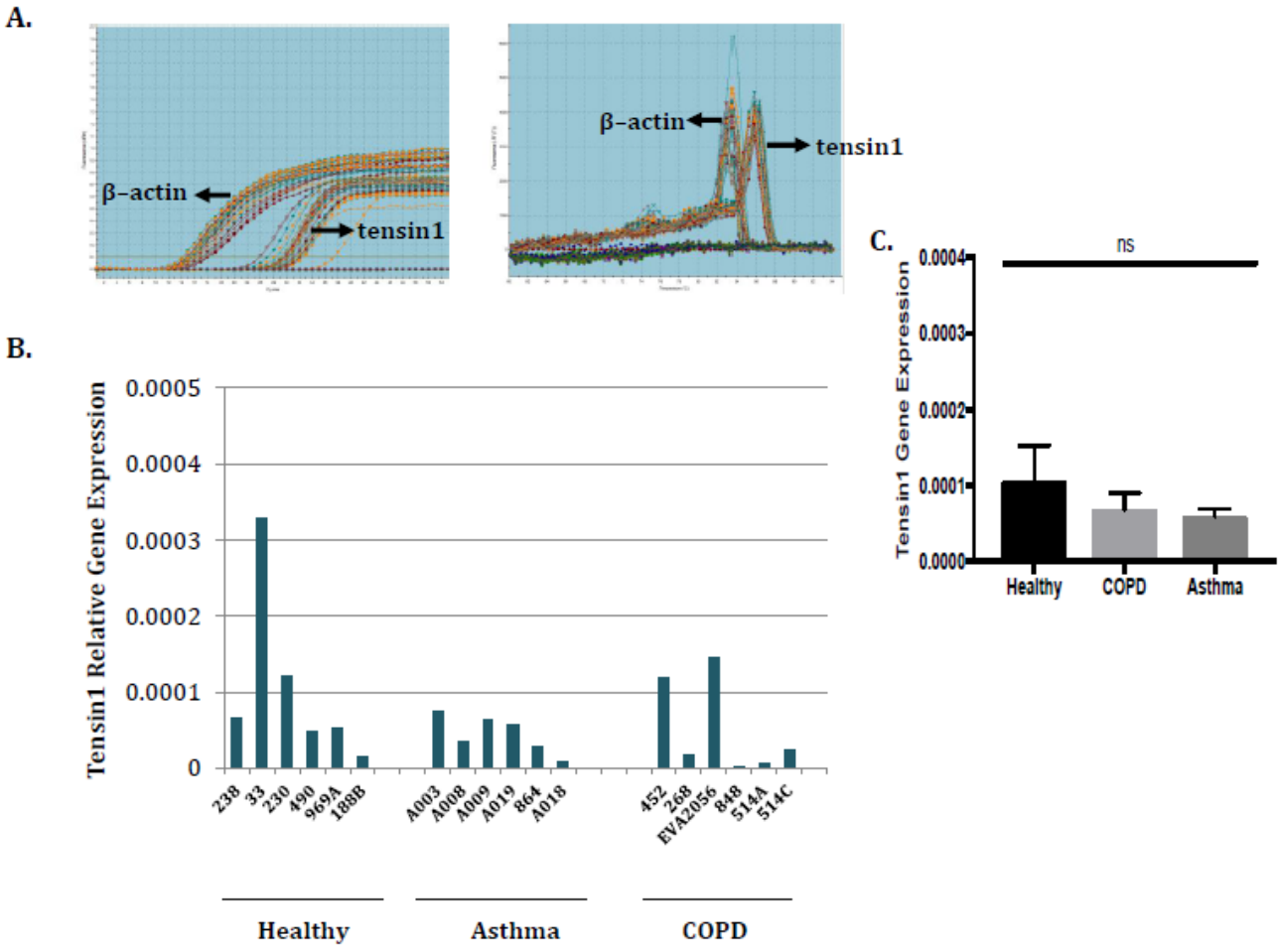

Figure 3.12: qRT-PCR showing expression of tensin1 in HBECs. (A) Tensin1 was detected in monolayers of primary HBECs isolated from both patients with COPD and asthma, and healthy controls, alongside the housekeeping gene β-actin. qPCR was used to quantify tensin1 expression in health and disease. Both, amplification and dissociation plots indicate the amplification of a single product. **(B)** The relative amount of tensin1 expression was calculated using the 2^-(ΔCt) method. **(C)** The mean±sem relative tensin1 expression in HBECs derived from healthy, asthmatic and COPD subjects is illustrated in this graph.

3.2.2.3 TGFβ1 increases tensin1 expression in HASMCs and HLMFs

The effect of TGFβ1 (an inflammatory and fibrotic growth factor) was also investigated with respect to tensin1 expression. Differences in tensin1 mRNA expression in TGFβ1- and non-stimulated cells were assessed using one-way ANOVA with Tukey's multiple comparison test. HASMCs and HLMF were stimulated with TGFβ1 (10 ng/ml) for 24 hours and expression was assessed using qRT-PCR. TGFβ1 stimulation resulted in a significant increase in tensin1 mRNA expression in HASMCs derived from both healthy (n=3) (**p=0.0042) and COPD (n=3) (*p=0.0418) subjects. Tensin1 mRNA expression was also significantly increased in TGFβ1-stimulated HLMF in both healthy and IPF subjects (n=3 of each) (**Figure 3.13** & **Figure 2 (Appendix)**).

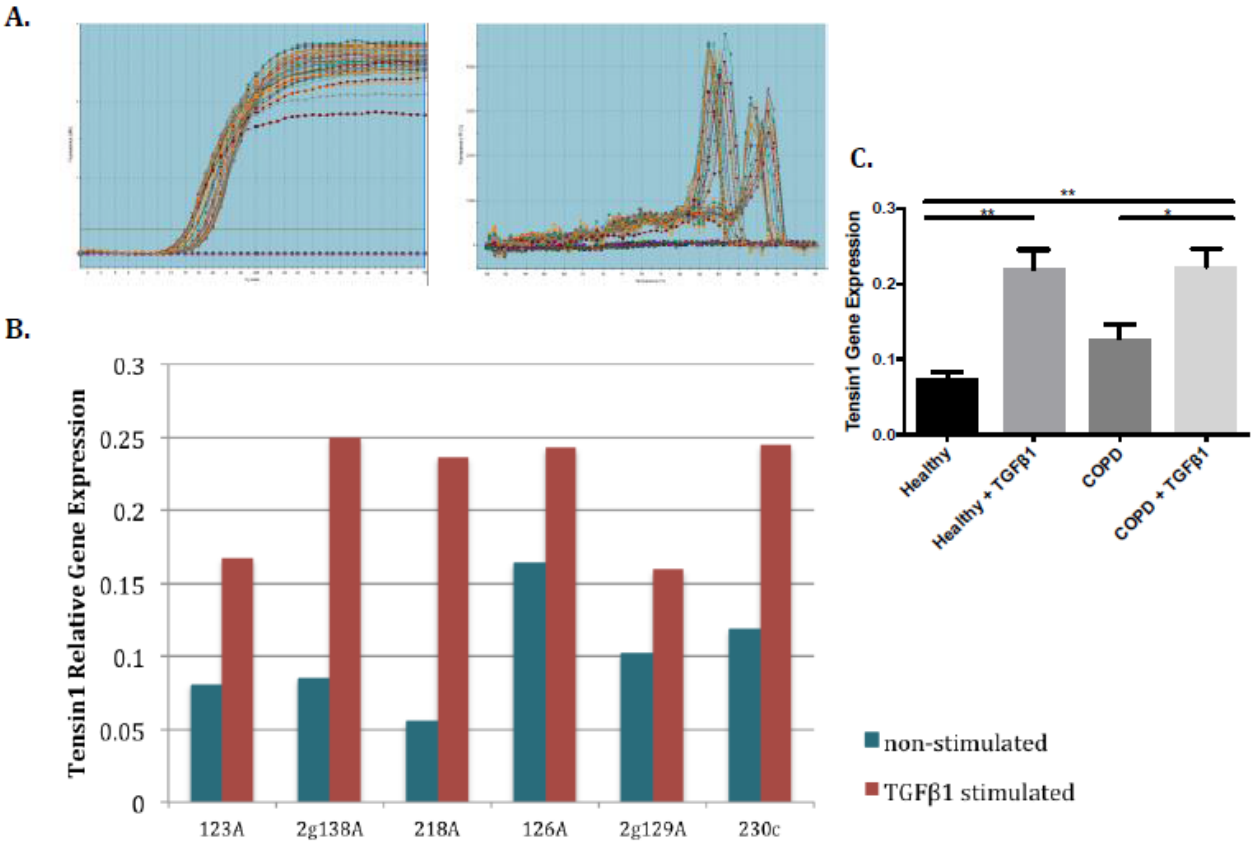

Figure 3.13: The effect of TGFβ1 on tensin1 mRNA expression in HASMCs. (A) Cells were stimulated with TGFβ1 for 24 h. qPCR was used to quantify tensin1 expression in health and disease after stimulation with TGFβ1. **(B)** The relative amount of tensin1 expression was calculated using the 2^-(ΔCt) method. **(C)** The mean±sem relative tensin1 expression in healthy and disease subjects in HASMCs is illustrated. TGFβ1 significantly increased tensin1 expression in HASMCs derived from both healthy and COPD subjects (*p<0.05, **p<0.01).

3.2.3 HASMCs express tensin1 protein

Tensin1 protein expression in HASMCs was first examined using western blot analysis. Multiple bands were detected in addition to the predicted band size of ~220kDa (**Figure 3.14**). Tensins are known to be highly susceptible to proteolytic degradation (Chuang, Lin and Lin 1995). To validate the tensin1 antibody further (Sigma-Aldrich), siRNA downregulation and immunoprecipitation were performed. Silencing markedly reduced tensin1 mRNA expression (**Figure 3.24**), and all the bands seen in the western blot analysis of non-transfected cells were eliminated with tensin1 downregulation. This provides confirmatory evidence that the Sigma-Aldrich antibody recognises tensin1 protein, and the additional bands on western blots were likely a result of proteolytic degradation (**Figure 3.14**). A more detailed description of the siRNA development and analysis on cell function is provided in Section 3.4.

Immunoprecipitation carried out using the two different tesnin1 antibodies (from Sigma-Aldrich and Santa-Cruz) and probed with the alternative antibody, generated a single band of ~220kDa molecular weight, further illustrating their specificity for tensin1 (**Figure 3.15**). Taken together, these data provide strong evidence that HASMCs express tensin1 protein, and that the tensin1 antibody (SAB4200283/Sigma-Aldrich) used for immunohistochemistry, western blotting and immunofluorescent staining (below) is selective for tensin1.

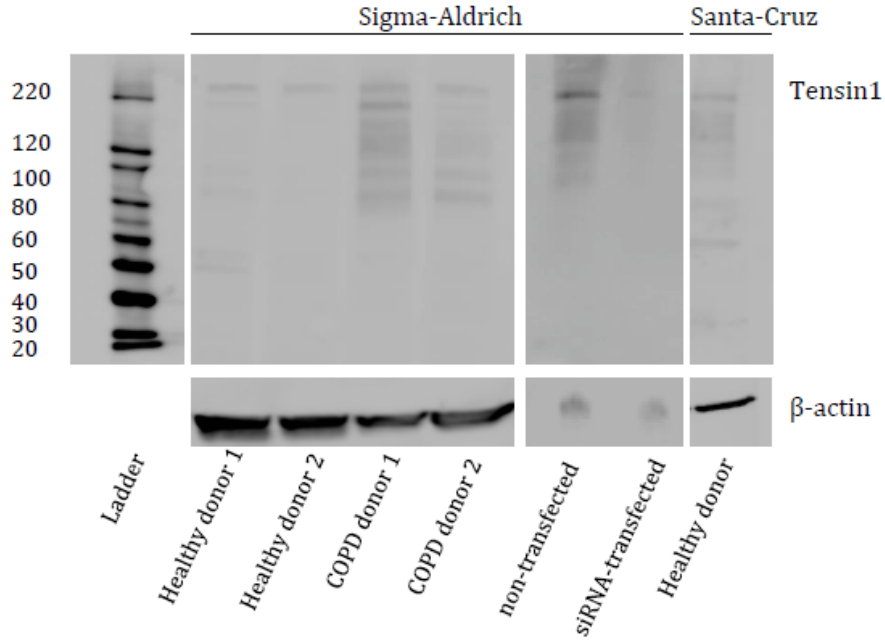

Figure 3.14: Tensin1 protein expression in HASMCs in health and disease. Tensin1 protein (size ~220kDa) was detected in monolayers of primary HASM isolated from both patients with COPD (n=2) and healthy controls (n=2), alongside the housekeeping protein β-actin using tensin1 antibody (Sigma-Aldrich). All the bands detected in the western blotting analysis in the non-tranfected cells were eliminated with tensin1 silencing. Similar tensin1 protein expression was detected using the tensin1 antibody from Santa-Cruz.

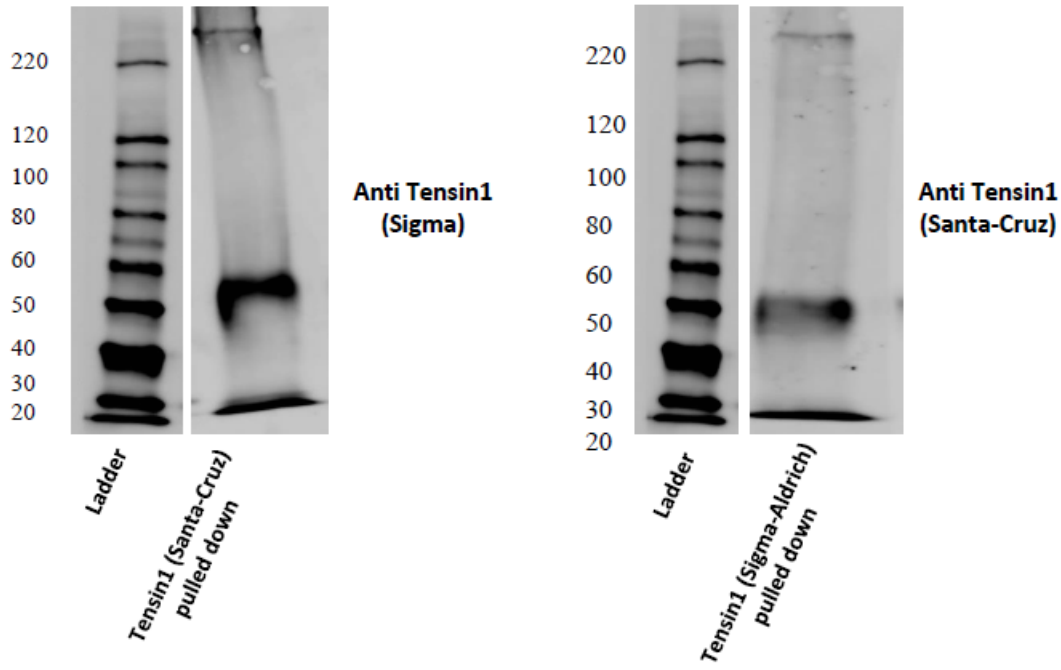

Figure 3.15: Immunoprecipitation to validate tensin1 antibody in HASMC lysates. Immunoprecipitation was carried out using two tensin1 antibodies (from Sigma-Aldrich and Santa-Cruz). A single band of ~220kDa molecular weight was detected with both antibodies further illustrating their specificity for tensin1.

Tensin1 protein expression and localisation was also examined using immunofluorescence staining on HASMCs derived from healthy controls (n=6) and COPD donors (n=6) using the tensin1 antibody from Sigma (SAB4200283). Immunostaining for αSMA and mouse and rabbit isotype controls were used as positive and negative controls. The rabbit and mouse isotype control slides did not produce any staining, whereas the αSMA actin showed cell staining as expected. For tensin1, both cytoskeletal and focal and fibrillar adhesion immunostaining were observed as illustrated in **Figure 3.16**. Quantification of the immunofluorescence staining was performed using the Cell F software. Tensin1 expression was analysed using nonparametric t-test (Mann-Whitney test). No difference was observed in the overall grey scale of tensin1 immunostaining between healthy and COPD-derived HASMCs as shown in **Figure 3.17**.

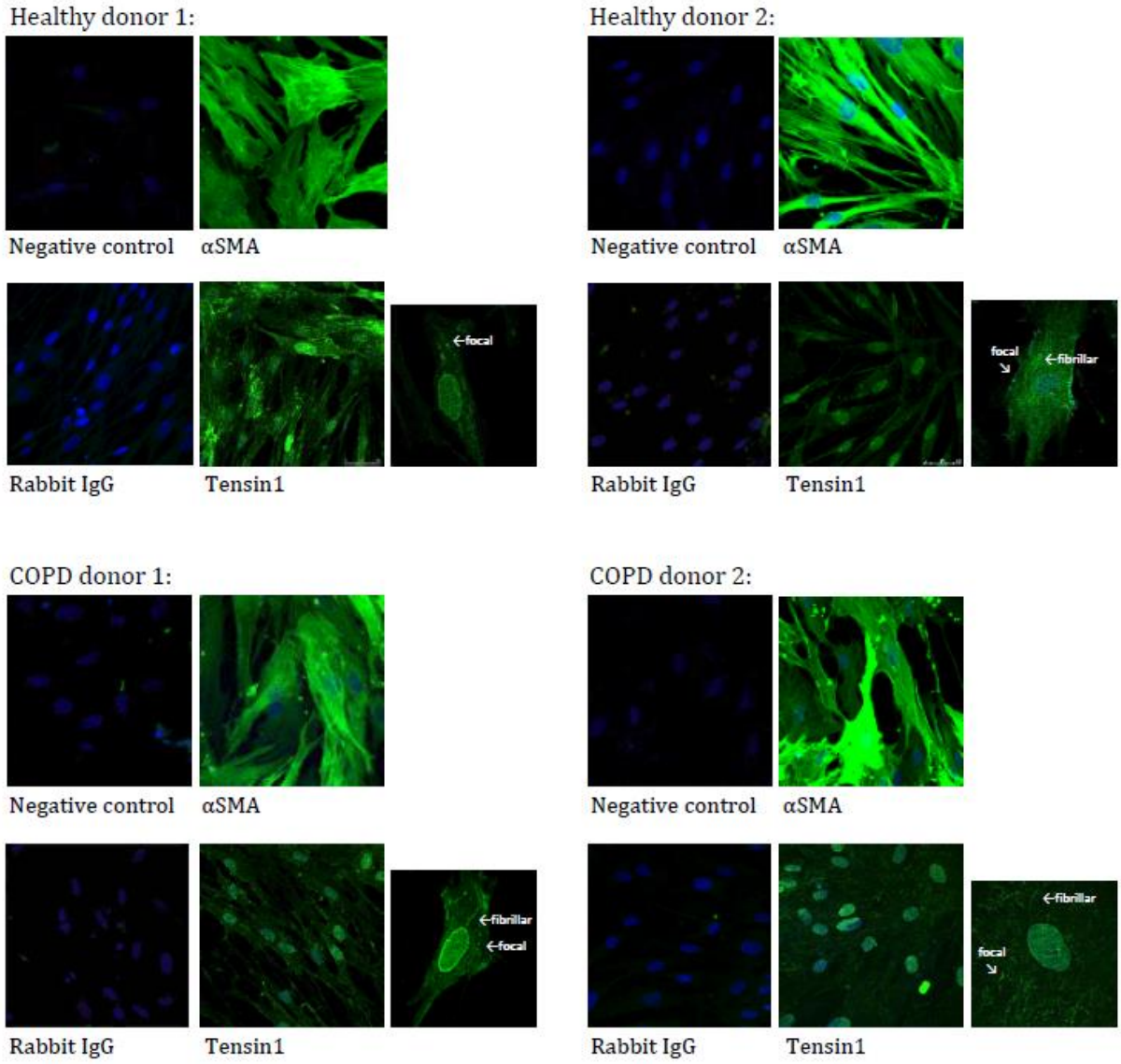

Figure 3.16: Tensin1 immunostaining in healthy and disease subjects. Tensin1 immunofluorescence staining was performed on HASMCs. Tensin1 protein localisation and expression was examined in n=6 healthy and n=6 COPD subjects.

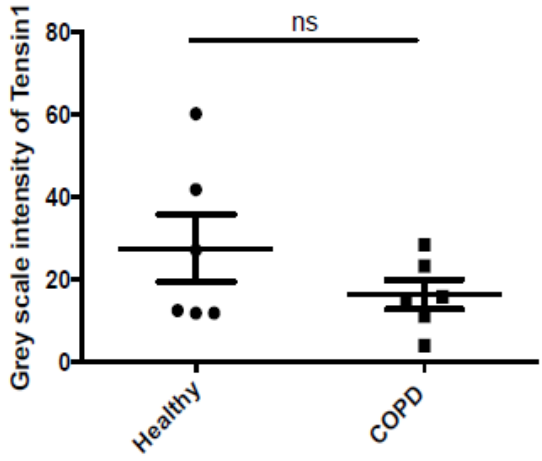

Figure 3.17: No difference in the tensin1 immunostaining in healthy and disease subjects. HASMC tensin1 expression was measured by grey scale intensity in n=6 healthy and n=6 COPD subjects. No difference was observed in the grey scale intensity of tensin1 immunostaining in the two phenotypes (mean ± sem).

The effect of TGFβ1 and fibronectin on tensin1 immunostaining was also examined. Slides were coated with human recombinant fibronectin prior to seeding and HASMCs were then seeded and stimulated with TGFβ1 (10 ng/ml) for 24 h. Although, stimulation with TGFβ1 and/or fibronectin did not significantly increase overall tensin1 protein expression analysed using one-way ANOVA with Dunnett's multiple comparison test (**Figure 3.18**), the distribution of tensin1 immunostaining was affected markedly. The length of the adhesions was significantly longer in the TGFβ1 alone (*p=0.0386) and TGFβ1 and fibronectin (*** p=0.0002) stimulated cells in both healthy (n=3) and COPD subjects (n=3), with no difference between health and COPD (**Figure 3.19**). Again, these data were analysed using one-way ANOVA with Dunnett's multiple comparison test.

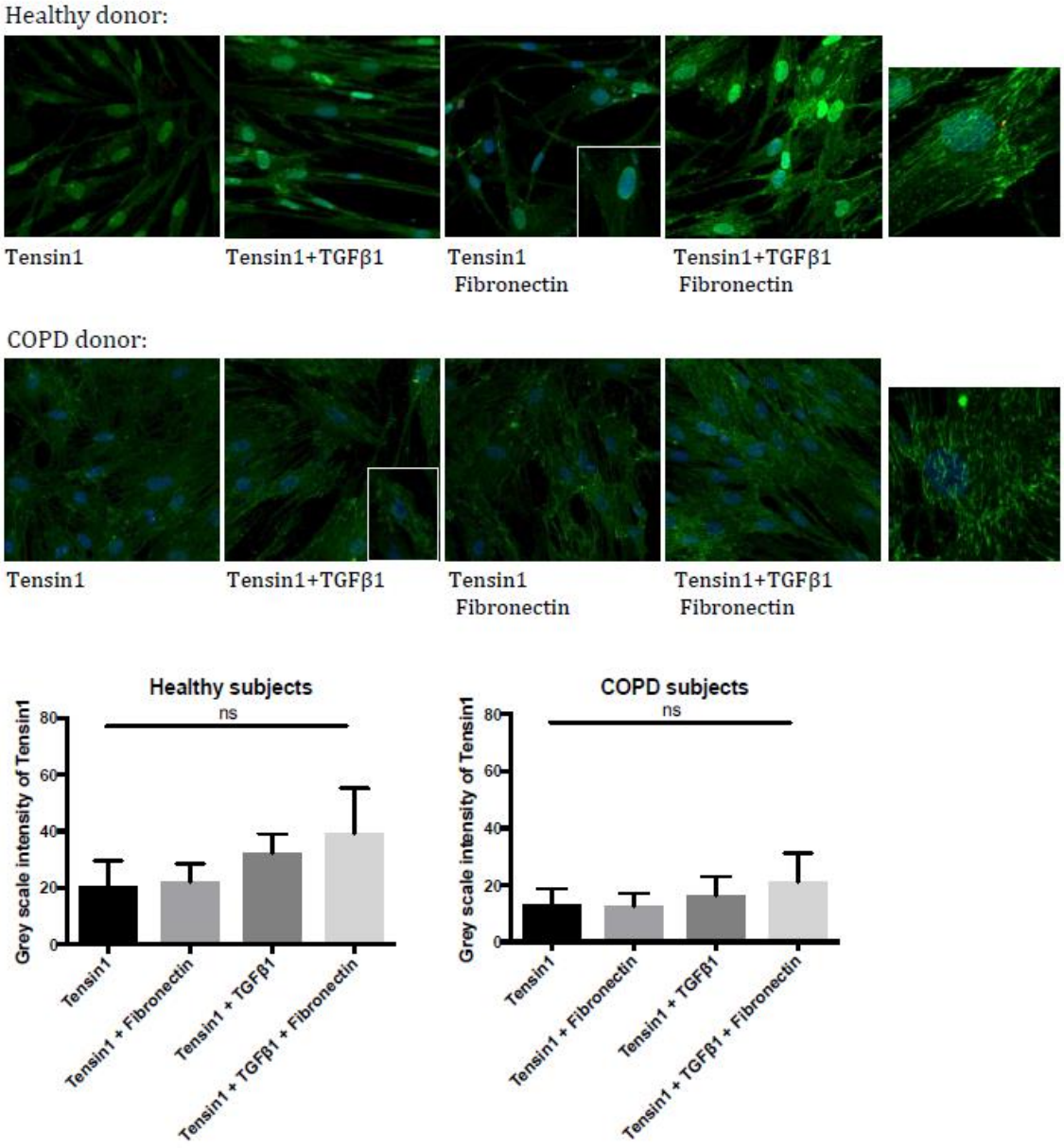

Figure 3.18: TGFβ1 and fibronectin stimulation did not cause increased tensin1 immunostaining. Cells were stimulated with TGFβ1 and/or fibronectin. Stimulation with TGFβ1 and fibronectin did not significantly increase the grey scale intensity of tensin1 in healthy (n=3) and COPD (n=3) subjects (mean±sem).

Healthy donor:

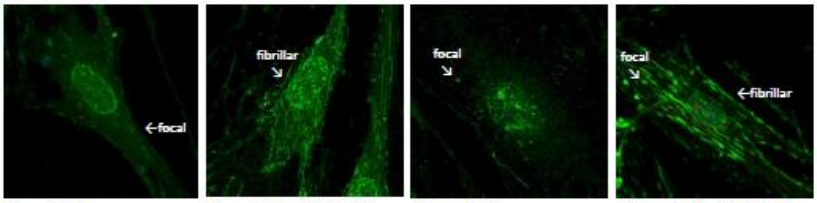

Tensin1 | Tensin1+TGFβ1 | Tensin1 Fibronectin | Tensin1+TGFβ1 Fibronectin

COPD donor:

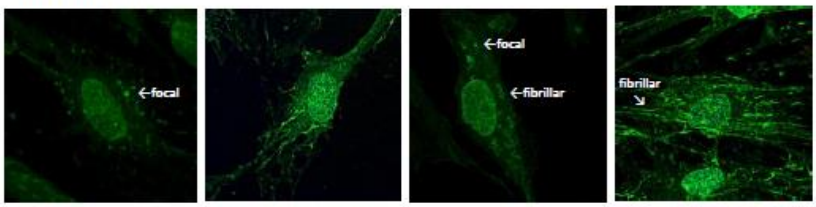

Tensin1 | Tensin1+TGFβ1 | Tensin1 Fibronectin | Tensin1+TGFβ1 Fibronectin

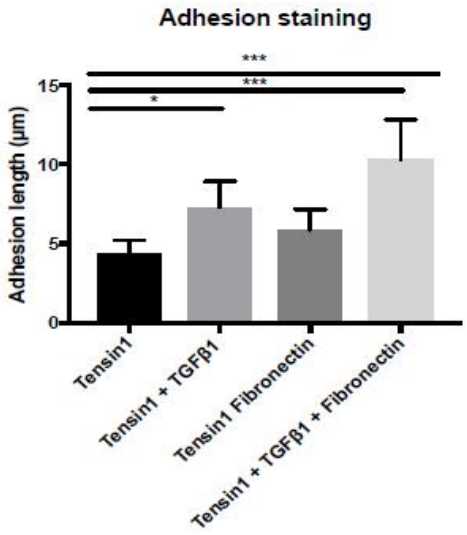

Figure 3.19: The effect of TGFβ1 and fibronectin on adhesion formation. Cells were stimulated with TGFβ1 and/or fibronectin. Stimulation with TGFβ1 and fibronectin did not significantly increase the grey scale intensity of tensin1, however the distribution of tensin1 immunostaining was affected. The fibrillar adhesions were significantly longer in the TGFβ1 only and TGFβ1 and fibronectin stimulated cells. Data shown is pooled COPD and healthy donors which did not differ (n=3, mean±sem) (*p<0.05, ***p<0.001).

3.3 Tensin1 and αSMA Interact in HASMCs

αSMA constitutes the most abundant protein in HASMCs. Therefore, investigating the association of tensin1 with αSMA was of particular interest considering the close interaction of tensin1 with actin filaments. Tensin1 and αSMA co-immunostaining was performed on non-stimulated and TGFβ1-stimulated HASMCs derived from healthy controls (n=3) and COPD individuals (n=3) on non-coated and fibronectin-coated slides. In all conditions, strong co-localisation of tensin1 and αSMA immunofluorescence was observed as shown in **Figure 3.20**. Quantification of tensin1 and αSMA co-localisation was performed using JaCoP. JaCoP measured Mander's overlap coefficient and Pearson's correlation to confirm the association of the two proteins. High levels of co-localised signals (Mander's overlap coefficient=0.8) and true correlation of approximately 0.6 revealed a strong association between the two proteins in both health and disease subjects (**Figure 3.21**).

Interaction of the two proteins was also shown using co-immunoprecipitation. Co-immunoprecipitation was carried out in HASMC lysates from a healthy control subject. Rabbit IgG and tensin1 immunoprecipitates were probed against a monoclonal anti-αSMA antibody. Rabbit IgG immunoprecipitate detected only the denatured heavy and light chains of the HRP-conjugated secondary antibody. In contrast three main bands, the heavy and light chains and a band of 42kDa, consistent with αSMA were detected in the tensin1 immunoprecipitate (**Figure 3.22**). These results suggest that tensin1 and αSMA both co-localise and interact physically, either directly or indirectly.

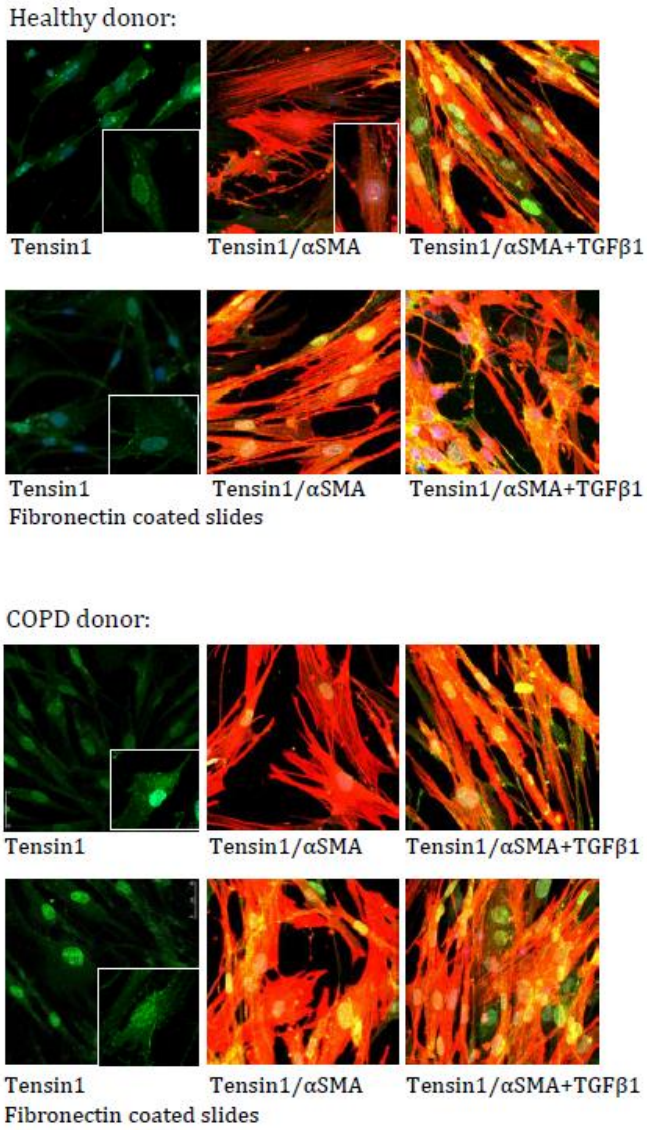

Figure 3.20: Tensin1 co-localisation with αSMA illustrated by confocal immunofluorescence staining. Association of tensin1 and αSMA was investigated using immunofluorescence analysis. HASMCs were co-stained for tensin1 and αSMA probed against FITC and Alexa Fluor 594 respectively. Co-localisation of tensin1 and αSMA proteins was indicated by the orange staining detected (tensin1 shown in green and αSMA in red).

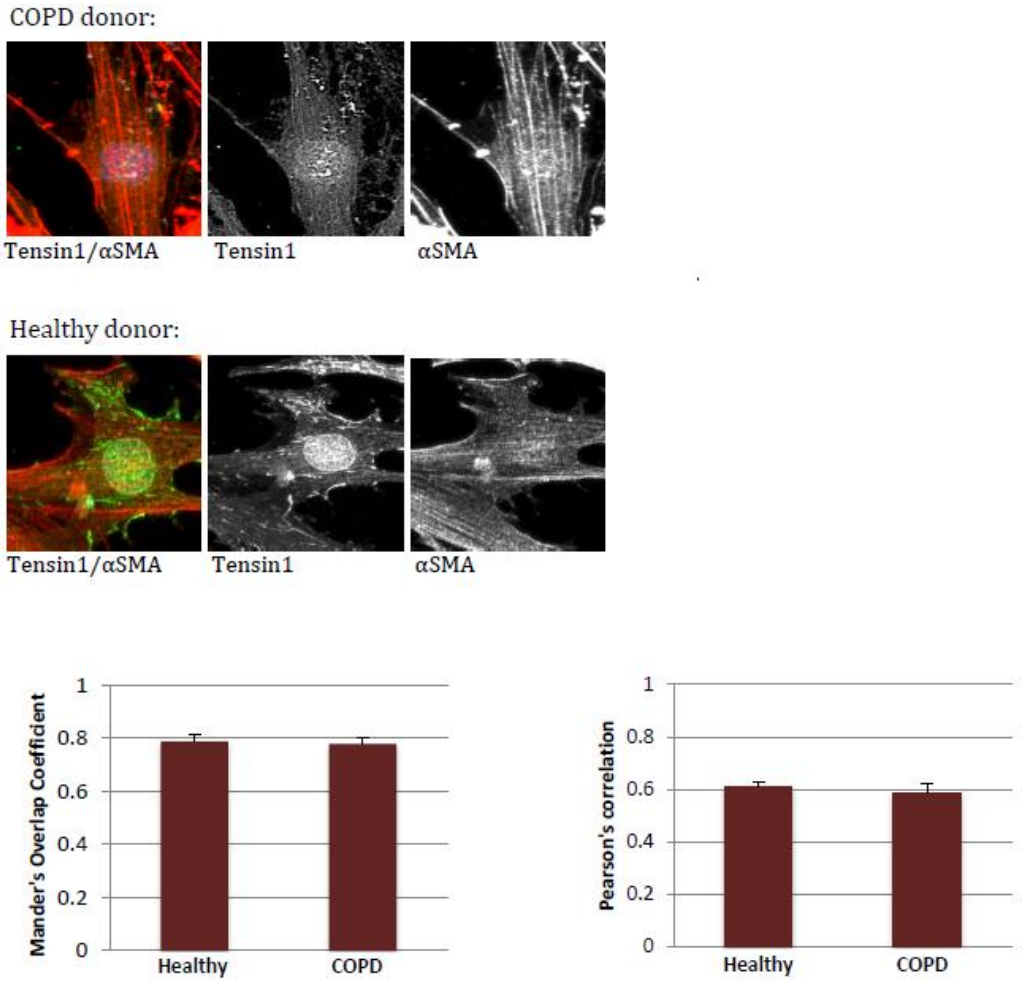

Figure 3.21: Tensin1 co-localises, but also correlates with αSMA. Association of tensin1 and αSMA was investigated using confocal immunofluorescence analysis. Quantification of co-localisation of tensin1 and αSMA was performed using JaCoP. Mander's overlap coefficient and Pearson's correlation were calculated to confirm association of the two proteins on n=3 healthy and n=3 COPD subjects (tensin1 shown in green and αSMA in red) (mean ± sem).

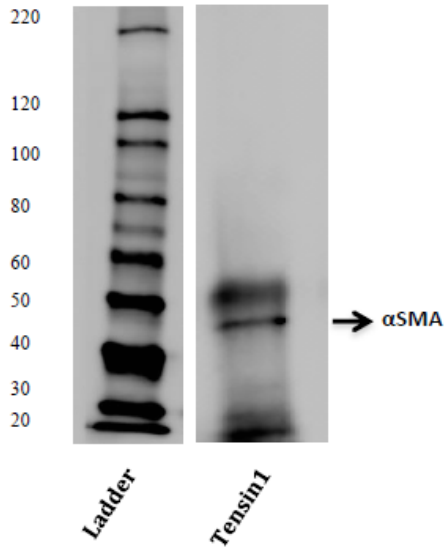

Figure 3.22: Tensin1 interaction with αSMA illustrated by immunoprecipitation. Co-immunoprecipitation was carried out to show interaction of tensin1 and αSMA. Tensin1 immunoprecipitates were analysed by western blotting analysis using an αSMA antibody, alongside rabbit IgG immunoprecipitates. A band of 42kDa was detected suggesting the interaction of the two proteins.

3.4 Effect of Tensin1 Silencing on Human Airway Smooth Muscle Cell Function

siRNA constitutes the most commonly used tool for induction of short-term silencing of protein coding genes. Depleting tensin1 was of extreme importance in order to investigate its function in HASMCs in properties such as proliferation, expression profile and contraction.

3.4.1 Optimising conditions for the siRNA technique with siGLO RISC FREE transfection

This experiment was performed on HASMCs derived from a healthy control subject. The efficiency of delivering a fluorescently-tagged, non-functional, non-targeting siRNA into HASMCs was examined. Cells were transfected with four different volumes of the transfection reagent Lipofectamine 2000 and a final 100nM concentration of this siGLO siRNA to determine the optimal Lipofectamine volume. 48 hour post-transfection, the cells were fixed with iced cold methanol, stained with DAPI and mounted prior to analysis by fluorescence microscopy. Images were acquired using the Leica TCS SP5 Confocal Immunofluorescence microscope. 6µl of Lipofectamine 2000 is the optimal volume to acquire 100% transfection efficiency on the HASMCs without causing toxicity to the cells (**Figure 3.23**).

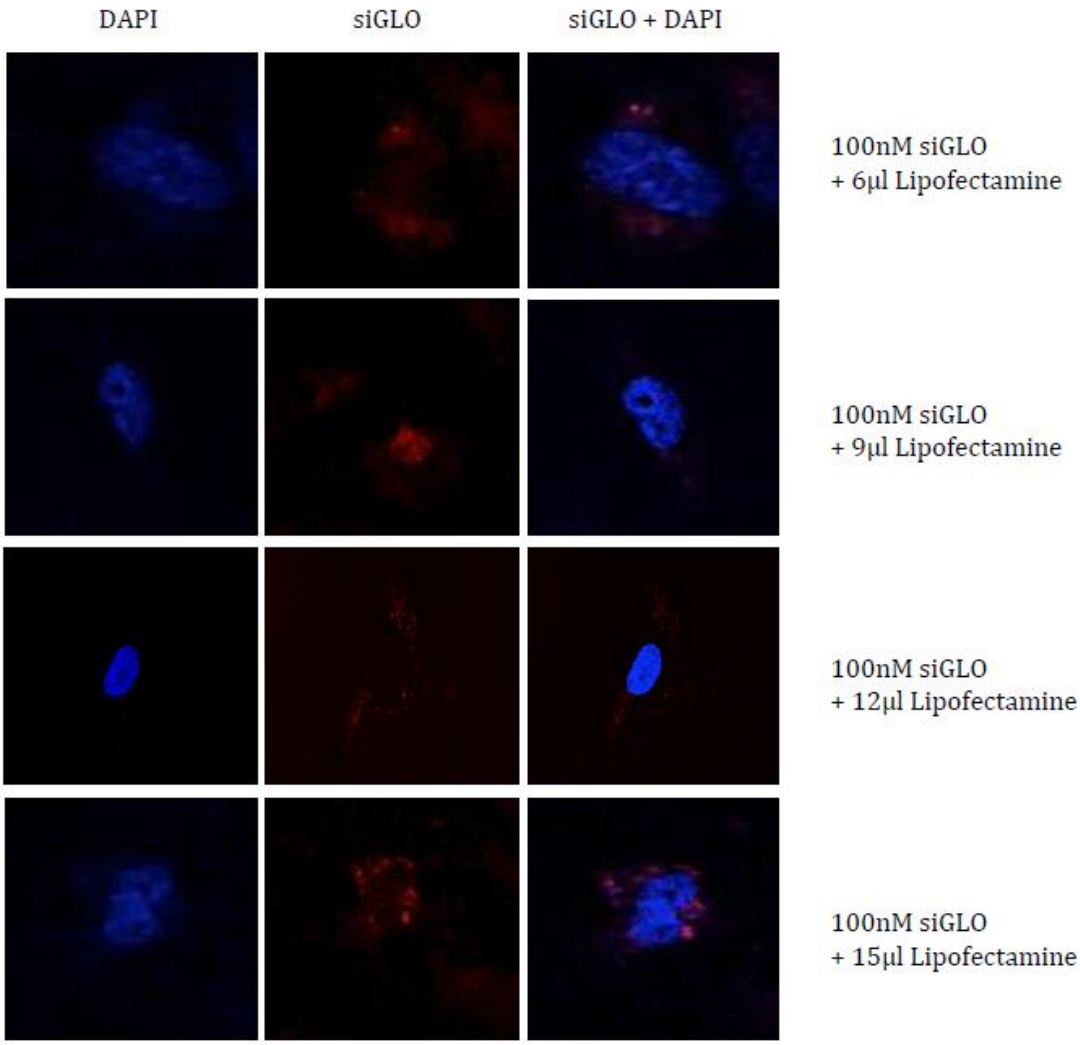

Figure 3.23: Successful delivery of oligonucleotides in HASMCs. siGLO was used to determine the volume of Lipofectamine needed and whether 100nM of oligonucleotides can successfully be delivered to all the cells. Even the lowest volume Lipofectamine achieved successful delivery of oligonucleotides to cells.

3.4.2 Successful knockdown of tensin1

sihT1 oligonucleotides were introduced to HASMCs at a final concentration of 100nM with 6µl of the transfection reagent. Success of tensin1 knockdown was assessed by qRT-PCR and western blot analysis. Knockdown was successful with approximately 92% downregulation at the mRNA level (p=0.0177). All the bands detected in the western blotting analysis in the non-transfected cells were eliminated following silencing, suggesting that tensin1 protein expression was also reduced (**Figure 3.24**).

3.4.3 Downregulation of tensin1 has no effect on HASMC survival and proliferation

HASMCs were transfected with siRNA directed against tensin1 and the appropriate controls; non-transfected, transfection reagent only (mock) and siCON controls. HASMC survival and proliferation was assessed using the trypan blue and MTS assays. Knockdown of tensin1 did not have any effect on the survival and spontaneous proliferation of HASMCs (n=4 health and n=4 COPD) in these two assays. Tensin1 siRNA survival and proliferation was compared to control using one-way ANOVA with Dunnett's multiple comparison test (**Figure 3.25** & **Figure 3.26**).

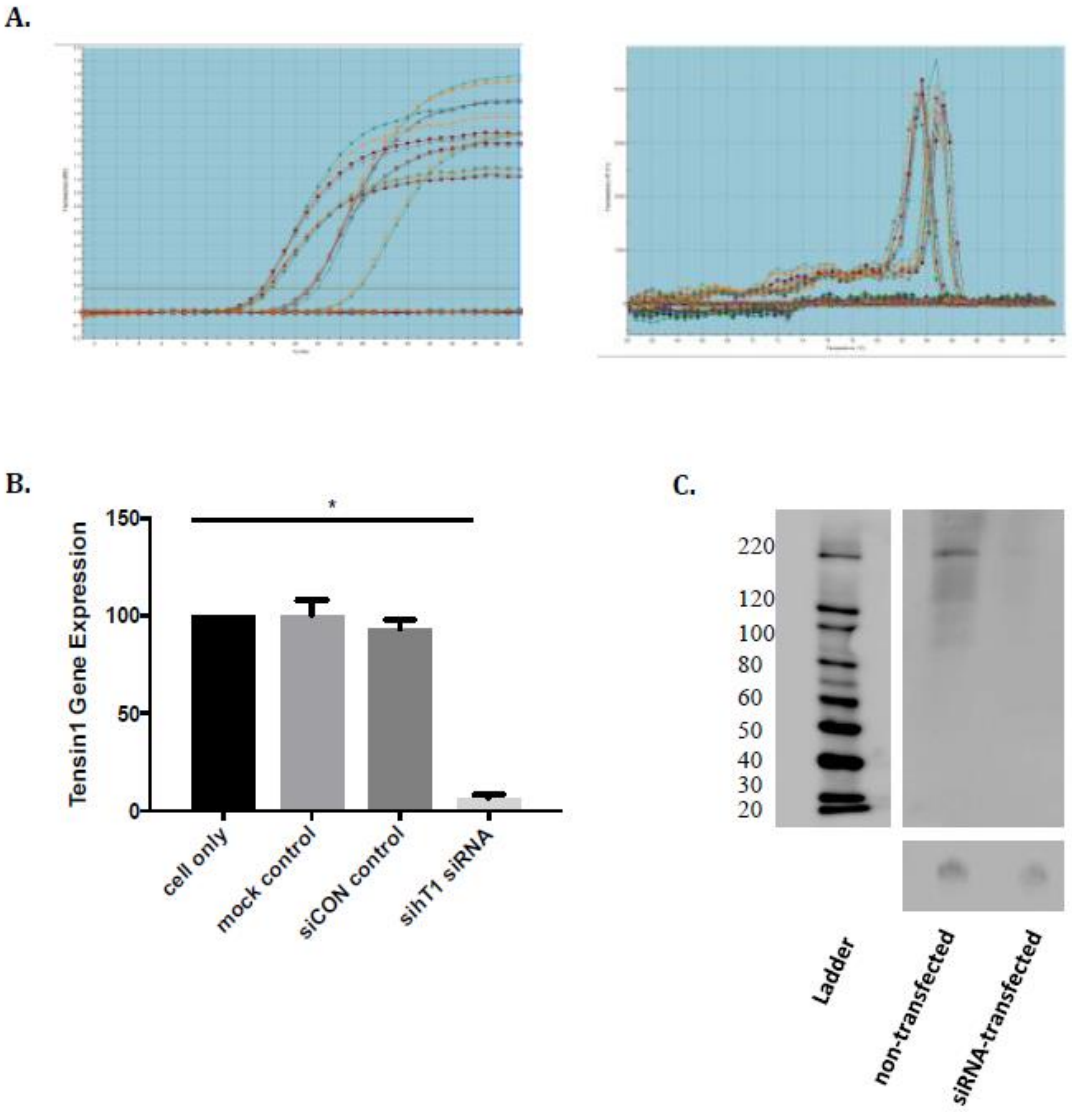

Figure 3.24: Successful tensin1 silencing using siRNA complexes. (A & B) Silencing tensin1 using siRNA was assessed using qPCR and was analysed using the 2^-(ΔCt) method. Appoximately 92% downregulation was achieved (mean±sem, n=3). **(C)** Tensin1 silencing was also assessed using western blotting analysis. All the bands detected in the non-tranfected cells were eliminated with tensin1 silencing (*p<0.05).

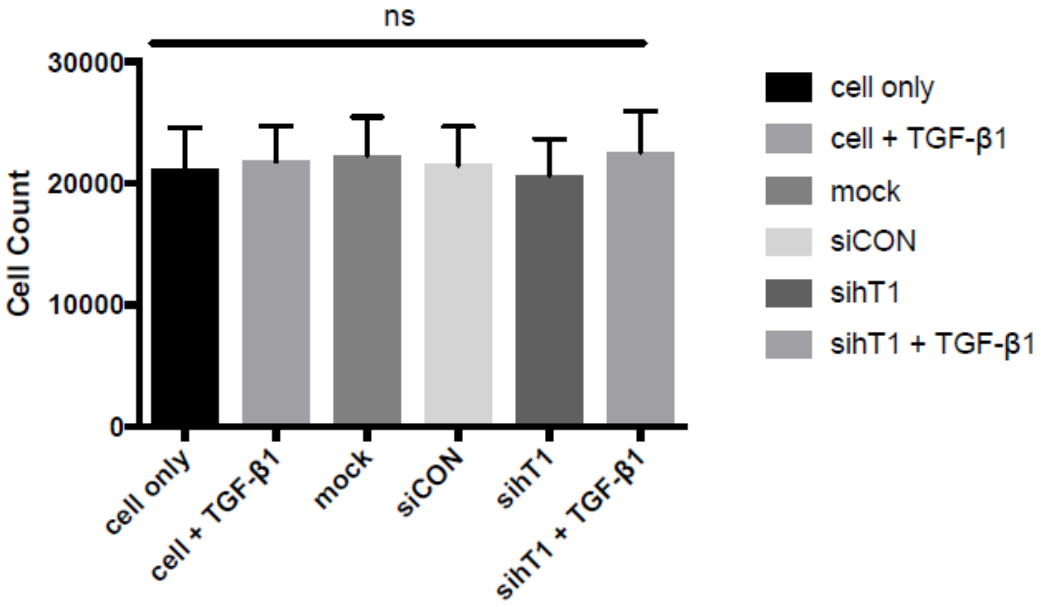

Figure 3.25: Tensin1 silencing has no effect on cell proliferation/survival illustrated by trypan blue assay. Cells were transfected with siRNA directed against tensin1. After tensin1 silencing was achieved, cell viability was assessed by trypan blue assay. Knockdown of tensin1 did not have any effect on HASMC proliferation/survival rates when compared to the controls. Data shown are pooled from COPD (n=4) and healthy donors (n=4) which did not differ (mean ± sem).

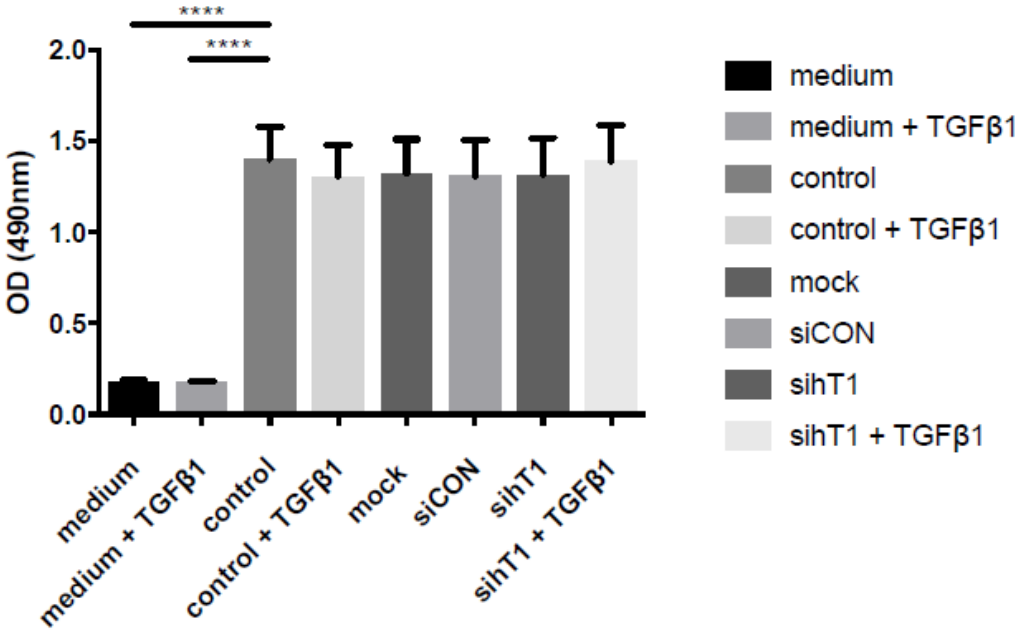

Figure 3.26: Tensin1 silencing has no effect on cell proliferation/survival illustrated by MTS assay. Cells were transfected with siRNA directed against tensin1. After tensin1 silencing was achieved, cell viability was assessed by MTS assay. Knockdown of tensin1 did not affect HASMC proliferation/survival rates when compared to the controls, confirming results acquired from trypan blue assay. Data shown are pooled from COPD (n=4) and healthy donors (n=4) which did not differ (mean ± sem).

3.4.4 Downregulation of tensin1 reduces αSMA expression

Interaction of tensin1 with αSMA has been illustrated and whether depletion of tensin1 can affect αSMA expression was tested. The ability of HASMCs to express αSMA after tensin1 depletion at the mRNA level was examined using qRT-PCR. Tensin1 knockdown was performed along with the controls and αSMA expression was quantified using the 2^-(ΔCt) method in n=4 COPD subjects. Both non-stimulated and TGFβ1-stimulated tensin1-depleted HASMCs, exhibited significantly lower αSMA mRNA expression compared to controls assessed by one-way ANOVA with Tukey's multiple comparison test (**Figure 3.27**).

The effect of tensin1 depletion on αSMA protein expression was also assessed. Tensin1 siRNA-transfected HASMCs derived from healthy (n=3) and COPD (n=3) individuals along with the controls (untreated cells, mock and siCON control) were immunostained for both tensin1 and αSMA. Cells were also stimulated with TGFβ1 (10 ng/ml) to examine its role on αSMA expression after silencing tensin1. Tensin1 downregulation significantly reduced αSMA protein expression in both non-stimulated and TGFβ1-stimulated cells ($p \leq 0.05$) (**Figure 3.28** & **Figure 3.29**). This effect of tensin1 depletion on αSMA expression in HASMCs was further investigated using western blot analysis (n=4 healthy and n=4 COPD), and revealed again greatly reduced αSMA protein expression in tensin1-depleted cells when compared to controls in both healthy and COPD subjects. With both immunofluorescence staining and western blot analysis, no difference on αSMA protein expression was detected in the mock and siCON controls when compared to the non-transfected cells eliminating any possibility of this to be an effect of

the transfection process. These data were analysed using one-way ANOVA with Tukey's multiple comparison test (**Figure 3.30** & **Figure 3.31**).

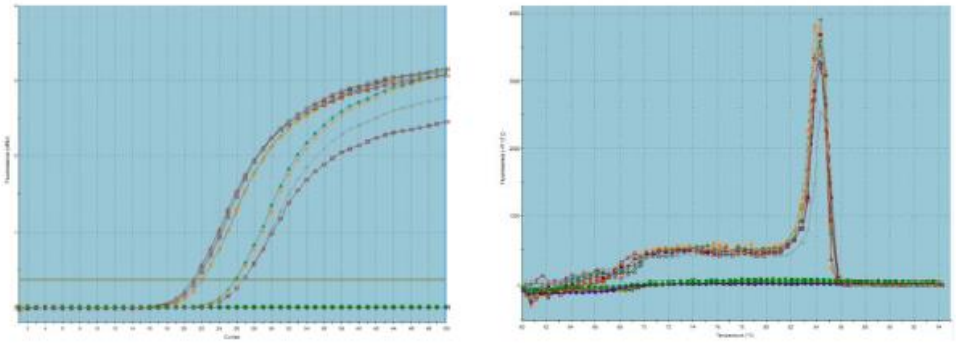

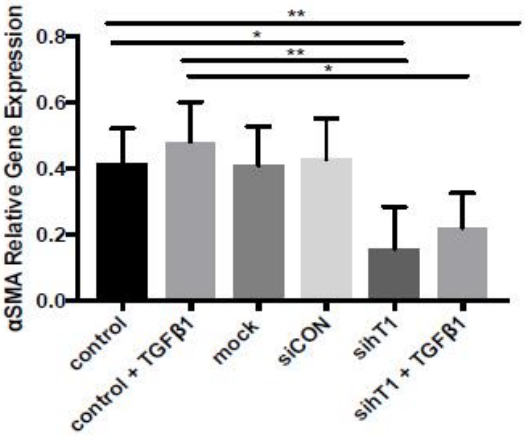

Figure 3.27: Reduced αSMA mRNA expression in tensin1 depleted HASMCs. Cells were transfected with siRNA directed against tensin1. The effects of depleting tensin1 on HASMC αSMA mRNA expression was assessed using qRT-PCR. αSMA mRNA (PCR product 222 size bp) was quantified using the 2^-(ΔCt) method in n=4 COPD subjects, alongside the housekeeping gene β-actin. Tensin1 depleted HASMCs revealed a significantly lower ability to express αSMA when compared to controls both in the absence or presence of TGFβ1 (mean ± sem) (*p<0.05, **p<0.01).

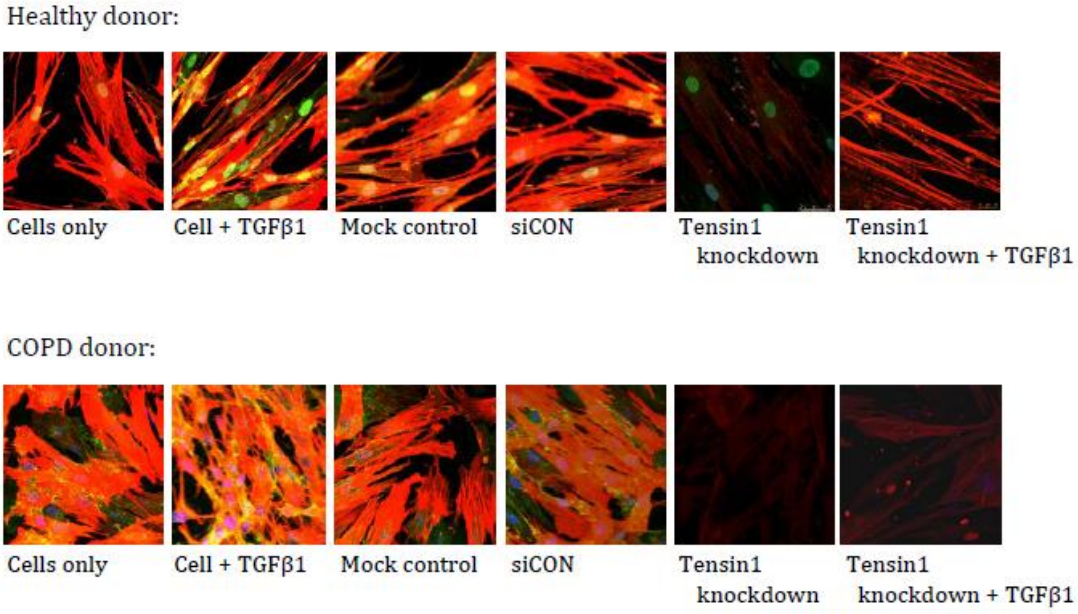

Figure 3.28: Reduced αSMA protein expression in tensin1 depleted HASMCs shown by confocal immunofluorescence analysis. Cells were transfected with siRNA directed against tensin1 and assessed for αSMA expression using immunofluorescence analysis. HASMCs were co-stained for tensin1 and αSMA probed against FITC and Alexa Fluor 594 respectively. Co-localisation of tensin1 and αSMA proteins was indicated by the orange staining detected. Reduced αSMA expression was detected in the siRNA transfected HASMCs when compared to untransfected cells in n=3 healthy and n=3 COPD subjects. Representative tensin1 and αSMA immunostaining in HASMCs derived from healthy and COPD subjects, along with the appropriate transfection controls (tensin1 shown in green and αSMA in red).

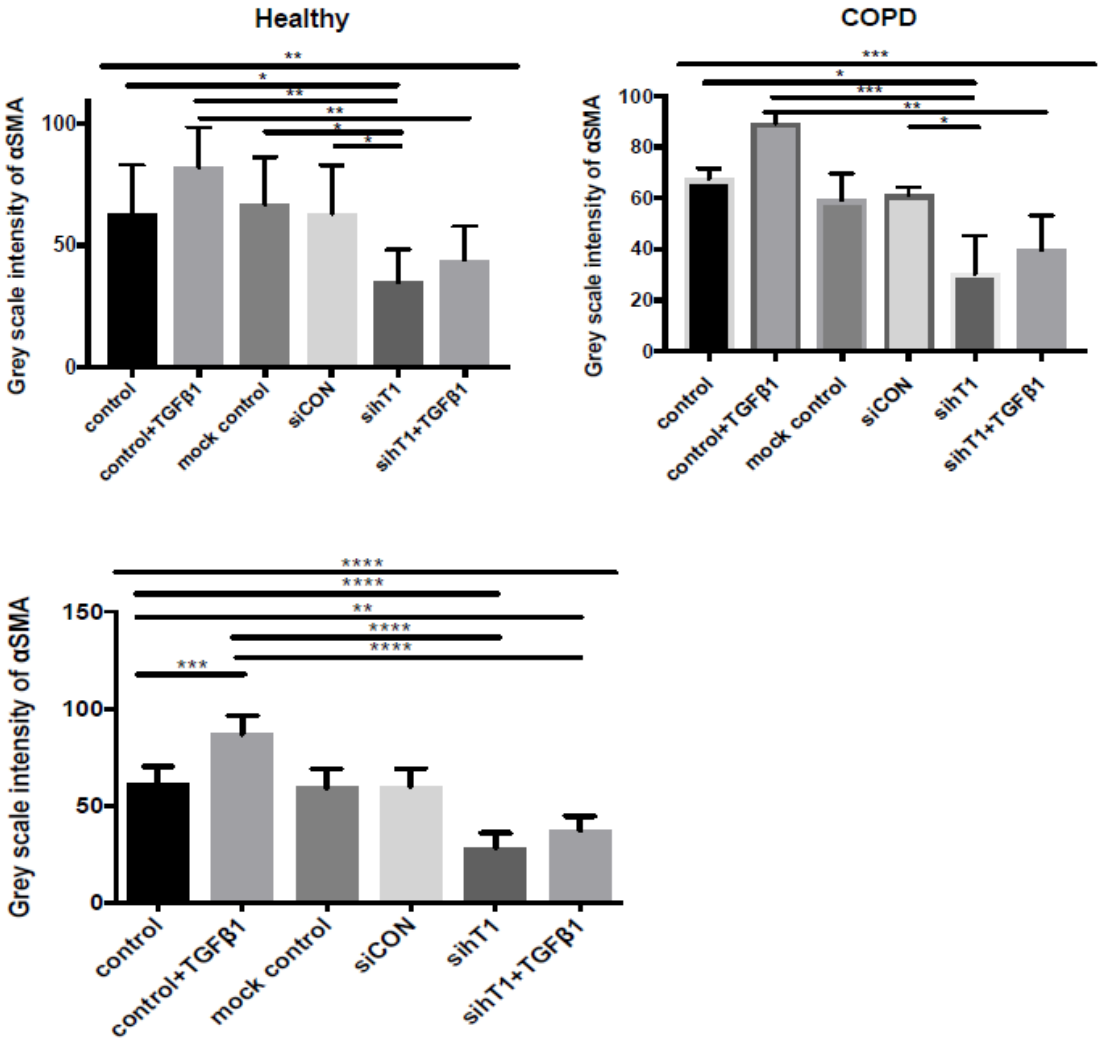

Figure 3.29: Quantification of reduced αSMA protein expression in tensin1 depleted HASMCs shown by immunofluorescence analysis. Cells were transfected with siRNA directed against tensin1 and assessed for αSMA expression using immunofluorescence analysis. Reduced HASMC αSMA expression was measured by grey scale intensity in n=3 healthy and n=3 COPD subjects. Tensin1 depleted HASMCs had significantly lower intensity of αSMA when compared to controls both in the absence or presence of TGFβ1 (mean±sem) (*p<0.05, **p<0.01, ***p<0.001, ****p<0.0001).

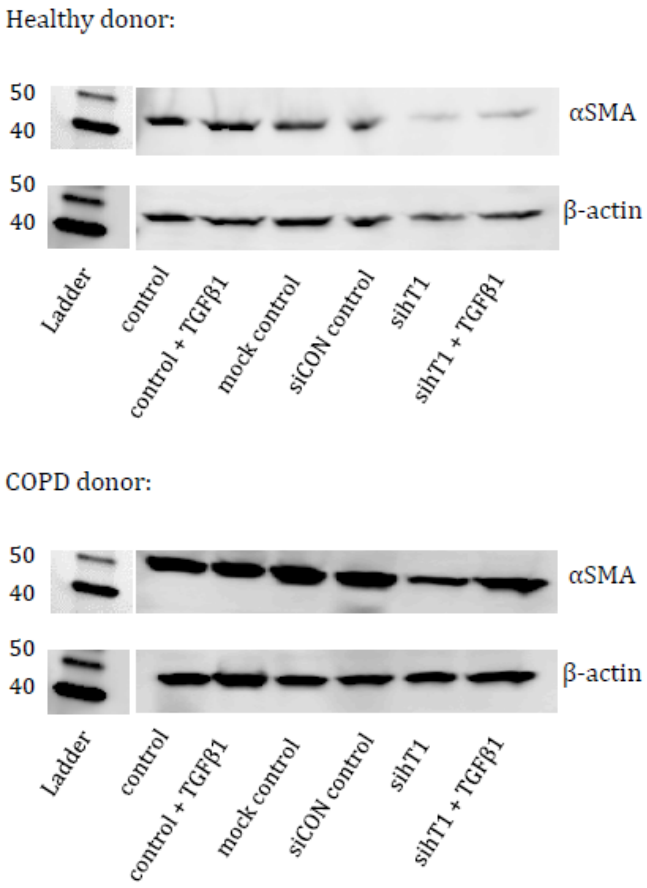

Figure 3.30: Reduced αSMA protein expression in tensin1 depleted HASMCs shown by western blotting analysis. The effects of depleting tensin1 on HASMC αSMA protein expression was also confirmed using western blotting analysis. Reduced αSMA expression was detected in the siRNA transfected HASMCs when compared to untransfected cells in n=3 healthy and n=3 COPD subjects. Representative αSMA immunoblotting staining in HASMCs derived from healthy and COPD subjects, along with the appropriate transfection controls and housekeeping protein β-actin.

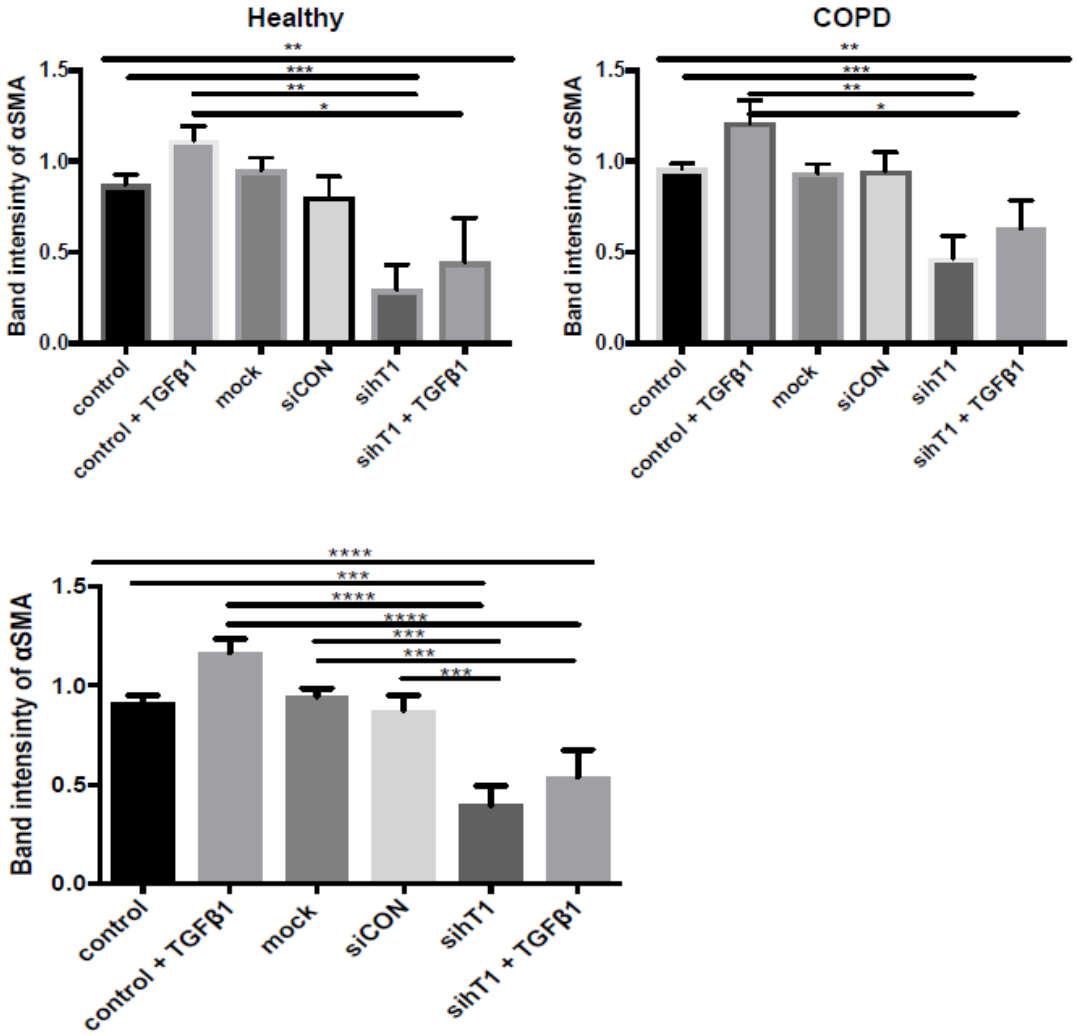

Figure 3.31: Quantification of reduced αSMA protein expression in tensin1 depleted HASMCs shown by western blotting analysis. The effects of depleting tensin1 on HASMC αSMA protein expression was also confirmed using western blotting analysis. αSMA expression was measured by band intensity in n=4 healthy and n=4 COPD subjects. Representative blots are shown for healthy and COPD donors. Data shown are pooled from COPD and healthy donors which did not differ (mean±sem). Representative blots are shown for healthy and COPD donors (*p<0.05, **p<0.01, ***p<0.001, ****p<0.0001).

3.4.5 Tensin1 silencing reduces HASMC contractility

Collagen gel assays provide a convenient platform to investigate spontaneous and agonist-dependent HASMC contraction ex vivo (Sakota et al. 2014, Lewis et al. 2016). As tensin1 interacted with αSMA, the ability of tensin1-depleted HASMCs to spontaneously contract collagen gels was tested over time (4, 18, 24 and 48 h). A series of images of the collagen gels were taken and a representative example of a HASM collagen gel assay can be seen in **Figure 3.32**. Tensin1-depleted HASMCs from both healthy (n-4) and COPD (n=4) subjects demonstrated a greatly reduced ability to contract collagen gels spontaneously. Contraction time course data were analysed using two-way ANOVA with Dunnett's post test (**Figure 3.33**). Difference in the collagen area was observed in 18 (*p=0.0118), 24 (**p=0.0027) and 48 h (****p=0.0001) in the graph with pooled COPD and healthy controls (**Figure 3.33A**). Again, mock and siCON controls exhibited a similar ability to contract the collagen gels as non-transfected cells suggesting a tensin1-specific effect.

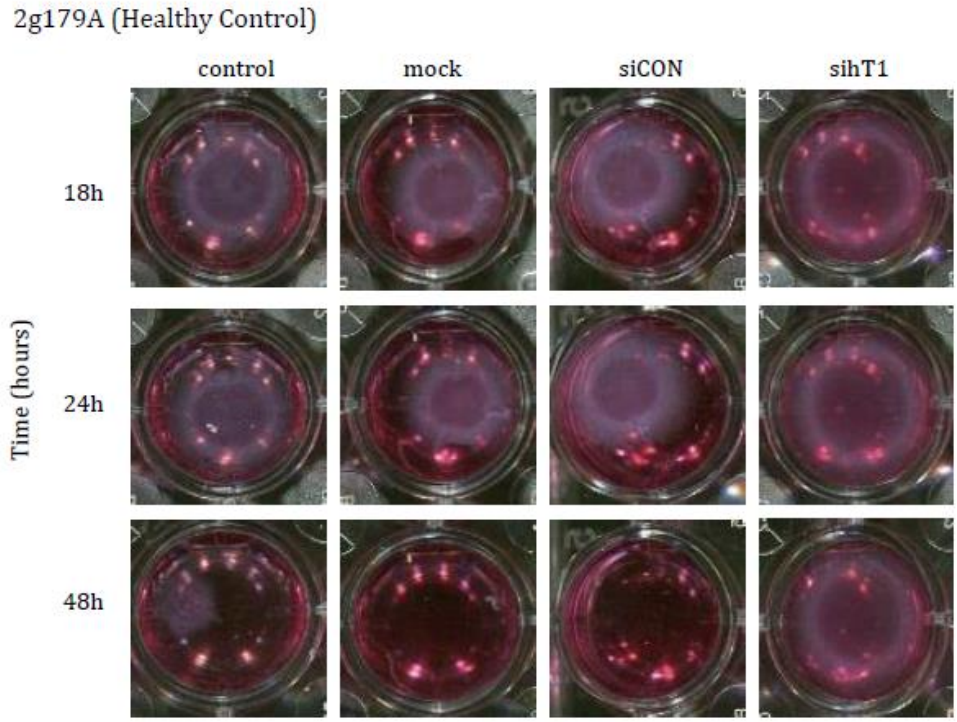

Figure 3.32: Collagen gel contraction by HASMCs is dependent on tensin1. Cells were transfected with siRNA directed against tensin1 and incubated within 3D collagen gels. The extend of spontaneous collagen gel contraction was recorded at 4, 18, 24 and 48 h time points. Assays were performed on 4 healthy and 4 COPD donors.

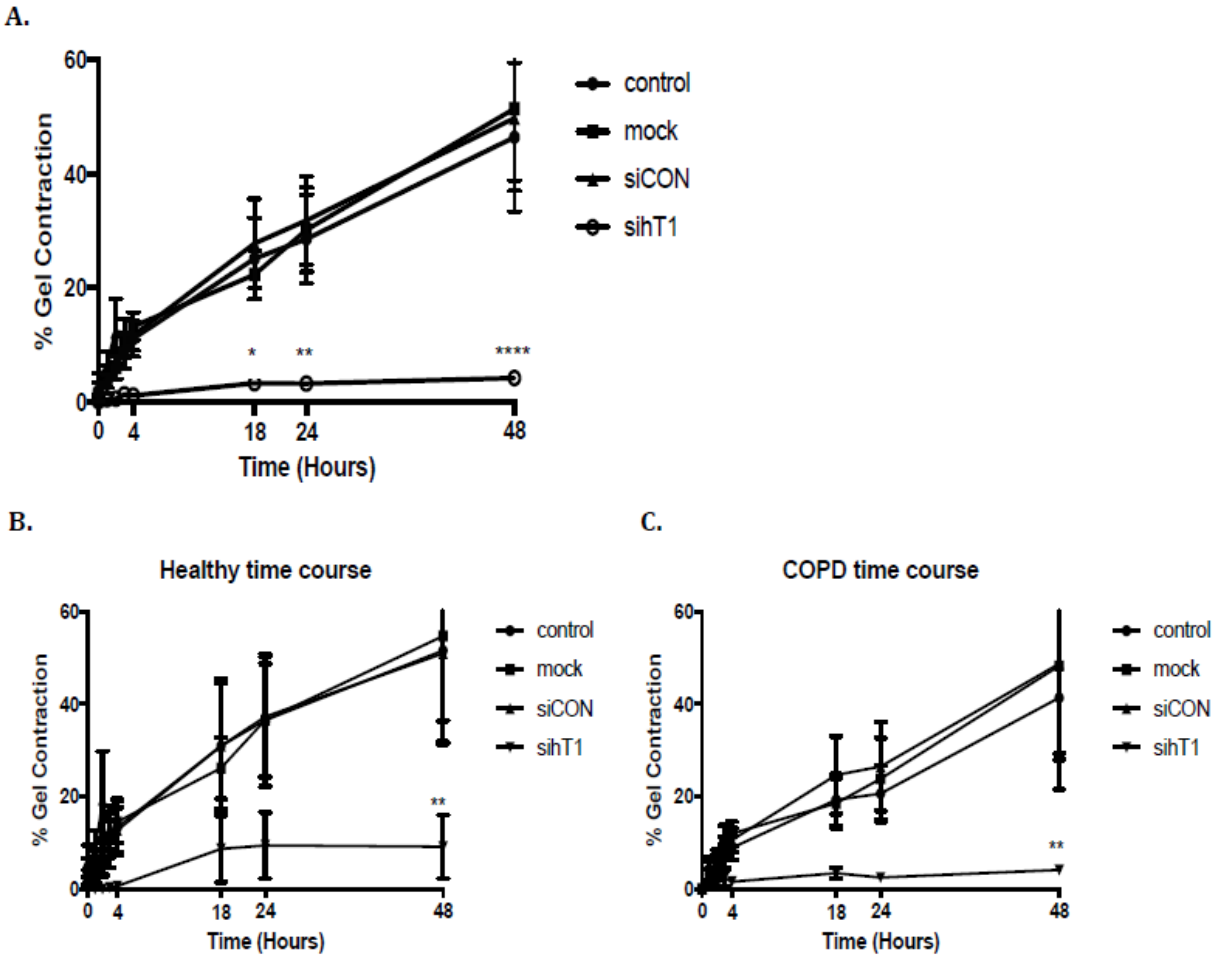

Figure 3.33: Collagen gel contraction by HASMCs is dependent on tensin1 in both health and disease. (A) Quantification of collagen gel contraction using gel area measurement (n=8, mean±SEM). Data shown are pooled COPD and healthy donors. HASMCs transfected with tensin1 siRNA SMARTpool showed a greatly reduced ability to contract. **(B & C)** Quantification of collagen gel contraction shown in healthy (n=4) and COPD (n=4) subjects separately (*p<0.05, **p<0.01, ****p<0.0001).

The role of TGFβ1 (10 ng/ml) on the ability of HASMCs to contract after tensin1 silencing was also examined. TGFβ1 did not have any effect on 24 h and 48 h HASMC contraction in tensin1-depleted cells. Although, TGFβ1 increased HASMC gel contraction compared to control, this did not reach significance. Data were analysed using one-way ANOVA with Dunnett's multiple comparison test (**Figure 3.34** & **Figure 3.35**).

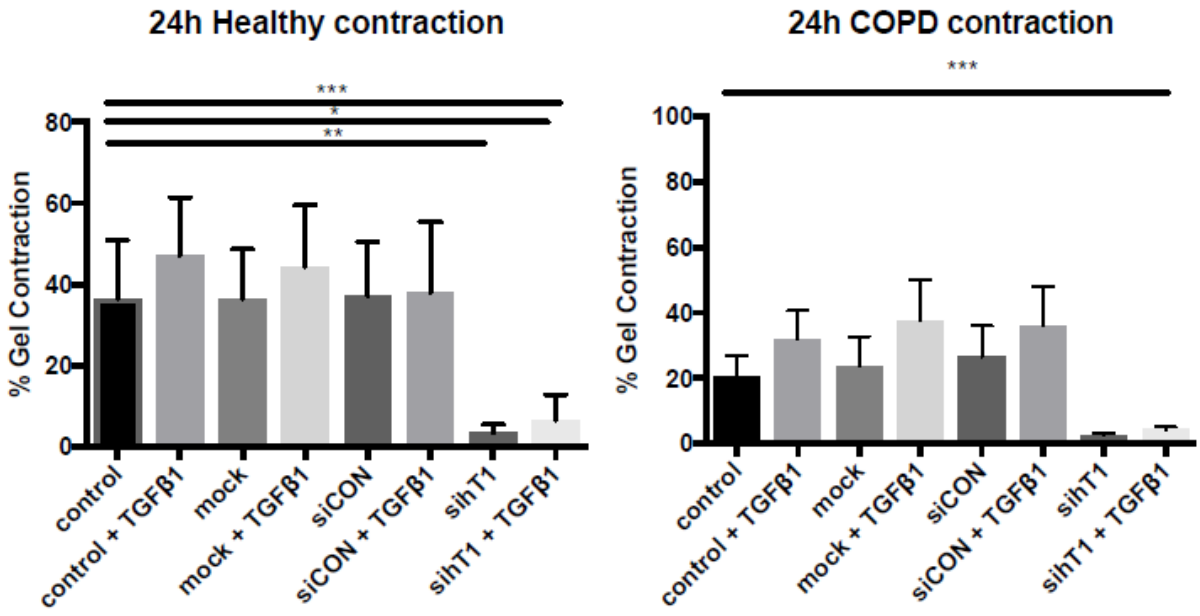

Figure 3.34: TGFβ1 does not have a significant effect on HASMC contractility at 24 h. Cells were transfected with siRNA directed against tensin1 and incubated within 3D collagen gels. HASMCs were then stimulated with TGFβ1. Quantification of collagen gel contraction shown in healthy (n=4) and COPD (n=4) subjects was performed at 24 hour incubation (mean±sem) (*p<0.05, **p<0.01, ***p<0.001).

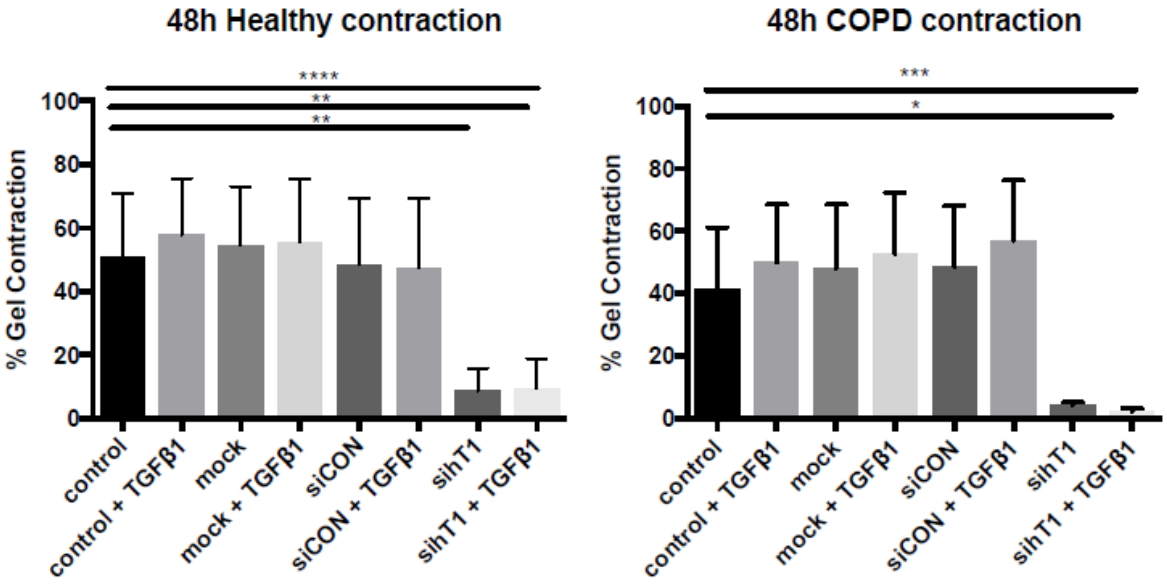

Figure 3.35: TGFβ1 does not have a significant effect on HASMC contractility at 48 h. Cells were transfected with siRNA directed against tensin1 and incubated within 3D collagen gels. HASMCs were then stimulated with TGFβ1. Quantification of collagen gel contraction shown in healthy (n=4) and COPD (n=4) subjects was performed at 48 hour incubation (mean±sem) (*p<0.05, **p<0.01, ***p<0.001, ****p<0.0001).

3.5 Genotyping Subjects for the Presence of the SNP Identified in GWAS

3.5.1 Restriction Fragment Length Polymorphism Mapping (RFLP) optimisation

RFLP was used to genotype subjects for the presence of the R1197W SNP. The association of the R1197W SNP with reduced FEV_1 has been revealed in a GWAS study (Repapi et al. 2010) and therefore examining its prevalence was of particular significance. The SNP causes the missense amino acid change R1197W (CGG>TGG), which disrupts the formation of an Eag1 restriction enzyme site (C^GGCCG). The aim is to genotype subjects by performing an Eag1 restriction digest on PCR products. If tensin1 is in its wild-type form, R1197, the restriction site is formed and the Eag1 enzyme performs digestion and two bands are evident. If the mutation is present, then the site for Eag1 is not formed DNA remains uncut, giving one band on gel. However, if tensin1 is in its heterozygote form, three bands will be detected (**Figure 2.2**).

To optimise the method, amplification of a single product during PCR was confirmed and primer efficiency was tested in order to achieve a good restriction digest of the PCR products (**Figure 3.36**). Furthermore, pEGFP constructs containing either the full length of tensin1 with the SNP or wild-type tensin1 were used as controls to validate the method. Digestion of the pEGFP construct containing the R1197 wild-type tensin1 resulted in the production of two bands. Restriction digestion of the pEGFP construct containing the R1197W SNP tensin1 resulted in the production of a single band as expected, shown in **Figure 3.37**.

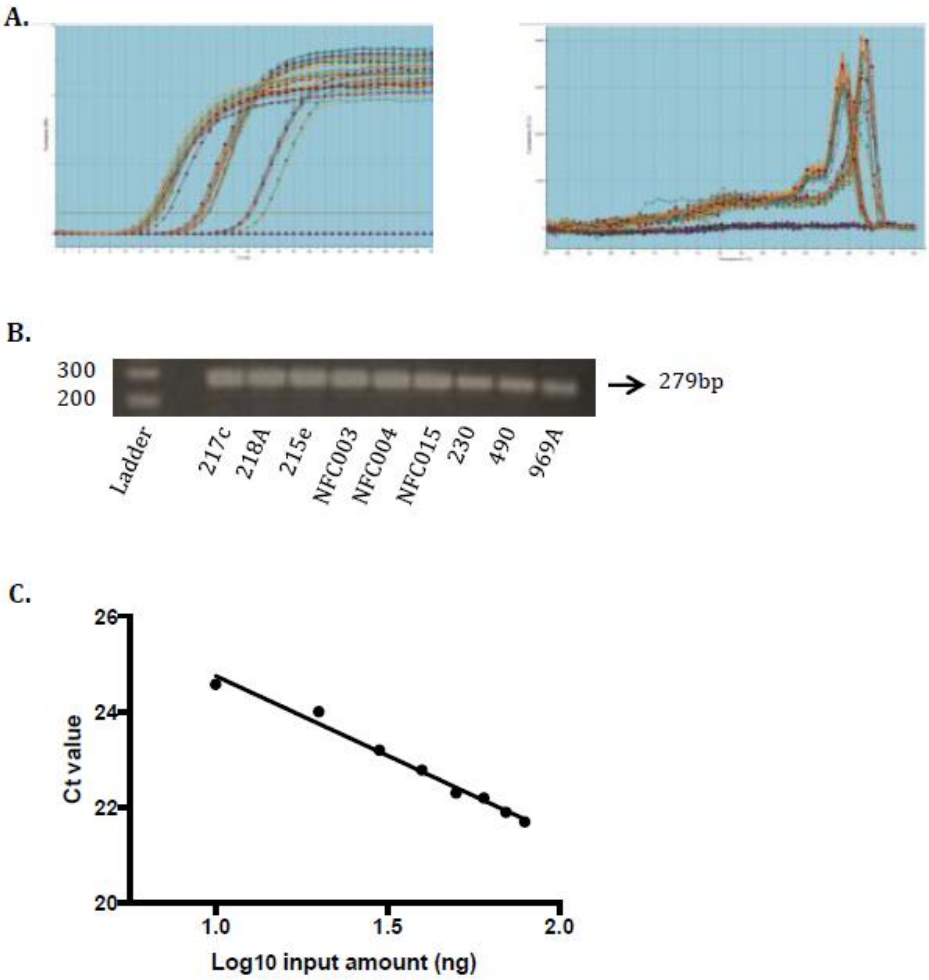

Figure 3.36: Optimisation of primers used for HASMC genotyping. (A) Primers covering the region of interest were tested using qRT-PCR. **(B)** PCR products were run on an agarose gel to confirm amplification of a single product. **(C)** Different concentrations of RNA were used to examine primer effiency and determine the optimal concentration of RNA to be used for genotyping subjects.

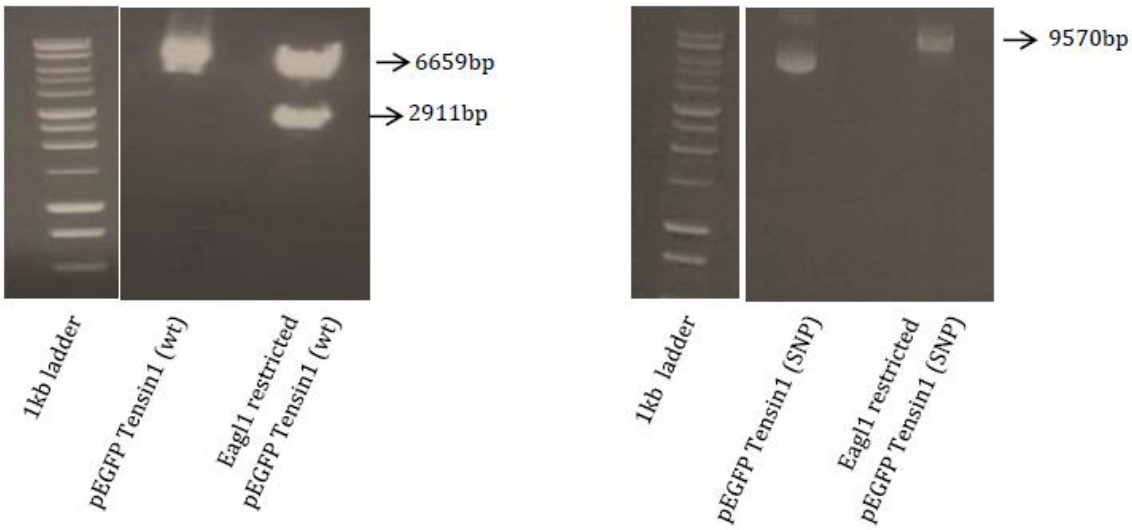

Figure 3.37: Validation of the RFLP method using pEGFP constructs containing the wild-type R1197 and R1197W SNP tensin1. pEGFP-C1 constructs with the mutant (homozygous –TT-) and wild-type (homozygous –CC-) tensin1 were used as controls to confirm validity of the RFLP technique. Eag1 restriction digestion was performed and as expected, two bands and a single band were detected in the pEGFP containing wild-type and mutant tensin1 respectively, on an electrophoresis gel.

3.5.2 The pattern of expression of the R1197W SNP in healthy and disease subjects

In **Figure 3.38**, the PCR-RFLP detection assay shows the detection of the SNP in healthy and disease subjects. ImageJ was used to confirm restriction efficiency by band intensity measurement and number of bands detected in each sample, an example of subjects with wild-type, mutant and heterozygote form of tensin1 can be seen in **Figure 3.39**. RFLP revealed the presence of the R1197 wild-type tensin1 in healthy controls (n=12) but not in COPD donors (n=10) (p=0.0005, Fisher's exact test) (**Figure 3.40**). COPD and asthmatic donors were predominantly –TC- heterozygotes or occasionally –TT- homozygotes (encoding for R1197W).

A.

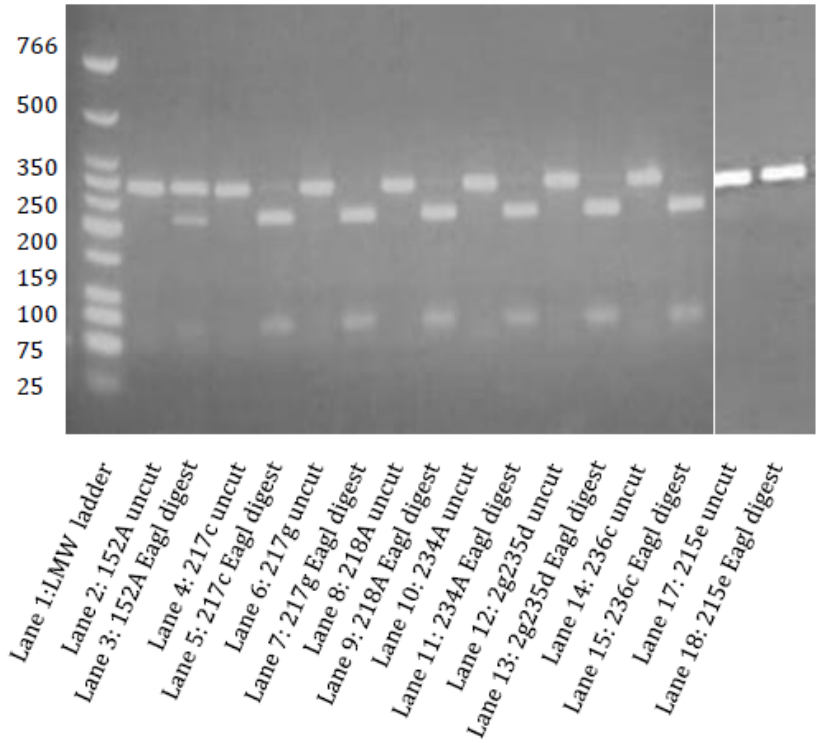

Figure 3.38: An agarose gel illustrating the different tensin1 phenotypes. PCR products from HASMCs were analysed by restriction digestion with Eag1. Non-digested and digested DNA products were run on an agarose gel to investigate whether the mutation is present or not. An agarose gel image illustrating the different tensin1 phenotypes is illustrated above. Lane 3 = Heterozygous, Lane 5, 7, 11, 13 and 15 = homozygous (-CC-) (encodes R1197 tensin1) and Lane 17 = homozygous (-TT-) (encodes R1197W tensin1).

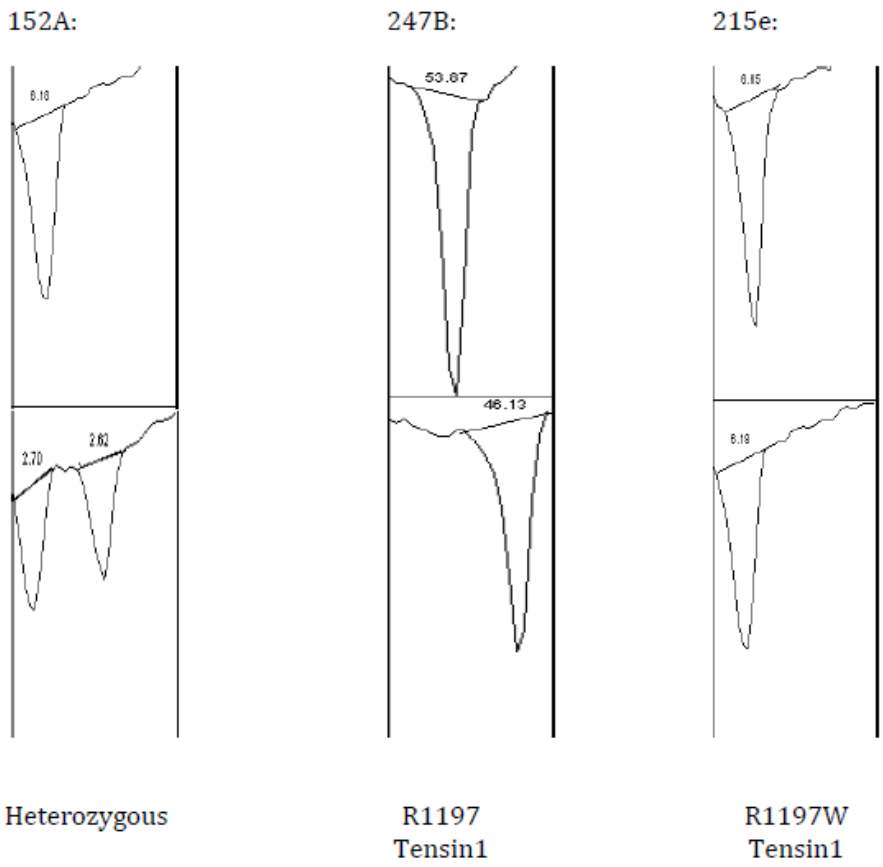

Figure 3.39: Intensity measurement of the bands detected in RFLP. Intensity measurement of the bands obtained from RFLP was performed using ImageJ to establish the presence of the three different tensin1 phenotypes; Heterozygous, homozygous (-CC-) R1197 tensin1 and homozygous (-TT-) R1197W tensin1.

Group	Number	Genotype frequency, no. (%)	
		CC	CT or TT
Healthy	12	9 (75%)	2+1 (25%)
COPD	10	-	9+1 (100%)
Asthma	9	1 (11.11%)	6+2 (88.89%)

Figure 3.40: The R1197 wild-type tensin1 (homozygous –CC-) is present predominantly in healthy subjects. HASMCs from 12 healthy control, 10 COPD and 9 asthmatic subjects were genotyped for the two tensin1 variants. RFLP revealed the presence of the homozygous (-CC) R1197 variant only in healthy controls, while COPD and asthmatic donors were predominantly –TC- heterozygotes or occasionally homozygotes (-TT-) R1197W.

3.5.3 The effect of R1197W SNP on contraction

Collagen gel contraction assays were performed on genotyped subjects to examine the effect of the R1197W SNP on 24 h and 48 h HASMC contraction. The assay was performed on HASMCs derived from COPD (n=4) and healthy subjects (n=4). Subjects with wild-type tensin1 had a trend towards increased contraction compared to heterozygotes, but this was not statistically significant (**Figure 3.41**). Increasing the sample size and examining the effects of contractile agonists will be important in future experiments. Data were analysed using nonparametric Mann-Whitney U test. However, the population size was not enough to draw any conclusions.

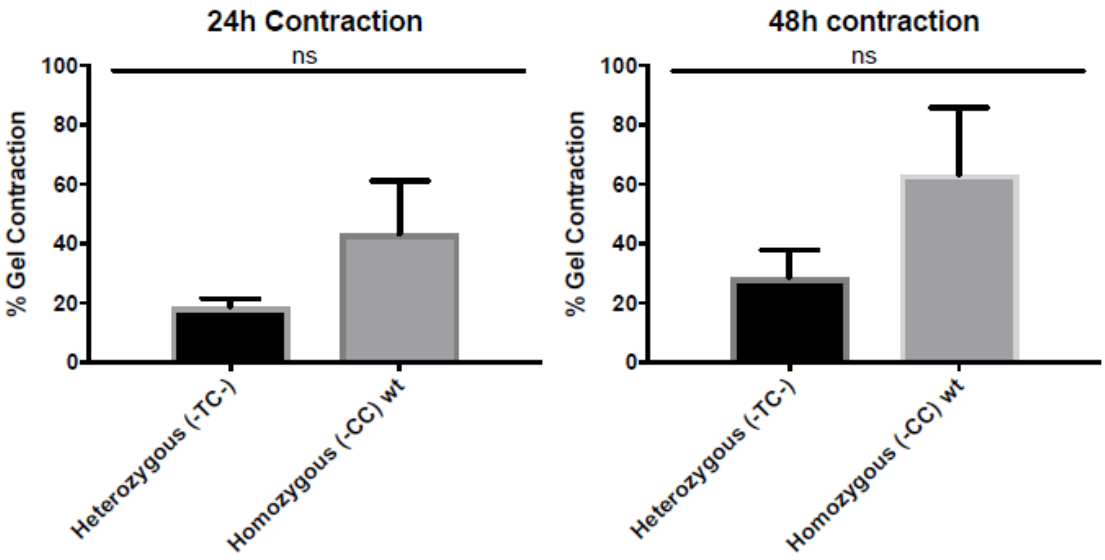

Figure 3.41: The effect of the two tensin1 variants on contraction. Collagen gel contraction assay was performed to investigate the effect that the different tensin1 genotypes have on the ability of human airway smooth muscle cells to contract spontaneously.

3.6 Effect of Overexpression of Tensin1 Containing the Wild-Type and the R1197W SNP on cell function

3.6.1 Successful overexpression of tensin1 in HASMCs

pEGFP C1 constructs were introduced to HASMCs at a concentration of 5 μg with 5 μl lipofectamine LTX and 5 μl of PLUS reagent. Success of pEGFP C1 tensin1 delivery was assessed by qRT-PCR and immunofluorescence. A Ct value of ~15 was detected in the pEGFP-transfected cells compared to a Ct value of ~21 detected in the non-transfected cells suggesting earlier amplification, thus increased expression of tensin1. Transfected cells were visualised under an immunofluorescence microscope where focal and fibrillar adhesion localisation of tensin1 was detected. pEGFP constructs were successfully delivered in 4 out of 10 HASMC cultures. A non-transfected control was used along experiments (**Figure 3.42**).

3.6.2 Effect of pEGFP C1 construct introduction on HASMC proliferation/survival illustrated by MTS assay

HASMCs were transfected with pEGFP C1 constructs containing wild-type and mutant tensin1 and the appropriate controls; non-transfected and pEGFP C1 alone controls. HASMC survival and proliferation was assessed using the MTS assay. Transfection with both constructs did not have any effect on the survival and spontaneous proliferation of HASMCs derived from COPD subjects in this assay. The healthy donors revealed significantly decreased proliferative ability following transfection with the pEGFP C1 construct containing mutant tensin1 (-TT-) ($p=0.0094$), whereas transfection with the pEGFP C1 construct containing

wild-type tensin1 (-CC-) did not have any effect. Tensin1 overexpression survival and proliferation was compared to control using one-way ANOVA with Dunnett's multiple comparison test (**Figure 3.43**).

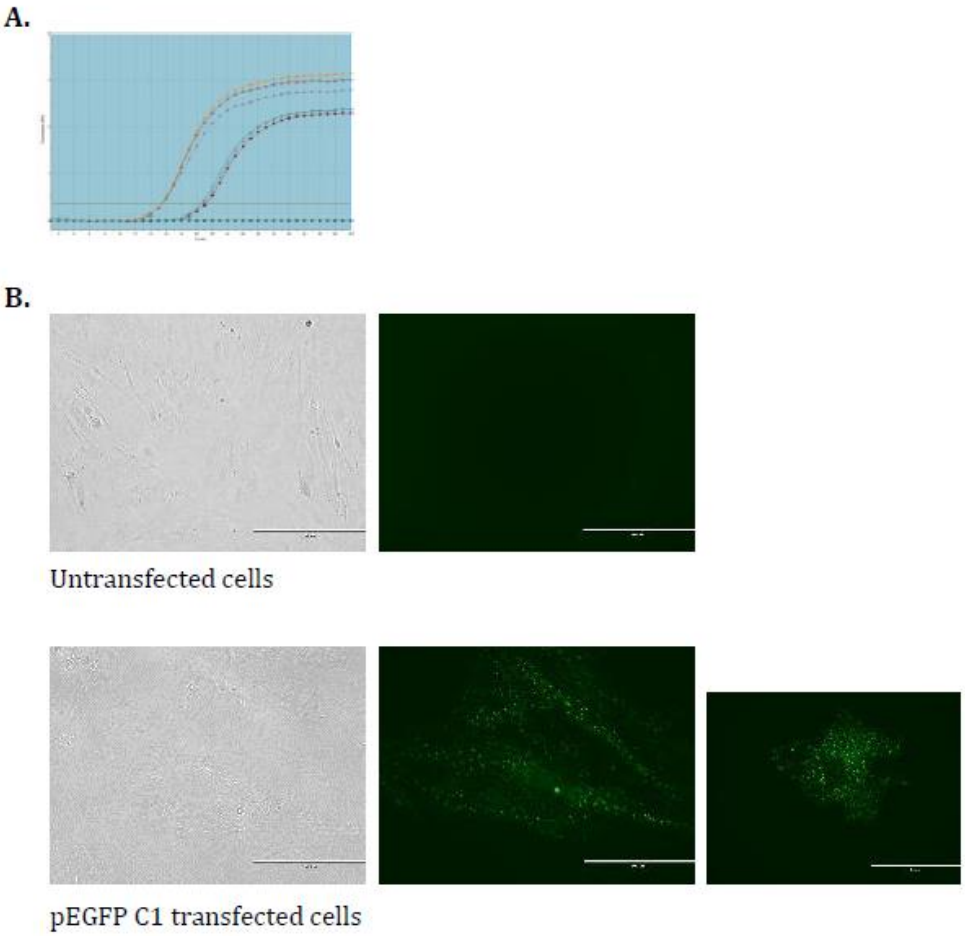

Figure 3.42: Successful delivery of pEGFP containing tensin1 construct in HASMCs. (A) Successful delivery of the construct was assessed using qPCR. Transfected cells expressed higher levels of tensin1 when compared to untransfected cells. **(B)** Overexpression of pEGFP containing tensin1 construct was assessed also using a conventional immunofluorescence microscope. Transfection was confirmed as adhesion staining was observed in the transfected and not in the untransfected cells.

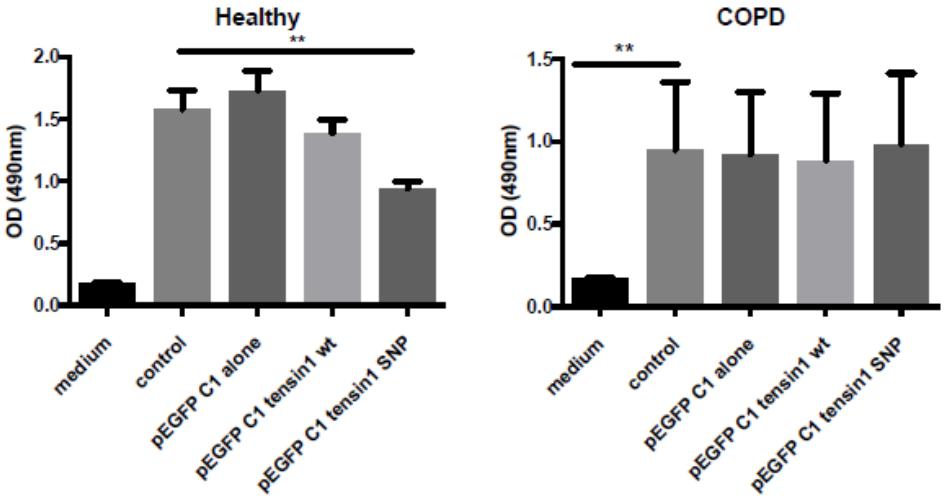

Figure 3.43: Delivery of pEGFP C1 containing mutant tensin1 has an effect on cell proliferation/survival on healthy subjects illustrated by MTS assay. Cells were transfected with pEGFP C1 constructs containing tensin1, wild-type and mutant. After successful delivery of the constructs, cell viability was assessed by MTS assay. Construct transfections did not have any effect on HASMC proliferation/survival rates derived from COPD subjects (n=3) when compared to the controls. However, construct transfection containing mutant tensin1 resulted in significantly decreased proliferative ability of HASMC derived from healthy subjects (n=3) when compared to controls (mean ± sem) (**p<0.01).

3.6.3 Transfection of COPD-derived HASMCs with pEGFP C1 containing the wild-type and mutant tensin1-effects on contraction in collagen gels

Genotyping subjects revealed the presence of the homozygous -CC- variant (which generates R1197) only in healthy subjects, while COPD subjects were predominantly heterozygotes -TC- or occasionally homozygotes -TT- (which generates R1197W). Therefore, it was of interest to examine whether introduction of the pEGFP C1 constructs containing the -CC- wild-type and -TT-SNP tensin1 could have an effect on HASMC collagen gel contraction. This experiment was performed on 3 COPD subjects. Representative examples of HASM collagen gel assays after transfection of cells with the pEGFP C1 constructs can be seen in **Figure 3.46**. A series of images of the collagen gels were taken and the extent of spontaneous gel contraction was assessed at 4, 18, 24 and 48 h using two-way ANOVA with Sidak's multiple comparison test (**Figure 3.44**). Quantification of contraction by % of gel area measurement revealed similar ability of the cells to contract despite genotype (**Figure 3.45**).

The effect of bradykinin, a contractile agonist, was also examined. HASMCs were transfected with the pEGFP C1 constructs and the appropriate controls. A series of images of the collagen gels were taken and extend of spontaneous gel contraction was assessed at 1, 2, 3, 4, 18, 24 and 48 h using two-way ANOVA with Sidak's multiple comparison test (**Figure 3.46**). Quantification of contraction by % of gel area measurement revealed slightly increased ability of the cells to contract following bradykinin stimulation in the non-transfected, pEGFP C1 alone and pEGFP C1 containing wild-type tensin1, when compared to non-stimulated cells. However, this did not reach significance. Bradykinin

stimulation of the pEGFP C1 containing mutant tensin1 did not have any effect on contraction, when compared to non-stimulated cells (**Figure 3.46**). This was assessed using one-way ANOVA with Dunnett's multiple comparison test.

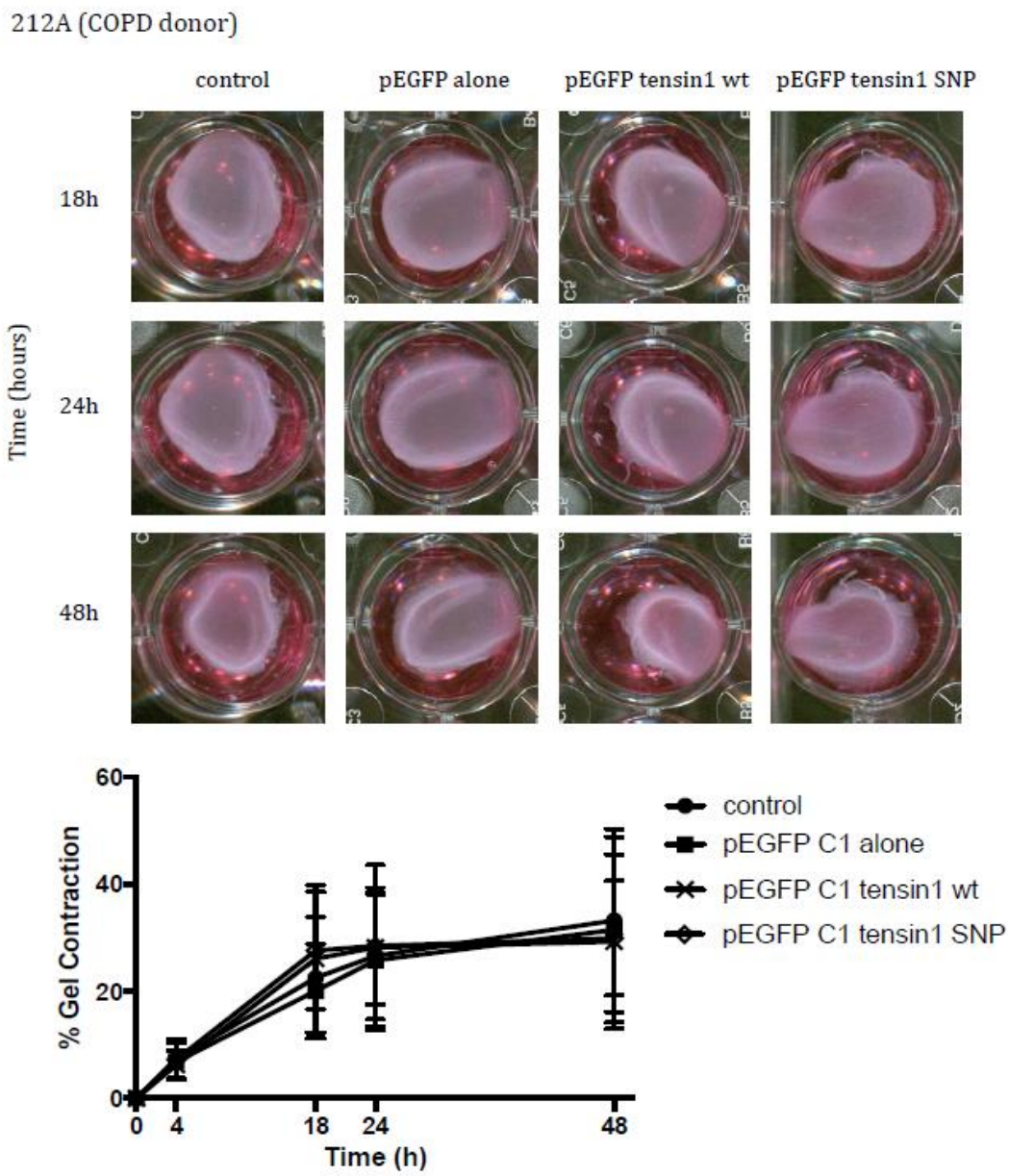

Figure 3.44: The effect of overexpression of pEGFP C1 containing the wild-type and SNP tensin1 on contraction in COPD subjects. HASMCs derived from COPD subjects were transfected with the pEGFP C1 construct containing the wild-type (homozygous –CC-) and SNP (heterozygous –TT-) tensin1 and incubated within 3D collagen gels, along with untransfected and pEGFP alone control cells. The extend of spontaneous gel contraction was assessed at 4, 18, 24 and 48 h. Assays were performed on 3 COPD subjects.

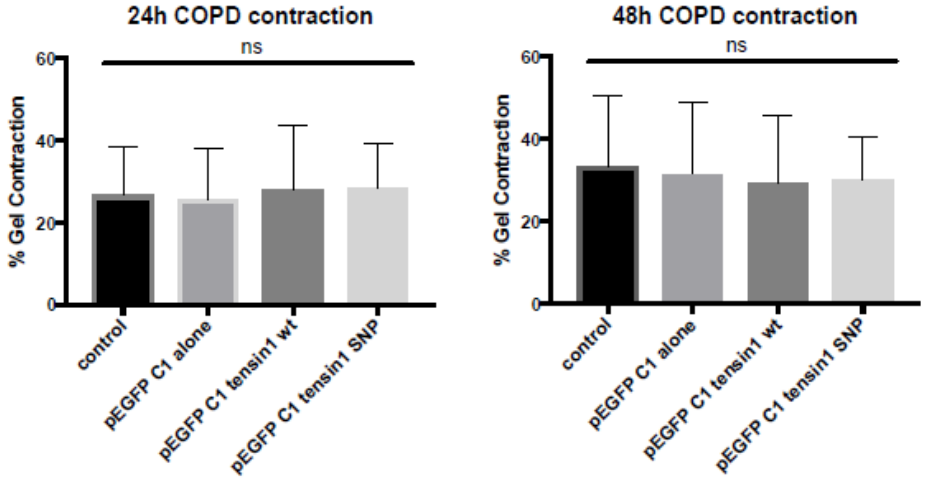

Figure 3.45: Extend of contraction of cells transfected with pEGFP C1 containing the homozygous (-CC-) wild-type and homozygous (-TT-) SNP tensin1 at 24 and 48 h. Quantification of collagen gel contraction shown in COPD (n=3) subjects was performed at 24 and 48 hour incubation (mean±sem). pEGFP C1 transfection containing either wild-type or mutant tensin1 did not impair the ability of the cells to contract.

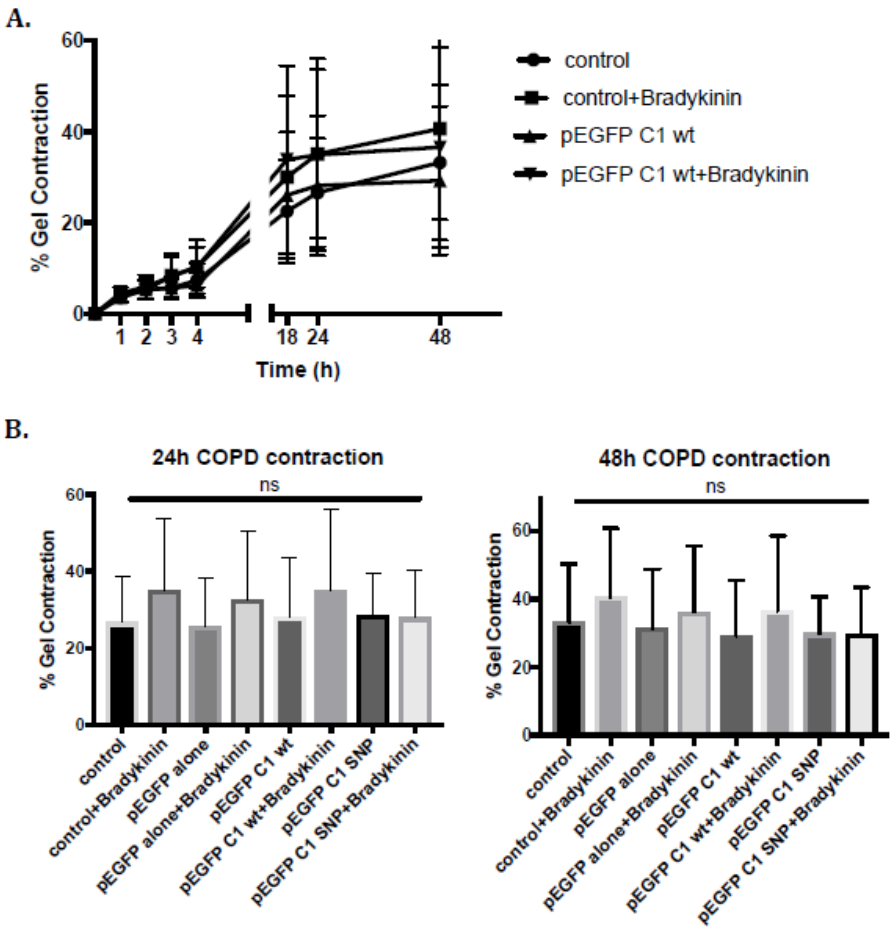

Figure 3.46: Bradykinin does not have a significant effect on HASMC contractility derived from COPD subjects. (A) HASMCs derived from COPD subjects were transfected with the pEGFP C1 construct containing the wild-type and SNP tensin1 and incubated within 3D collagen gels. HASMCs were then stimulated with bradykinin. The extend of spontaneous gel contraction was assessed at 1, 2, 3, 4, 18, 24 and 48 h. Assays were performed on 3 COPD subjects. **(B)** Quantification of collagen gel contraction shown in COPD (n=3) subjects was performed at 24 and 48 hour incubation (mean±sem). Bradykinin did not have a significant effect on contraction in all different conditions.

3.6.4 Transfection of healthy-derived HASMCs with pEGFP C1 containing the wild-type and mutant tensin1-effects on contraction in collagen gels

As mentioned above, genotyping subjects revealed the presence of the homozygous -CC- variant (which generates R1197) only in healthy subjects. It was of interest to examine whether introduction of the pEGFP C1 constructs containing the -CC- wild-type and -TT- SNP tensin1 could impair HASMC contraction. This experiment was performed on 3 healthy subjects. Representative examples of HASM collagen gel assays after transfection of cells with the pEGFP C1 constructs can be seen in **Figure 3.47**. A series of images of the collagen gels were taken and the extent of spontaneous gel contraction was assessed at 4, 18, 24 and 48 h using two-way ANOVA with Sidak's multiple comparison test (**Figure 3.47**). Quantification of contraction by % of gel area measurement revealed a significantly decreased ability of the cells to contract ($p=0.0382$) spontaneously following transfection with the pEGFP C1 constructs containing wild-type (-CC-) and mutant (-TT-) tensin1 (**Figure 3.48**).

The effect of bradykinin, a contraction agonist, was also examined. Again, HASMCs were transfected with the pEGFP C1 constructs and the appropriate controls. A series of images of the collagen gels were taken and extend of spontaneous gel contraction was assessed at 1, 2, 3, 4, 18, 24 and 48 h using two-way ANOVA with Sidak's multiple comparison test (**Figure 3.49**). Quantification of contraction was performed by % of gel area measurement. Bradykinin stimulation of cells did not have a significant effect on contraction in all four different conditions.

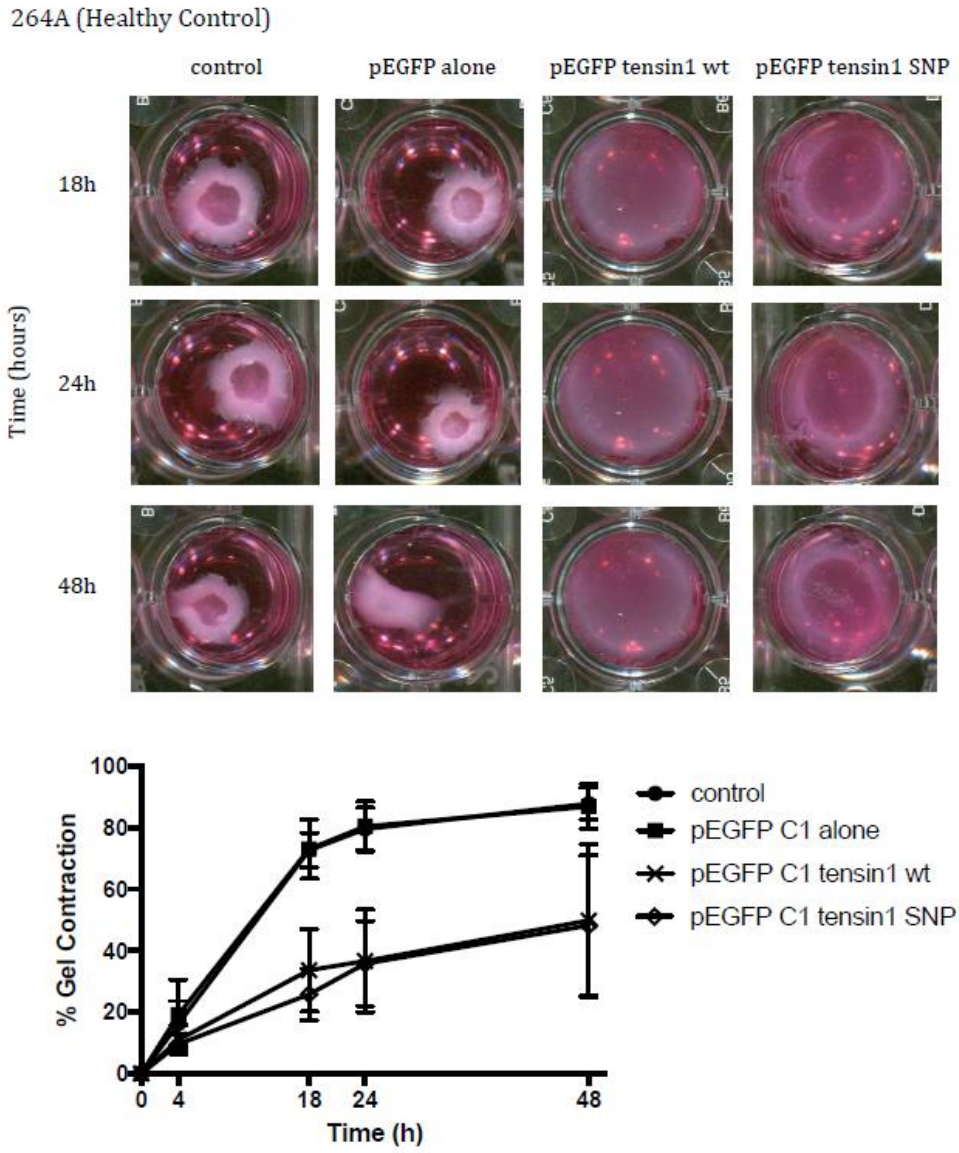

Figure 3.47: The effect of overexpression of pEGFP C1 containing the wild-type and SNP tensin1 on contraction in healthy subjects. HASMCs derived from healthy subjects were transfected with the pEGFP C1 construct containing the wild-type and SNP tensin1 and incubated within 3D collagen gels, along with untransfected and pEGFP alone control cells. The extend of spontaneous gel contraction was assessed at 4, 18, 24 and 48 h. Assays were performed on 3 healthy subjects.

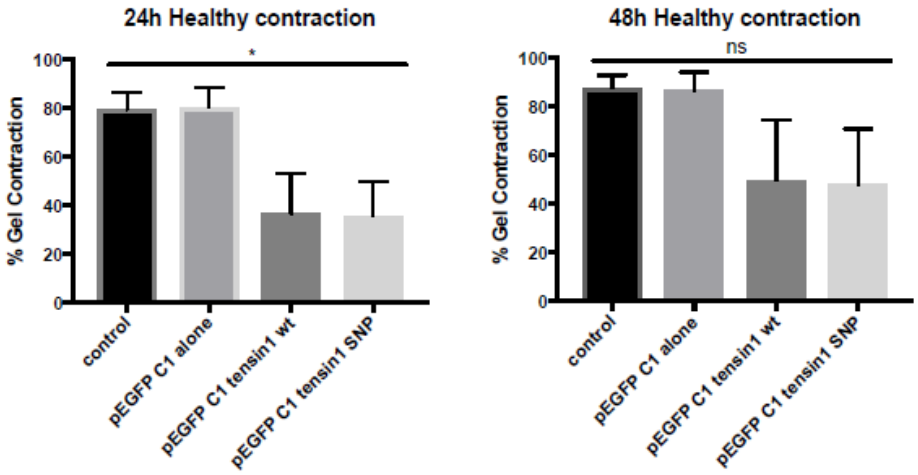

Figure 3.48: Extend of contraction of cells transfected with pEGFP C1 containing the homozygous (-CC-) wild-type homozygous (-TT-) SNP tensin1 at 24 h and 48 h. Quantification of collagen gel contraction shown in healthy subjects (n=3) was performed at 24 and 48 hour incubation. Decreased contractility was observed in the transfected cells when compared to controls (*$p<0.05$).

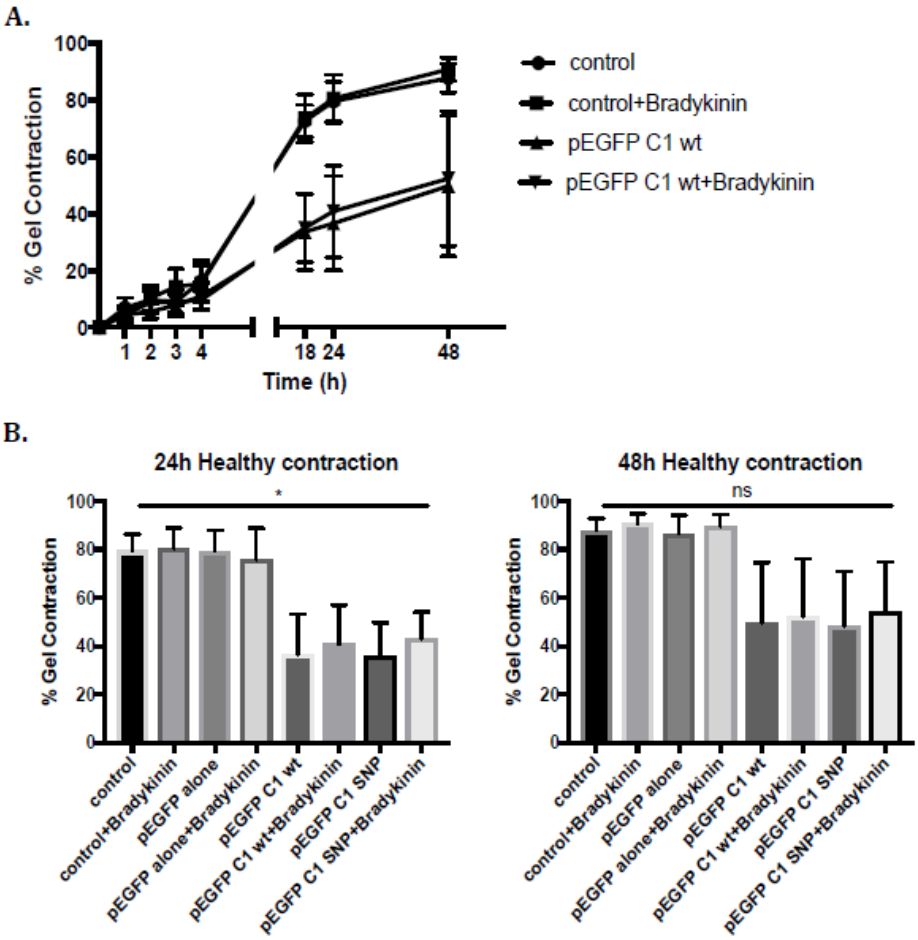

Figure 3.49: Bradykinin stimulation does not have a significant effect on HASMC contractility derived from healthy subjects. (A) HASMCs derived from healthy subject were transfected with the pEGFP C1 construct containing the wild-type and SNP tensin1 and incubated within 3D collagen gels. HASMCs were then stimulated with bradykinin. The extend of spontaneous gel contraction was assessed at 1, 2, 3, 4, 18, 24 and 48 h. Assays were performed on 3 healthy subjects. **(B)** Quantification of collagen gel contraction shown in healthy (n=3) subjects was performed at 24 and 48 hour incubation (mean±sem). Bradykinin did not have a significant effect on contraction in all different conditions (*p<0.05).

Chapter 4: Discussion

4.1 Localisation of Tensin1 in Endobronchial Biopsies and Lung Resections

This is the first study to investigate the protein localisation and expression of tensin1 in both healthy and asthmatic endobronchial biopsies and healthy and COPD lung resections. Two tensin1 antibodies were tested and revealed identical immunostaining on lung resections. Specificity of immunostaining was confirmed using isotype controls. Antibodies were further validated using immunoprecipitation and siRNA downregulation. Positive tensin1 immunoreactivity was detected in the apical epithelium, ASM bundles and lamina propria in in both healthy and COPD lung resections (small airways), and healthy and asthmatic endobronchial biopsies (large airways). A significant increase of tensin1 immunostaining was detected in the ASM and lamina propria in COPD subjects when compared to healthy controls, but no differences were evident between asthma and health. However, this might be the result of differential tensin1 expression in different airway compartments (small and large airways) or it might be disease specific. A recent study revealed increased tensin1 expression in fibroblastic foci from lungs with idiopathic pulmonary fibrosis (IPF), when compared to healthy tissue (Bernau et al. 2016). It is possible that tensin1 might be involved in the pathological remodelling evident in both COPD and IPF.

To help evaluate the role of tensin1 in COPD, correlations between tensin1 immunostaining and FEV_1 and FEV_1/FVC ratio were examined. FEV_1 and FEV_1/FVC ratio are routinely used as measures of airway obstruction. Although, a non-synonymous SNP (rs2571445) in the TNS1 gene is associated with airflow obstruction in GWAS studies (Repapi et al. 2010), here there was

no significant correlation between the extent tensin1 immunostaining and the FEV_1 value or FEV_1/FVC ratio. However, correlations should only be considered to be hypothesis-generating as they do not in themselves confirm cause and effect, and the absence of significant correlations between tensin1 expression and lung function does not therefore exclude a role for tensin1 in COPD pathogenesis.

4.2 Tensin1 mRNA and Protein Expression in Human Airway Structural Cells

Tensin1 mRNA and protein expression were evident in human airway structural cells. In this study, we have shown tensin1 mRNA expression in all HASMCs, HBECs and HLMFs tested. Relatively low expression of tensin1 was detected in the HBECs when compared to the other two cell types, consistent with our immunohistochemistry data revealing localisation of tensin1 mainly in the apical region of the epithelium. Similar levels of tensin1 mRNA and protein expression were detected in HASMCs derived from healthy and COPD subjects investigated using qRT-PCR and confocal immunofluorescence staining respectively. This indicates a disconnect between the increased tensin1 expression present in tissue, and that present in cultured HASMCs. This is most likely a consequence of the removal of the cultured cells from their normal airway microenvironment, and suggests that there is not an underlying genetic or epigenetic abnormality that explains the differences seen in vivo. However, we also need to take in consideration that tensin1 expression in tissue was examined on lung resections, specimens derived from the small airways of subjects. Whereas, these experiments were performed on primary cells derived from endobronchial biopsies and this might indicate that increased expression of tensin1 occurs only in the small airways of COPD subjects, and not in the large airways. Thus, examining tensin1 expression in primary cells grown from lung resections is of particular interest in order to understand tensin1 expression in disease and in the airways in general.

Confocal immunofluorescence staining revealed cytoskeletal focal and fibrillar adhesion localisation of the tensin1 protein. It is previously established that

tensin1 exhibits similar affinity for both $\alpha_V\beta_3$ and $\alpha_5\beta_1$ integrins and is responsible for the translocation of $\alpha_5\beta_1$ integrin to fibrillar adhesions. Therefore, tensin1 localisation in both focal and fibrillar adhesions is expected (Pankov et al. 2000, Chen et al. 2000).

The effect of two factors, TGFβ1 and fibronectin, on tensin1 expression was then examined. TGFβ1 constitutes a key mediator of inflammatory, fibrotic and remodelling diseases. It has been shown that TGFβ in general can result in ASM hypertrophy and hyperplasia (Goldsmith et al. 2006, Cohen et al. 2000). Fibronectin constitutes a rigid extracellular matrix component that is mainly bound to $\alpha_5\beta_1$ integrin and therefore tensin1 in fibrillar adhesions (Zamir et al. 2000). It has been demonstrated that increased expression of fibronectin occurs in obstructed COPD patients when compared to non-obstructed COPD and healthy subjects and its expression is inversely correlated with lung function (Annoni et al. 2012). Furthermore, the roles of fibronectin in stiffening the overall airway wall and impairing the relaxation of ASM cells in the presence of bronchoconstrictors have been illustrated suggesting its importance in COPD pathogenesis (Bidan et al. 2015). As a consequence, it was of a particular interest to examine the effect that these factors may have on tensin1 expression and localisation. TGFβ1 stimulation resulted in a significant increase in tensin1 mRNA expression in HASMCs derived from both healthy and COPD subjects. Confocal immunofluorescence staining for tensin1 after stimulation of the cells with TGFβ1 and/or fibronectin did not result in an overall increase of tensin1 protein expression, but the distribution of tensin1 immunostaining was markedly affected. A significant increase in the length of the adhesions was

observed after TGFβ1 and/or fibronectin stimulation. The response of the cells to these two growth factors was largely similar irrespective of their source. This is particularly interesting as these regions are extremely important for the interaction of tensin1 with other proteins (such as $\alpha_5\beta_1$ integrin (McCleverty et al. 2007), actin and vinculin (Zamir et al. 2000, Romer et al. 2006), which enables its participation in several signaling pathways (JNK and p38 pathway) (Katz et al. 2000b). Since the completion of this study, Bernau et al. (Bernau et al. 2016) demonstrated the effect of these two components in the formation of fibrillar adhesions in cultured HLMFs derived from healthy and IPF subjects. Furthermore, it has been previously reported that TGFβ1 can alter organisation of another type of adhesions, the adherens junction (Leikauf et al. 2012). These findings suggest that TGFβ1 and fibronectin are of a great significance for the reorganisation of tensin1-dependent adhesions from focal adhesions to fibrillar adhesions.

To summarise, tensin1 expression was studied extensively in this set of experiments in HASMCs. Tobacco smoking and air pollution constitute the two main causative factors for the development of COPD. However, it has been reported that association of tensin1 with COPD was not attenuated by qualitative or quantitative adjustments for smoking exposure in a GWAS study (Soler Artigas et al. 2011). Our dataset was too small to examine the effect of cigarette smoke on tensin1 expression. However, this can also be examined in air pollution and cigarette smoke-induced animal models. Animal models offer the advantage of recapitulating critical features of human disease in a short time frame and as a consequence facilitating the testing of novel therapeutics (Vlahos

et al. 2006). COPD exacerbations for example, the feature of COPD accounting for the increased rate of disease progression, can be induced on animal models using LPS installation, bacterial or viral infections and components involved can be easily identified (Spond et al. 2004, Drannik et al. 2004, Donovan et al. 2016).

4.3 Tensin1 and αSMA Association in HASMCs

Tensin1 localises in the integrin-mediated focal and fibrillar adhesions and this enables its interaction with several proteins (McCleverty et al. 2007). In particular, its N-terminus contains an actin-binding domain (ABD) I a and b, localised in the third quarter of its amino acid sequence, that enables tensin1 interaction with actin filaments (Lo 2004, Weigt et al. 1992). Actins, in general, are highly conserved proteins in eukaryotic cells and the actin filaments form part of the cytoskeleton, which have an extremely important role in cell shape and movement (Pollard and Cooper 2009). Association of tensin1 with F-actin has been established and illustrated in several studies (Zamir et al. 2000, Bernau et al. 2016). F-actin is a filamentous actin important for several cellular functions, such as mobility and contraction of cells during division (Onfelt et al. 2006). αSMA is abundant in HASMCs and it is mostly localised in the stress fibers, contractile organelles responsible for actin polymerisation and modulation of tension (Skalli et al. 1986, Katoh et al. 1998). For the first time, we show that tensin1 co-localises and correlates with αSMA in both health and disease in HASMCs. This is of significance as αSMA is involved in many processes related to airway hyperresponsiveness and remodelling (Tang 2015). This is discussed further below.

4.4 Effect of Tensin1 Silencing on HASMC Function

As discussed above, we have examined tensin1 expression in human lung tissue and airway cells derived from healthy and COPD subjects and are the first to report increased tensin1 expression in the airway smooth muscle in COPD subjects, when compared to healthy controls. However, the function of tensin1 in the airways needed to be elucidated. A knockdown method was pioneered to examine this. Survival and proliferation was firstly assessed in HASMCs following tensin1 silencing, as impaired proliferation of airway cells can be the reason for airway remodelling and obstruction seen in COPD (Burgess et al. 2009, Xia et al. 2013). Furthermore, a study revealed that tensin1 overexpression resulted in activation of two pathways, the JNK and p38 pathway, pathways with an established role in proliferation (Katz et al. 2000b). So, it was of particular interest to examine the role of tensin1 in this process. Tensin1 silencing did not have any effect on the proliferation of the cells as HASMCs derived from both healthy and COPD subjects revealed similar ability to proliferate. Interestingly, another study showed that tensin3, another member of the tensin family, also did not demonstrate any role in cellular proliferation (Martuszewska et al. 2009). This suggests that tensin1 is not contributing to COPD pathogenesis by promoting the proliferative properties of ASM cells in the airways.

So far, we have showed that tensin1 co-localises and interacts physically with αSMA in actin stress fibres. However, it was unknown whether tensin1 can regulate αSMA expression, mRNA and protein. Intriguingly, tensin1 silencing produced a marked downregulation of expression on both the mRNA and protein level of αSMA. Downregulation of αSMA mRNA expression indicates a defect in

the transcriptional process of αSMA caused by tensin1 depletion. The function of αSMA transcription factor may be inhibited by tensin1 knockdown. Impaired function of a transcription factor involves impaired splicing and histone methylation, processes essential for regulation of transcription. This suggests a potential positive feedback loop between the two proteins. As mentioned above αSMA is involved in several processes in eukaryotic cells and it is of extreme importance for HASMCs, as it is the most abundant protein and contributes to their contractility. It has been shown previously that short-term exposure of ASM tissue to actin polymerization inhibitors resulted in profound inhibition of the cells' shortening or constriction (Smith et al. 2005). The role of tensin isoforms, and tensin1 in particular, in cell-matrix interactions has been shown previously as tensin-silenced fibroblasts exhibited a strongly reduced ability to contract (Clark et al. 2010, Saintigny et al. 2008). The question that has risen from this was whether tensin1-depleted HASMCs would be able to retain their contractile properties.

Although the mechanism of upregulated tensin1 expression in COPD tissue is unclear, TGFβ1 is upregulated in COPD airways and a likely contributory factor. Furthermore, the ability of TGFβ1 to promote the formation of long tensin1 fibrillar adhesions, the strong co-localisation of tensin1 to αSMA stress fibres, and evidence of a physical interaction between tensin1 and αSMA, suggested that tensin1 might contribute to the contractile properties of HASMCs. This was clearly the case, as silencing of tensin1 markedly reduced the ability of HASMCs in collagen gels to contract. Therefore, tensin1 appears to make an important contribution to the contractile properties of HASMCs and this observation

provides the first insight into how the GWAS signals linking a TNS1 SNP to airflow obstruction (Repapi et al. 2010) and COPD (Soler Artigas et al. 2011) may be relevant to disease pathogenesis. Increased expression of contractile proteins, and in particular αSMA has been demonstrated in the airways of COPD subjects supporting the hypothesis that tensin1 might contribute to the development of airway obstruction and COPD (Lofdahl et al. 2011) through its interaction with αSMA and ability to enhance the contractile properties of HASMCs. TGFβ1 did not have any effect on HASMC contractile properties on non-stimulated and tensin1-depleted cells. This has also been demonstrated by another study illustrating the effect of TGFβ1 on HASMC proliferation, but not on contraction (Stamatiou et al. 2012).

The above observations indicate that tensin1 plays a significant role in HASMC contraction. However, tensin1 expression was not increased in asthma compared to health, suggesting that there is something specific to COPD which leads to increased expression. COPD is characterised by fixed airflow obstruction, and it is often assumed that the contribution of ASM contraction is limited as β2-agonist bronchodilators are of poor efficacy. However an alternative hypothesis is that there is drug resistant bronchoconstriction in COPD, and if true, that overexpression of tensin1 and perhaps altered tensin1 function, in someway linked to tryptophan at amino acid 1197, contributes to this.

Finally to further evaluate the functional role of tensin1 in HASMCs and COPD in general, molecular inhibitors can be used. There is a major need to develop new treatments for COPD and recent advances in understanding the cellular and molecular mechanisms underlying disease led to the discovery of several

components involved in these processes. The role of muscarinic receptors in generating bronchoconstriction in COPD has been established and inhibitors can be used to induce bronchodilation in the airways of COPD subjects (Selivanova et al. 2012). An example is the tiotropium bromide and it has recently become available in some countries. Leukotriene B4, TNF-α and NF-κB inhibitors are examples of components that can be used for the treatment and management of COPD (Markham and Lamb 2000, Nasuhara et al. 1999, Crooks et al. 2000). Leukotriene B4 contributes to the recruitment of neutrophils in the airways and the use of specific antagonist resulted in resolving neutrophilic inflammation (Crooks et al. 2000). TNF-α inhibitors have also been used for the management of other chronic diseases such as rheumatoid arthritis and it has been shown that increased levels of TNF-α can result in activation of the NF-κB pathway and subsequently activation of other cytokines (Markham and Lamb 2000). These molecular inhibitors can be used on tensin1 knockdown experiments to determine its role in resolving or worsen processes involved in COPD pathophysiology and to examine its potential as a therapeutic target.

4.5 Prevalence of R1197W SNP in Healthy and COPD Subjects and its Effects on Cell Function

The GWAS studies (Repapi et al. 2010, Soler Artigas et al. 2011) revealed the association of the non synonymous SNP (rs2571445) in the TNS1 gene with lung function on the risk of chronic obstructive pulmonary disease. The same non synonymous SNP in TNS1 gene was also associated with more transient early wheeze and therefore lung function in early childhood in another GWAS study (Kerkhof et al. 2014). The base pair change encoded by this SNP leads to the amino acid substitution R1197W (arginine to tryptophan). The SNP is present in approximately 40% of the population, and its presence was actually associated with reduced lung function in the GWAS study (Repapi et al. 2010). It was therefore remarkable, that in spite of the relatively small number of subjects, there was very strong segregation between homozygotes for R1197 (-CC-, arginine) who were largely healthy, and patients with COPD and asthma who were predominantly heterozygous (-CT-) or occasionally homozygous (-TT-) for tryptophan. This data supports the GWAS findings, and suggests that R1197 is potentially protective against the development of COPD in smokers, or alternatively, the presence of tryptophan in tensin1 is an important co-factor promoting the development of COPD. However, asthmatic subjects revealed a similar genotype with COPD subjects suggesting that the mutation is involved in a pathological feature common in both diseases.

Tensin1 protein expression was upregulated in the ASM bundles in COPD patients, but it seems unlikely that the different genotypes influencing amino acid 1197 play a role as tensin1 mRNA and protein expression in HASMCs from

health and COPD in vivo were similar. Furthermore, the expression response to TGFβ1 exposure in vitro was similar between both health and COPD. However, it is possible that there is a differential response to stimulation by other pro-inflammatory mediators present in COPD or a longer exposure to TGFβ1, or that the genotype is a co-factor influencing gene expression, for example in response to airway stretch. These various hypotheses will need testing in future work. Tensin1 depletion markedly reduced the ability of HASMCs to contract and this response was similar irrespective of the source of the cells. Therefore, examining the effect of R1197W SNP on the contractile properties of HASMCs was of particular interest. Subjects with R1197 tensin1 had a trend towards increased contraction compared to heterozygotes, but this was not statistically significant Increasing the sample size and examining the effects of contractile agonists will be important in future experiments.

4.6 Effect of Overexpression of Wild-Type and Mutant Tensin1 on Cell Function

Genotyping subjects revealed the presence of the homozygous -CC- variant (which generates R1197) only in healthy subjects, while COPD subjects were predominantly heterozygotes -TC- or occasionally homozygotes -TT- (which generates R1197W). This strong division was compelling and therefore the effect of the two different genotypes on functional responses was examined using an overexpression technology. As previously mentioned, the R1197W SNP is associated with reduced FEV_1 in a GWAS study (Repapi et al. 2010). Therefore, it was of interest to examine whether introduction of the pEGFP C1 constructs containing the -CC- wild-type and -TT- SNP tensin1 could have an effect on HASMC proliferation and collagen gel contraction derived from both healthy and COPD subjects. Transfection with both constructs did not have any effect on the survival and spontaneous proliferation of HASMCs derived from COPD subjects. However, HAMSCs derived from 3 healthy donors revealed decreased proliferative ability following transfection with the pEGFP C1 construct containing mutant tensin1 (-TT-), whereas transfection with the pEGFP C1 construct containing wild-type tensin1 (-CC-) had a minimal effect on HASMC proliferation. The reasons behind this discrepancy between COPD and health are not immediately obvious, and before making firm conclusions it will be important to increase the number of experiments. The results are also counter intuitive, as we would have expected that if anything, the disease –TT- construct would increase healthy HASMC proliferation because increased ASM mass is a feature of both COPD and asthma.

So far, we have shown that HASMC contraction is dependent on tensin1 and also that tensin1 expression is upregulated in the ASM bundles in COPD subjects. Hence, it was of great significance to examine the effect of the two tensin1 genotypes on HASMC contraction. Overexpression of tensin1, despite genotype, did not reduce or enhance the contractile properties of HASMCs derived from COPD subjects. However, HASMCs derived from healthy subjects revealed a greatly reduced contractility following overexpression of tensin1 despite genotype. Intriguingly, overexpression of tensin1 impaired both the proliferative and contractile properties of cells derived from healthy subjects suggesting a detrimental role of higher levels of tensin1 in the ASM. Again, the population size is too small to draw any firm conclusions. Furthermore, the cells were only transiently transfected with an efficiency of approximately 40%, which could result in the masking of any effect induced by overexpression of tensin1 by the untransfected cell population.

Bradykinin is a powerful bronchoconstrictor and its effects are mediated through $G\alpha_{q/11}$-coupled receptors present on HASM cells, which show an increase in cytosolic calcium concentrations $[Ca^{2+}]_i$ upon stimulation (Farmer, Ensor and Burch 1991). Bradykinin is widely used in experiments as a contractile agonist. HASMCs revealed a slightly increased ability to contract following bradykinin stimulation. Again, these are preliminary experiments which need further work before firm conclusions can be drawn. Studies suggest that the presence of cytokines, such as IL-1β and TNF-α, in patients can directly impair the calcium homeostasis and contribute to airway smooth muscle hyperresponsiveness to contractile agonists (Amrani and Panettieri 1998).

Therefore, stimulating cells with these cytokines may enhance response to the contractile agonist. Increasing the sample size is also important to further examine the effect of this contractile agonist.

4.7 Summary

In conclusion, we have demonstrated localisation of tensin1 in the airway smooth muscle, lamina propria and airway epithelium in human lung tissue. Tensin1 expression was increased in the airway smooth muscle and lamina propria cells in COPD donors when compared to healthy controls. Tensin1 is highly dynamic and is enriched in fibrillar adhesions upon stimulation with TGFβ1 and fibronectin and this is of great importance as it allows its interaction with other proteins and activation of signaling pathways. Tensin1 plays a critical role in regulating αSMA expression and contraction suggesting its importance in COPD pathology. Finally, preliminary data suggest that the R1197 tensin1 genotype is present predominantly in healthy subjects suggesting that the polymorphism R1197W constitutes a co-factor promoting the development of COPD.

4.8 Future Work

Firstly, tensin1 expression was examined in this study. Upregulated tensin1 expression was observed in the ASM bundles in COPD patients when compared to healthy controls. However, tensin1 expression was similar in HASMCs derived from both healthy and COPD subjects. Furthermore, the expression response to TGFβ1 exposure in vitro was similar between both health and COPD. It is possible that there is a differential response to stimulation by other pro-inflammatory mediators present in COPD or a longer exposure to TGFβ1. These various hypotheses will need testing in future work. Additionally, co-staining of tensin1 with integrins, $\alpha_5\beta_1$ and $\alpha_V\beta_3$ integrin will further demonstrate localisation of tensin1 in fibrillar adhesions mostly following TGFβ1 and fibronectin stimulation.

This study has also shown that tensin1 silencing inhibits αSMA mRNA and protein expression and contraction of HASMCs. Identifying the interacting partners of tensin1 is of extreme importance to define new therapeutic strategies in COPD. A recent study revealed that tensin1 inhibition of contraction was associated with a substantial reduction in Rho activity (Clark et al. 2010). A collagen contraction assay on tensin1 knockdown HASMCs stimulated with Rho inhibitor can be performed to examine whether tensin1 role in contraction is mediated by its interaction with Rho DLC-1 protein. Interaction of these two proteins is well established (Hall et al. 2010, Hall et al. 2009). Airway obstruction and COPD pathogenesis can be the result of impaired migratory properties of the cells (Parameswaran et al. 2006). Previous studies established the role of tensin1 in

migration and it will be of great significance to identify a role of tensin1 in cell migration in COPD (Chen et al. 2002, Hall et al. 2009).

Additionally, we have demonstrated a very strong segregation between homozygotes for R1197 (-CC-, arginine) who were largely healthy, and patients with COPD and asthma who were predominantly heterozygous (-CT-) or occasionally homozygous (-TT-). Subjects with R1197 tensin1 had a trend towards increased contraction compared to heterozygotes, but this was not statistically significant. Increasing the sample size and examining the effects of contractile agonists will be important in future experiments. Examining other functional responses, such as cell migration, is also of extreme importance in order to determine the role of the tensin1 variant in COPD pathogenesis.

Overexpression of constructs containing wild-type and mutant tensin1 in HASMCs derived from COPD subjects did not have any effect on their proliferative and contractile properties. However, HASMCs derived from healthy subjects revealed a greatly reduced proliferation and contractility following overexpression of tensin1 despite genotype. Increasing the sample size is essential in order to be able to draw any conclusions from this set of experiments. Finally, bradykinin, a contractile agonist, did not demonstrate any significant response in regards to the contractile properties of HASMCs following overexpression of both wild-type and mutant tensin1. Use of other contractile agonists and/or stimulation with cytokines stimulating contraction can be done in future experiments. As mentioned above, any effect induced by overexpression of tensin1 could be masked as only 40% of the cells were transiently transfected.

Developing a new overexpression model or improving the current one could facilitate observations.

Appendix

	HLMFs	
	Healthy	IPF
Age (y), mean±SEM	69±3.1	58.6±4.4
Gender (M/F)	3/4	6/1
FEV_1, mean±SEM	88.5±11.8	45.7±5.4
FVC, mean±SEM	79.8±4.3	64.7±3.9
Pack Years (y), mean±SEM	27.2±9.1	12.1±3.4
DLCO (% predicted), mean±SEM	ND	17.7±4.9
PA mean (% predicted), mean±SEM	ND	27.7±2.9
Treatment-Prednisone	0	7
Age of Onset, mean±SEM	NA	55.2±2.9

Table 1: Clinical characteristics of healthy controls and IPF subjects used for cell culture studies.

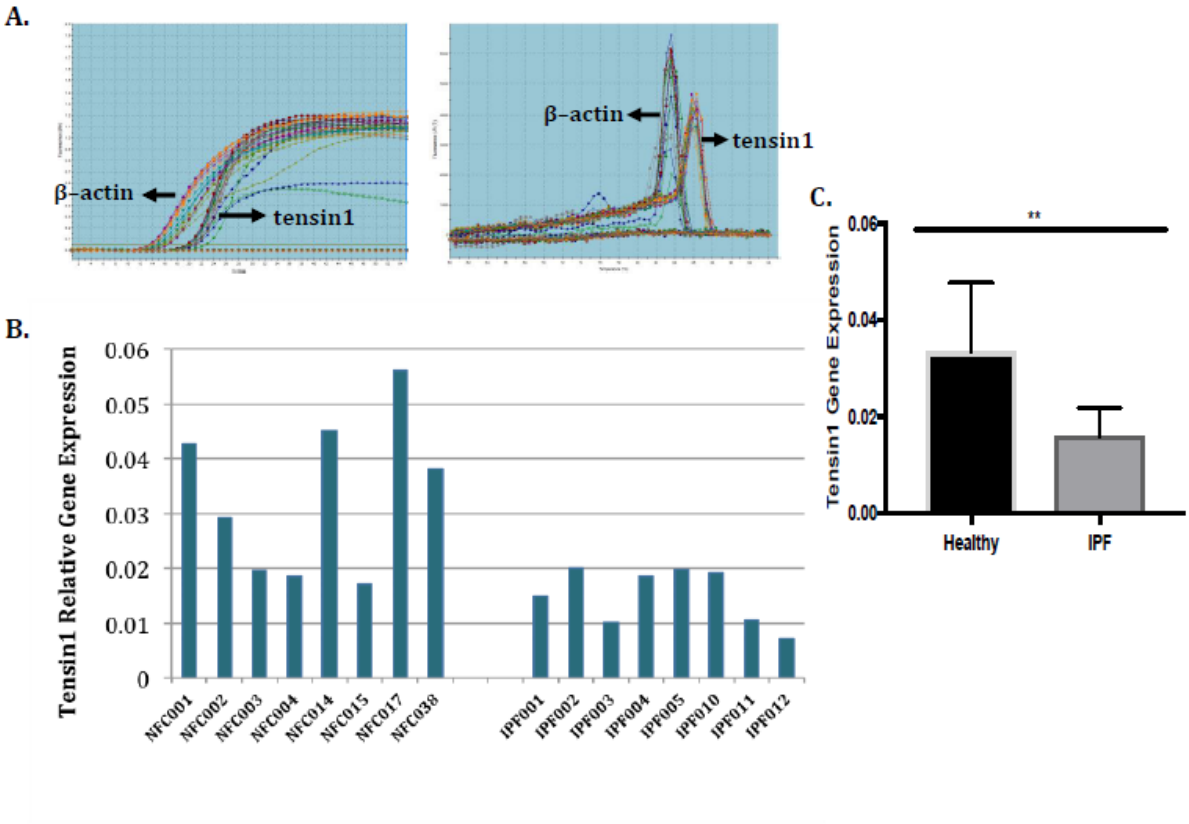

Figure 1: qRT-PCR showing expression of tensin1 in HLMF. (A) Tensin1 was detected in HLMF isolated from both patient with IPF and healthy controls, alongside the housekeeping gene β–actin. qPCR was used to quantify tensin1 expression in health and disease. Both, amplification and dissociation curves indicate the amplification of a single product. **(B)** The relative amount of tensin1 expression was calculated using the 2^-(ΔCt) method. **(C)** Graph illustrates the mean±sem relative tensin1 expression in healthy and disease subjects in HLMF (*p<0.05).

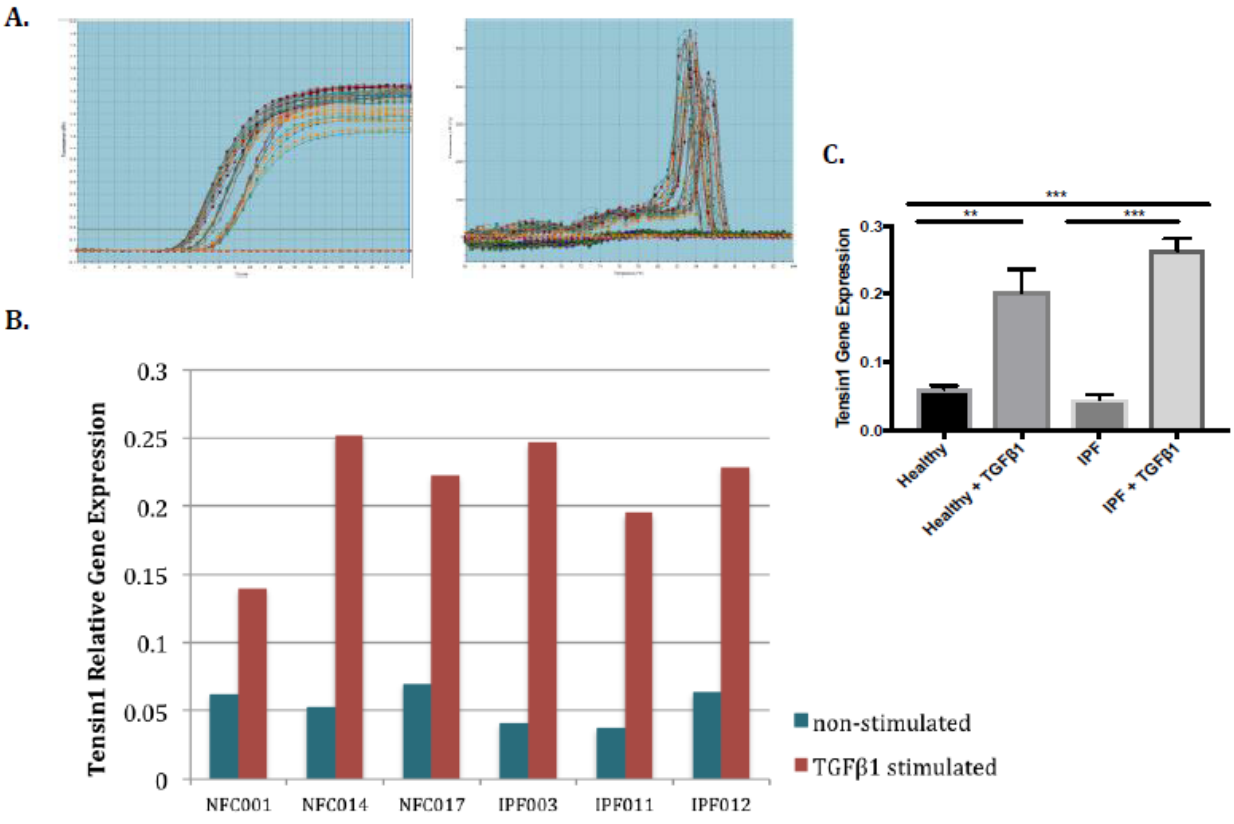

Figure 2: The effect of TGFβ1 on tensin1 mRNA expression in HLMF. (A) Cells were stimulated with TGFβ1 for 24 h. qPCR was used to quantify tensin1 expression in health and disease after stimulation with TGFβ1. **(B)** The relative amount of tensin1 expression calculated using the 2^-(ΔCt) method. **(C)** Graph shows the mean±sem relative tensin1 expression in healthy and disease subjects in HLMF. TGFβ1 significantly increased tensin1 expression in HLMF derived from both healthy and IPF subjects (**p<0.01, ***p<0.001).

References

(1985) The definition of emphysema. Report of a National Heart, Lung, and Blood Institute, Division of Lung Diseases workshop. *Am Rev Respir Dis,* 132**,** 182-5.

BTS (2001) British Thoracic Society guidelines on diagnostic flexible bronchoscopy. *Thorax,* 56**,** i1-i21.

Aalbers, R., J. Ayres, V. Backer, M. Decramer, P. A. Lier, P. Magyar, J. Malolepszy, R. Ruffin & G. W. Sybrecht (2002) Formoterol in patients with chronic obstructive pulmonary disease: a randomized, controlled, 3-month trial. *Eur Respir J,* 19**,** 936-43.

Abboud, R. T. & S. Vimalanathan (2008) Pathogenesis of COPD. Part I. The role of protease-antiprotease imbalance in emphysema. *Int J Tuberc Lung Dis,* 12**,** 361-7.

Abraham, S. N. & A. L. St John (2010) Mast cell-orchestrated immunity to pathogens. *Nat Rev Immunol,* 10**,** 440-52.

Adeloye, D., S. Chua, C. Lee, C. Basquill, A. Papana, E. Theodoratou, H. Nair, D. Gasevic, D. Sridhar, H. Campbell, K. Y. Chan, A. Sheikh & I. Rudan Global and regional estimates of COPD prevalence: Systematic review and meta–analysis. *J Glob Health,* 5.

Adler, J. & I. Parmryd (2010) Quantifying colocalization by correlation: the Pearson correlation coefficient is superior to the Mander's overlap coefficient. *Cytometry A,* 77**,** 733-42.

Agusti, A., P. Sobradillo & B. Celli (2011) Addressing the complexity of chronic obstructive pulmonary disease: from phenotypes and biomarkers to scale-free networks, systems biology, and P4 medicine. *Am J Respir Crit Care Med,* 183**,** 1129-37.

Allen, I. C., J. M. Hartney, T. M. Coffman, R. B. Penn, J. Wess & B. H. Koller (2006) Thromboxane A2 induces airway constriction through an M3 muscarinic acetylcholine receptor-dependent mechanism. *Am J Physiol Lung Cell Mol Physiol,* 290**,** L526-33.

Amrani, Y. & R. Panettieri (1998) Cytokines induce airway smooth muscle cell hyperresponsiveness to contractile agonists. *Thorax,* 53**,** 713-6.

Anderson, W. H., R. D. Coakley, B. Button, A. G. Henderson, K. L. Zeman, N. E. Alexis, D. B. Peden, E. R. Lazarowski, C. W. Davis, S. Bailey, F. Fuller, M. Almond, B. Qaqish, E. Bordonali, M. Rubinstein, W. D. Bennett, M. Kesimer & R. C. Boucher (2015) The Relationship of Mucus Concentration (Hydration) to Mucus Osmotic Pressure and Transport in Chronic Bronchitis. *Am J Respir Crit Care Med,* 192**,** 182-90.

Annoni, R., T. Lancas, R. Yukimatsu Tanigawa, M. de Medeiros Matsushita, S. de Morais Fernezlian, A. Bruno, L. Fernando Ferraz da Silva, P. J. Roughley, S. Battaglia, M. Dolhnikoff, P. S. Hiemstra, P. J. Sterk, K. F. Rabe & T. Mauad (2012) Extracellular matrix composition in COPD. *Eur Respir J,* 40**,** 1362-73.

Anzueto, A., D. Tashkin, S. Menjoge & S. Kesten (2005) One-year analysis of longitudinal changes in spirometry in patients with COPD receiving tiotropium. *Pulm Pharmacol Ther,* 18**,** 75-81.

Aoshiba, K. & A. Nagai (2004) Differences in airway remodeling between asthma and chronic obstructive pulmonary disease. *Clin Rev Allergy Immunol,* 27**,** 35-43.

Au, D. H., C. L. Bryson, J. W. Chien, H. Sun, E. M. Udris, L. E. Evans & K. A. Bradley (2009) The effects of smoking cessation on the risk of chronic obstructive pulmonary disease exacerbations. *J Gen Intern Med,* 24**,** 457-63.

Auger, K. R., Z. Songyang, S. H. Lo, T. M. Roberts & L. B. Chen (1996) Platelet-derived growth factor-induced formation of tensin and phosphoinositide 3-kinase complexes. *J Biol Chem,* 271**,** 23452-7.

Baarsma, H. A., M. H. Menzen, A. J. Halayko, H. Meurs, H. A. Kerstjens & R. Gosens (2011) beta-Catenin signaling is required for TGF-beta1-induced extracellular matrix production by airway smooth muscle cells. *Am J Physiol Lung Cell Mol Physiol,* 301**,** L956-65.

Bafadhel, M., S. McKenna, S. Terry, V. Mistry, C. Reid, P. Haldar, M. McCormick, K. Haldar, T. Kebadze, A. Duvoix, K. Lindblad, H. Patel, P. Rugman, P. Dodson, M. Jenkins, M. Saunders, P. Newbold, R. H. Green, P. Venge, D. A. Lomas, M. R. Barer, S. L. Johnston, I. D. Pavord & C. E. Brightling (2011) Acute exacerbations of chronic obstructive pulmonary disease: identification of biologic clusters and their biomarkers. *Am J Respir Crit Care Med,* 184**,** 662-71.

Barker, D. J., K. M. Godfrey, C. Fall, C. Osmond, P. D. Winter & S. O. Shaheen (1991) Relation of birth weight and childhood respiratory infection to adult lung function and death from chronic obstructive airways disease. *Bmj,* 303**,** 671-5.

Barnes, P. J. (1998) New therapies for chronic obstructive pulmonary disease. *Thorax,* 53**,** 137-47.

--- (2004) Alveolar macrophages as orchestrators of COPD. *Copd,* 1**,** 59-70.

Barnes, P. J., S. D. Shapiro & R. A. Pauwels (2003) Chronic obstructive pulmonary disease: molecular and cellular mechanisms. *Eur Respir J,* 22**,** 672-88.

Benayoun, L., A. Druilhe, M. C. Dombret, M. Aubier & M. Pretolani (2003) Airway structural alterations selectively associated with severe asthma. *Am J Respir Crit Care Med,* 167**,** 1360-8.

Bernau, K. P., E. E. Torr, M. D. Evans, J. K. Aoki, C. R. Ngam & N. Sandbo (2016) TNS1 is Essential for Myofibroblast Differentiation and Extracellular Matrix Formation. *Am J Respir Cell Mol Biol*.

Bidan, C. M., A. C. Veldsink, H. Meurs & R. Gosens (2015) Airway and Extracellular Matrix Mechanics in COPD. *Front Physiol,* 6**,** 346.

Black, P. N., P. S. Ching, B. Beaumont, S. Ranasinghe, G. Taylor & M. J. Merrilees (2008) Changes in elastic fibres in the small airways and alveoli in COPD. *Eur Respir J,* 31**,** 998-1004.

Bockholt, S. M. & K. Burridge (1993) Cell spreading on extracellular matrix proteins induces tyrosine phosphorylation of tensin. *J Biol Chem,* 268**,** 14565-7.

Bonnans, C., J. Chou & Z. Werb (2014) Remodelling the extracellular matrix in development and disease. *Nat Rev Mol Cell Biol,* 15**,** 786-801.

Borchers, M. T., S. C. Wesselkamper, V. Curull, A. Ramirez-Sarmiento, A. Sanchez-Font, J. Garcia-Aymerich, C. Coronell, J. Lloreta, A. G. Agusti, J. Gea, J. A. Howington, M. F. Reed, S. L. Starnes, N. L. Harris, M. Vitucci, B. L. Eppert, G. T. Motz, K. Fogel, D. W. McGraw, J. W. Tichelaar & M. Orozco-Levi (2009) Sustained CTL activation by murine pulmonary epithelial cells promotes the development of COPD-like disease. *J Clin Invest,* 119**,** 636-49.

Bosken, C. H., B. R. Wiggs, P. D. Pare & J. C. Hogg (1990) Small airway dimensions in smokers with obstruction to airflow. *Am Rev Respir Dis,* 142**,** 563-70.

Bourdoulous, S., G. Orend, D. A. MacKenna, R. Pasqualini & E. Ruoslahti (1998) Fibronectin matrix regulates activation of RHO and CDC42 GTPases and cell cycle progression. *J Cell Biol,* 143**,** 267-76.

Bozinovski, S., R. Vlahos, D. Anthony, J. McQualter, G. Anderson, L. Irving & D. Steinfort (2016) COPD and squamous cell lung cancer: aberrant inflammation and immunity is the common link. *Br J Pharmacol,* 173**,** 635-48.

Bradding, P., I. H. Feather, P. H. Howarth, R. Mueller, J. A. Roberts, K. Britten, J. P. Bews, T. C. Hunt, Y. Okayama, C. H. Heusser & et al. (1992) Interleukin 4 is localized to and released by human mast cells. *J Exp Med,* 176**,** 1381-6.

Brightling, C. E., A. J. Ammit, D. Kaur, J. L. Black, A. J. Wardlaw, J. M. Hughes & P. Bradding (2005) The CXCL10/CXCR3 axis mediates human lung mast cell migration to asthmatic airway smooth muscle. *Am J Respir Crit Care Med,* 171**,** 1103-8.

Brusasco, V., G. Barisione & E. Crimi (2015) Pulmonary physiology: future directions for lung function testing in COPD. *Respirology,* 20**,** 209-18.

Burgess, J. K., C. Ceresa, S. R. Johnson, V. Kanabar, L. M. Moir, T. T. Nguyen, B. G. Oliver, M. Schuliga & J. Ward (2009) Tissue and matrix influences on airway smooth muscle function. *Pulm Pharmacol Ther,* 22**,** 379-87.

Calverley, P., R. Pauwels, J. Vestbo, P. Jones, N. Pride, A. Gulsvik, J. Anderson & C. Maden (2003) Combined salmeterol and fluticasone in the treatment of chronic obstructive pulmonary disease: a randomised controlled trial. *Lancet,* 361**,** 449-56.

Calverley, P. M., J. A. Anderson, B. Celli, G. T. Ferguson, C. Jenkins, P. W. Jones, J. C. Yates & J. Vestbo (2007) Salmeterol and fluticasone propionate and survival in chronic obstructive pulmonary disease. *N Engl J Med,* 356**,** 775-89.

Caramori, G., P. Casolari & I. Adcock (2013) Role of transcription factors in the pathogenesis of asthma and COPD. *Cell Commun Adhes,* 20**,** 21-40.

Casaburi, R. (2000) Skeletal muscle function in COPD. *Chest,* 117**,** 267s-71s.

Caulfield, M. P. & N. J. Birdsall (1998) International Union of Pharmacology. XVII. Classification of muscarinic acetylcholine receptors. *Pharmacol Rev,* 50**,** 279-90.

Celli, B. R. & J. Vestbo. 2011. The EXACT-Pro: measuring exacerbations of COPD. In *Am J Respir Crit Care Med*, 287-8. United States.

Chang, Y., L. Al-Alwan, P. A. Risse, A. J. Halayko, J. G. Martin, C. J. Baglole, D. H. Eidelman & Q. Hamid (2012) Th17-associated cytokines promote human airway smooth muscle cell proliferation. *Faseb j,* 26**,** 5152-60.

Chen, H., I. C. Duncan, H. Bozorgchami & S. H. Lo (2002) Tensin1 and a previously undocumented family member, tensin2, positively regulate cell migration. *Proc Natl Acad Sci U S A,* 99**,** 733-8.

Chen, H., A. Ishii, W. K. Wong, L. B. Chen & S. H. Lo (2000) Molecular characterization of human tensin. *Biochem J,* 351 Pt 2**,** 403-11.

Chen, H. & S. H. Lo (2003) Regulation of tensin-promoted cell migration by its focal adhesion binding and Src homology domain 2. *Biochem J,* 370**,** 1039-45.

Chen, Y., P. Thai, Y. H. Zhao, Y. S. Ho, M. M. DeSouza & R. Wu (2003) Stimulation of airway mucin gene expression by interleukin (IL)-17 through IL-6 paracrine/autocrine loop. *J Biol Chem,* 278**,** 17036-43.

Chuang, J. Z., D. C. Lin & S. Lin (1995) Molecular cloning, expression, and mapping of the high affinity actin-capping domain of chicken cardiac tensin. *J Cell Biol,* 128**,** 1095-109.

Chung, K. F. (2005) The role of airway smooth muscle in the pathogenesis of airway wall remodeling in chronic obstructive pulmonary disease. *Proc Am Thorac Soc,* 2**,** 347-54; discussion 371-2.

Clark, K., J. D. Howe, C. E. Pullar, J. A. Green, V. V. Artym, K. M. Yamada & D. R. Critchley (2010) Tensin 2 modulates cell contractility in 3D collagen gels through the RhoGAP DLC1. *J Cell Biochem,* 109**,** 808-17.

Cohen, P., R. Rajah, J. Rosenbloom & D. J. Herrick (2000) IGFBP-3 mediates TGF-beta1-induced cell growth in human airway smooth muscle cells. *Am J Physiol Lung Cell Mol Physiol,* 278**,** L545-51.

Cooper, M. D. (2015) The early history of B cells. *Nat Rev Immunol,* 15**,** 191-7.

Crooks, S. W., D. L. Bayley, S. L. Hill & R. A. Stockley (2000) Bronchial inflammation in acute bacterial exacerbations of chronic bronchitis: the role of leukotriene B4. *Eur Respir J,* 15**,** 274-80.

Curkendall, S. M., C. DeLuise, J. K. Jones, S. Lanes, M. R. Stang, E. Goehring, Jr. & D. She (2006) Cardiovascular disease in patients with chronic obstructive pulmonary disease, Saskatchewan Canada cardiovascular disease in COPD patients. *Ann Epidemiol,* 16**,** 63-70.

Davi, G., S. Basili, M. Vieri, F. Cipollone, S. Santarone, C. Alessandri, P. Gazzaniga, C. Cordova & F. Violi (1997) Enhanced thromboxane biosynthesis in patients with chronic obstructive pulmonary disease. The Chronic Obstructive Bronchitis and Haemostasis Study Group. *Am J Respir Crit Care Med,* 156**,** 1794-9.

de Torres, J. P., J. M. Marin, C. Casanova, C. Cote, S. Carrizo, E. Cordoba-Lanus, R. Baz-Davila, J. J. Zulueta, A. Aguirre-Jaime, M. Saetta, M. G. Cosio & B. R. Celli (2011) Lung cancer in patients with chronic obstructive pulmonary disease--incidence and predicting factors. *Am J Respir Crit Care Med,* 184**,** 913-9.

Deacon, K. & A. J. Knox (2015) Human airway smooth muscle cells secrete amphiregulin via bradykinin/COX-2/PGE2, inducing COX-2, CXCL8, and VEGF

expression in airway epithelial cells. *Am J Physiol Lung Cell Mol Physiol,* 309**,** L237-49.

Decramer, M., W. Janssens & M. Miravitlles (2012) Chronic obstructive pulmonary disease. *Lancet,* 379**,** 1341-51.

Deslee, G., J. C. Woods, C. M. Moore, L. Liu, S. H. Conradi, M. Milne, D. S. Gierada, J. Pierce, A. Patterson, R. A. Lewit, J. T. Battaile, M. J. Holtzman, J. C. Hogg & R. A. Pierce (2009) Elastin expression in very severe human COPD. *Eur Respir J,* 34**,** 324-31.

Dillon, L. M. & T. W. Miller (2014) Therapeutic targeting of cancers with loss of PTEN function. *Curr Drug Targets,* 15**,** 65-79.

Donovan, C., H. J. Seow, J. E. Bourke & R. Vlahos (2016) Influenza A virus infection and cigarette smoke impair bronchodilator responsiveness to beta-adrenoceptor agonists in mouse lung. *Clin Sci (Lond),* 130**,** 829-37.

Drannik, A. G., M. A. Pouladi, C. S. Robbins, S. I. Goncharova, S. Kianpour & M. R. Stampfli (2004) Impact of cigarette smoke on clearance and inflammation after Pseudomonas aeruginosa infection. *Am J Respir Crit Care Med,* 170**,** 1164-71.

Eurlings, I. M., M. A. Dentener, J. P. Cleutjens, C. J. Peutz, G. G. Rohde, E. F. Wouters & N. L. Reynaert (2014) Similar matrix alterations in alveolar and small airway walls of COPD patients. *BMC Pulm Med,* 14**,** 90.

Evans, S. E., Y. Xu, M. J. Tuvim & B. F. Dickey (2010) Inducible innate resistance of lung epithelium to infection. *Annu Rev Physiol,* 72**,** 413-35.

Fahy, J. V. & B. F. Dickey (2010) Airway mucus function and dysfunction. *N Engl J Med,* 363**,** 2233-47.

Farmer, S. G., J. E. Ensor & R. M. Burch (1991) Evidence that cultured airway smooth muscle cells contain bradykinin B2 and B3 receptors. *Am J Respir Cell Mol Biol,* 4**,** 273-7.

Fediuk, J., A. S. Sikarwar, N. Nolette & S. Dakshinamurti (2014) Thromboxane-induced actin polymerization in hypoxic neonatal pulmonary arterial myocytes involves Cdc42 signaling. *Am J Physiol Lung Cell Mol Physiol,* 307**,** L877-87.

Fernandez-Valdivia, R., Y. Zhang, S. Pai, M. L. Metzker & A. Schumacher (2006) l7Rn6 encodes a novel protein required for clara cell function in mouse lung development. *Genetics,* 172**,** 389-99.

Foreman, M. G., M. Campos & J. C. Celedon (2012) Genes and chronic obstructive pulmonary disease. *Med Clin North Am,* 96**,** 699-711.

Fowlkes, J. L., J. J. Enghild, K. Suzuki & H. Nagase (1994) Matrix metalloproteinases degrade insulin-like growth factor-binding protein-3 in dermal fibroblast cultures. *J Biol Chem,* 269**,** 25742-6.

Gentzsch, M., H. Dang, Y. Dang, A. Garcia-Caballero, H. Suchindran, R. C. Boucher & M. J. Stutts (2010) The cystic fibrosis transmembrane conductance regulator impedes proteolytic stimulation of the epithelial Na+ channel. *J Biol Chem,* 285**,** 32227-32.

Giancotti, F. G. & E. Ruoslahti (1999) Integrin signaling. *Science,* 285**,** 1028-32.

Goldsmith, A. M., J. K. Bentley, L. Zhou, Y. Jia, K. N. Bitar, D. C. Fingar & M. B. Hershenson (2006) Transforming growth factor-beta induces airway smooth muscle hypertrophy. *Am J Respir Cell Mol Biol,* 34**,** 247-54.

Gosens, R., J. Zaagsma, H. Meurs & A. J. Halayko (2006) Muscarinic receptor signaling in the pathophysiology of asthma and COPD. *Respir Res,* 7**,** 73.

Gosman, M. M., D. S. Postma, J. M. Vonk, B. Rutgers, M. Lodewijk, M. Smith, M. A. Luinge, N. H. Ten Hacken & W. Timens (2008) Association of mast cells with lung function in chronic obstructive pulmonary disease. *Respir Res,* 9**,** 64.

Gosselink, J. V., S. Hayashi, W. M. Elliott, L. Xing, B. Chan, L. Yang, C. Wright, D. Sin, P. D. Pare, J. A. Pierce, R. A. Pierce, A. Patterson, J. Cooper & J. C. Hogg (2010) Differential expression of tissue repair genes in the pathogenesis of chronic obstructive pulmonary disease. *Am J Respir Crit Care Med,* 181**,** 1329-35.

Grabiec, A. M. & T. Hussell (2016) The role of airway macrophages in apoptotic cell clearance following acute and chronic lung inflammation. *Semin Immunopathol,* 38**,** 409-23.

Grashoff, W. F., J. K. Sont, P. J. Sterk, P. S. Hiemstra, W. I. de Boer, J. Stolk, J. Han & J. M. van Krieken (1997) Chronic obstructive pulmonary disease: role of bronchiolar mast cells and macrophages. *Am J Pathol,* 151**,** 1785-90.

Gross, N. J. & M. S. Skorodin (1984) Role of the parasympathetic system in airway obstruction due to emphysema. *N Engl J Med,* 311**,** 421-5.

Gross, P., E. A. Pfitzer, E. Tolker, M. A. Babyak & M. Kaschak (1965) EXPERIMENTAL EMPHYSEMA: ITS PRODUCTION WITH PAPAIN IN NORMAL AND SILICOTIC RATS. *Arch Environ Health,* 11**,** 50-8.

Guyot, N., J. Wartelle, L. Malleret, A. A. Todorov, G. Devouassoux, Y. Pacheco, D. E. Jenne & A. Belaaouaj (2014) Unopposed cathepsin G, neutrophil elastase, and proteinase 3 cause severe lung damage and emphysema. *Am J Pathol,* 184**,** 2197-210.

Hall, E. H., J. L. Balsbaugh, K. L. Rose, J. Shabanowitz, D. F. Hunt & D. L. Brautigan (2010) Comprehensive analysis of phosphorylation sites in Tensin1 reveals regulation by p38MAPK. *Mol Cell Proteomics,* 9**,** 2853-63.

Hall, E. H., A. E. Daugherty, C. K. Choi, A. F. Horwitz & D. L. Brautigan (2009) Tensin1 requires protein phosphatase-1alpha in addition to RhoGAP DLC-1 to control cell polarization, migration, and invasion. *J Biol Chem,* 284**,** 34713-22.

Halwani, R., J. Al-Abri, M. Beland, H. Al-Jahdali, A. J. Halayko, T. H. Lee, S. Al-Muhsen & Q. Hamid (2011) CC and CXC chemokines induce airway smooth muscle proliferation and survival. *J Immunol,* 186**,** 4156-63.

Han, M. K. & G. J. Criner (2013) Update in chronic obstructive pulmonary disease 2012. *Am J Respir Crit Care Med,* 188**,** 29-34.

Hanania, N. A., H. Mullerova, N. W. Locantore, J. Vestbo, M. L. Watkins, E. F. Wouters, S. I. Rennard & A. Sharafkhaneh (2011) Determinants of depression in the ECLIPSE chronic obstructive pulmonary disease cohort. *Am J Respir Crit Care Med,* 183**,** 604-11.

Hardaker, E. L., A. M. Bacon, K. Carlson, A. K. Roshak, J. J. Foley, D. B. Schmidt, P. T. Buckley, M. Comegys, R. A. Panettieri, Jr., H. M. Sarau & K. E. Belmonte (2004) Regulation of TNF-alpha- and IFN-gamma-induced CXCL10 expression: participation of the airway smooth muscle in the pulmonary inflammatory response in chronic obstructive pulmonary disease. *Faseb j,* 18**,** 191-3.

Haroon, S., R. Jordan, Y. Takwoingi & P. Adab (2015) Diagnostic accuracy of screening tests for COPD: a systematic review and meta-analysis. *BMJ Open,* 5**,** e008133.

Haynie, D. T. (2014) Molecular physiology of the tensin brotherhood of integrin adaptor proteins. *Proteins,* 82**,** 1113-27.

Hiemstra, P. S. (2013) Altered macrophage function in chronic obstructive pulmonary disease. *Ann Am Thorac Soc,* 10 Suppl**,** S180-5.

Hodge, S., G. Hodge, J. Ahern, H. Jersmann, M. Holmes & P. N. Reynolds (2007) Smoking alters alveolar macrophage recognition and phagocytic ability: implications in chronic obstructive pulmonary disease. *Am J Respir Cell Mol Biol,* 37**,** 748-55.

Hoenderdos, K. & A. Condliffe (2013) The neutrophil in chronic obstructive pulmonary disease. *Am J Respir Cell Mol Biol,* 48**,** 531-9.

Hogg, J. C., F. Chu, S. Utokaparch, R. Woods, W. M. Elliott, L. Buzatu, R. M. Cherniack, R. M. Rogers, F. C. Sciurba, H. O. Coxson & P. D. Pare (2004) The nature of small-airway obstruction in chronic obstructive pulmonary disease. *N Engl J Med,* 350**,** 2645-53.

Holtzman, M. J., L. M. Fabbri, P. M. O'Byrne, B. D. Gold, H. Aizawa, E. H. Walters, S. E. Alpert & J. A. Nadel (1983) Importance of airway inflammation for hyperresponsiveness induced by ozone. *Am Rev Respir Dis,* 127**,** 686-90.

Houghton, A. M. 2015. Matrix metalloproteinases in destructive lung disease. In *Matrix Biol*, 167-74. Netherlands: 2015. Published by Elsevier B.V.

Houghton, A. M., P. A. Quintero, D. L. Perkins, D. K. Kobayashi, D. G. Kelley, L. A. Marconcini, R. P. Mecham, R. M. Senior & S. D. Shapiro (2006) Elastin fragments drive disease progression in a murine model of emphysema. *J Clin Invest,* 116**,** 753-9.

Ichimaru, Y., D. I. Krimmer, J. K. Burgess, J. L. Black & B. G. Oliver (2012) TGF-beta enhances deposition of perlecan from COPD airway smooth muscle. *Am J Physiol Lung Cell Mol Physiol,* 302**,** L325-33.

Ioannidis, I., F. Ye, B. McNally, M. Willette & E. Flano (2013) Toll-like receptor expression and induction of type I and type III interferons in primary airway epithelial cells. *J Virol,* 87**,** 3261-70.

Irie, H. Y., R. V. Pearline, D. Grueneberg, M. Hsia, P. Ravichandran, N. Kothari, S. Natesan & J. S. Brugge (2005) Distinct roles of Akt1 and Akt2 in regulating cell migration and epithelial-mesenchymal transition. *J Cell Biol,* 171**,** 1023-34.

Ishida, T., M. Ishida, J. Suero, M. Takahashi & B. C. Berk (1999) Agonist-stimulated cytoskeletal reorganization and signal transduction at focal adhesions in vascular smooth muscle cells require c-Src. *J Clin Invest,* 103**,** 789-97.

Ishii, A. & S. H. Lo (2001) A role of tensin in skeletal-muscle regeneration. *Biochem J,* 356**,** 737-45.

James, A. & N. Carroll (2000) Airway smooth muscle in health and disease; methods of measurement and relation to function. *Eur Respir J,* 15**,** 782-9.

Jansen, S. R., A. M. Van Ziel, H. A. Baarsma & R. Gosens (2010) {beta}-Catenin regulates airway smooth muscle contraction. *Am J Physiol Lung Cell Mol Physiol,* 299**,** L204-14.

Jiang, B., S. Yamamura, P. R. Nelson, L. Mureebe & K. C. Kent (1996) Differential effects of platelet-derived growth factor isotypes on human smooth muscle cell proliferation and migration are mediated by distinct signaling pathways. *Surgery,* 120**,** 427-31; discussion 432.

Jockusch, B. M., P. Bubeck, K. Giehl, M. Kroemker, J. Moschner, M. Rothkegel, M. Rudiger, K. Schluter, G. Stanke & J. Winkler (1995) The molecular architecture of focal adhesions. *Annu Rev Cell Dev Biol,* 11**,** 379-416.

John, M., B. T. Au, P. J. Jose, S. Lim, M. Saunders, P. J. Barnes, J. A. Mitchell, M. G. Belvisi & K. F. Chung (1998) Expression and release of interleukin-8 by human airway smooth muscle cells: inhibition by Th-2 cytokines and corticosteroids. *Am J Respir Cell Mol Biol,* 18**,** 84-90.

Johnson, P. R. (2001) Role of human airway smooth muscle in altered extracellular matrix production in asthma. *Clin Exp Pharmacol Physiol,* 28**,** 233-6.

Kan, H., G. Heiss, K. M. Rose, E. Whitsel, F. Lurmann & S. J. London (2007) Traffic exposure and lung function in adults: the Atherosclerosis Risk in Communities study. *Thorax,* 62**,** 873-9.

Kanoh, S., T. Tanabe & B. K. Rubin (2011) IL-13-induced MUC5AC production and goblet cell differentiation is steroid resistant in human airway cells. *Clin Exp Allergy,* 41**,** 1747-56.

Katoh, K., Y. Kano, M. Masuda, H. Onishi & K. Fujiwara (1998) Isolation and contraction of the stress fiber. *Mol Biol Cell,* 9**,** 1919-38.

Katz, B. Z., E. Zamir, A. Bershadsky, Z. Kam, K. M. Yamada & B. Geiger (2000a) Physical state of the extracellular matrix regulates the structure and molecular composition of cell-matrix adhesions. *Mol Biol Cell,* 11**,** 1047-60.

Katz, B. Z., M. Zohar, H. Teramoto, K. Matsumoto, J. S. Gutkind, D. C. Lin, S. Lin & K. M. Yamada (2000b) Tensin can induce JNK and p38 activation. *Biochem Biophys Res Commun,* 272**,** 717-20.

Katz, M., I. Amit, A. Citri, T. Shay, S. Carvalho, S. Lavi, F. Milanezi, L. Lyass, N. Amariglio, J. Jacob-Hirsch, N. Ben-Chetrit, G. Tarcic, M. Lindzen, R. Avraham, Y. C. Liao, P. Trusk, A. Lyass, G. Rechavi, N. L. Spector, S. H. Lo, F. Schmitt, S. S. Bacus & Y. Yarden (2007) A reciprocal tensin-3-cten switch mediates EGF-driven mammary cell migration. *Nat Cell Biol,* 9**,** 961-9.

Kerkhof, M., H. M. Boezen, R. Granell, A. H. Wijga, B. Brunekreef, H. A. Smit, J. C. de Jongste, C. Thijs, M. Mommers, J. Penders, J. Henderson, G. H. Koppelman & D. S. Postma (2014) Transient early wheeze and lung function in early childhood

associated with chronic obstructive pulmonary disease genes. *J Allergy Clin Immunol,* 133**,** 68-76.e1-4.

Khan, M. A. (2013) Inflammation signals airway smooth muscle cell proliferation in asthma pathogenesis. *Multidiscip Respir Med,* 8**,** 11.

Kielty, C. M., M. J. Sherratt & C. A. Shuttleworth (2002) Elastic fibres. *J Cell Sci,* 115**,** 2817-28.

Kistemaker, L. E. & R. Gosens (2015) Acetylcholine beyond bronchoconstriction: roles in inflammation and remodeling. *Trends Pharmacol Sci,* 36**,** 164-71.

Konigshoff, M., N. Kneidinger & O. Eickelberg (2009) TGF-beta signaling in COPD: deciphering genetic and cellular susceptibilities for future therapeutic regimen. *Swiss Med Wkly,* 139**,** 554-63.

Kook, S., D. H. Kim, S. R. Shim, W. Kim, J. S. Chun & W. K. Song (2003) Caspase-dependent cleavage of tensin induces disruption of actin cytoskeleton during apoptosis. *Biochem Biophys Res Commun,* 303**,** 37-45.

Koziol-White, C. J. & R. A. Panettieri, Jr. (2011) Airway smooth muscle and immunomodulation in acute exacerbations of airway disease. *Immunol Rev,* 242**,** 178-85.

Kranenburg, A. R., A. Willems-Widyastuti, W. J. Moori, P. J. Sterk, V. K. Alagappan, W. I. de Boer & H. S. Sharma (2006) Enhanced bronchial expression of extracellular matrix proteins in chronic obstructive pulmonary disease. *Am J Clin Pathol,* 126**,** 725-35.

Kwak, H. J., D. W. Park, J. Y. Seo, J. Y. Moon, T. H. Kim, J. W. Sohn, D. H. Shin, H. J. Yoon, S. S. Park & S. H. Kim (2015) The Wnt/beta-catenin signaling pathway regulates the development of airway remodeling in patients with asthma. *Exp Mol Med,* 47**,** e198.

Larsson, C. (1978) Natural history and life expectancy in severe alpha1-antitrypsin deficiency, Pi Z. *Acta Med Scand,* 204**,** 345-51.

Leikauf, G. D., H. Pope-Varsalona, V. J. Concel, P. Liu, K. Bein, A. Berndt, T. M. Martin, K. Ganguly, A. S. Jang, K. A. Brant, R. A. Dopico, Jr., S. Upadhyay, Y. P. Di, Q. Li, Z. Hu, L. J. Vuga, M. Medvedovic, N. Kaminski, M. You, D. C. Alexander, J. E. McDunn, D. R. Prows, D. L. Knoell & J. P. Fabisiak (2012) Integrative assessment of chlorine-induced acute lung injury in mice. *Am J Respir Cell Mol Biol,* 47**,** 234-44.

Lewis, R. J., L. Chachi, C. Newby, Y. Amrani & P. Bradding (2016) Bidirectional Counterregulation of Human Lung Mast Cell and Airway Smooth Muscle beta2 Adrenoceptors. *J Immunol,* 196**,** 55-63.

Li, X., Y. He, Y. Xu, X. Huang, J. Liu, M. Xie & X. Liu (2016) KLF5 mediates vascular remodeling via HIF-1alpha in hypoxic pulmonary hypertension. *Am J Physiol Lung Cell Mol Physiol,* 310**,** L299-310.

Liang, K. C., C. W. Lee, W. N. Lin, C. C. Lin, C. B. Wu, S. F. Luo & C. M. Yang (2007) Interleukin-1beta induces MMP-9 expression via p42/p44 MAPK, p38 MAPK, JNK, and nuclear factor-kappaB signaling pathways in human tracheal smooth muscle cells. *J Cell Physiol,* 211**,** 759-70.

Liao, Y. C. & S. H. Lo (2008) Deleted in liver cancer-1 (DLC-1): a tumor suppressor not just for liver. *Int J Biochem Cell Biol,* 40**,** 843-7.

Liu, X., B. Hao, A. Ma, J. He & J. Chen (2016) The Expression of NOX4 in Smooth Muscles of Small Airway Correlates with the Disease Severity of COPD. *Biomed Res Int,* 2016**,** 2891810.

Livak, K. J. & T. D. Schmittgen (2001) Analysis of relative gene expression data using real-time quantitative PCR and the 2(-Delta Delta C(T)) Method. *Methods,* 25**,** 402-8.

Lo, S. H. (2004) Tensin. *Int J Biochem Cell Biol,* 36**,** 31-4.

Lo, S. H., Q. C. Yu, L. Degenstein, L. B. Chen & E. Fuchs (1997) Progressive kidney degeneration in mice lacking tensin. *J Cell Biol,* 136**,** 1349-61.

Lofdahl, M., R. Kaarteenaho, E. Lappi-Blanco, G. Tornling & M. C. Skold (2011) Tenascin-C and alpha-smooth muscle actin positive cells are increased in the large airways in patients with COPD. *Respir Res,* 12**,** 48.

Lugade, A. A., P. N. Bogner, T. H. Thatcher, P. J. Sime, R. P. Phipps & Y. Thanavala (2014) Cigarette smoke exposure exacerbates lung inflammation and compromises immunity to bacterial infection. *J Immunol,* 192**,** 5226-35.

Lumsden, A. B., A. McLean & D. Lamb (1984) Goblet and Clara cells of human distal airways: evidence for smoking induced changes in their numbers. *Thorax,* 39**,** 844-9.

Ma, L., M. Brown, P. Kogut, K. Serban, X. Li, J. McConville, B. Chen, J. K. Bentley, M. B. Hershenson, N. Dulin, J. Solway & B. Camoretti-Mercado (2011) Akt activation induces hypertrophy without contractile phenotypic maturation in airway smooth muscle. *Am J Physiol Lung Cell Mol Physiol,* 300**,** L701-9.

Mak, J. C., J. N. Baraniuk & P. J. Barnes (1992) Localization of muscarinic receptor subtype mRNAs in human lung. *Am J Respir Cell Mol Biol,* 7**,** 344-8.

Mall, M. A., J. R. Harkema, J. B. Trojanek, D. Treis, A. Livraghi, S. Schubert, Z. Zhou, S. M. Kreda, S. L. Tilley, E. J. Hudson, W. K. O'Neal & R. C. Boucher (2008) Development of chronic bronchitis and emphysema in beta-epithelial Na+ channel-overexpressing mice. *Am J Respir Crit Care Med,* 177**,** 730-42.

Marin, L., P. Colombo, M. Bebawy, P. M. Young & D. Traini (2011) Chronic obstructive pulmonary disease: patho-physiology, current methods of treatment and the potential for simvastatin in disease management. *Expert Opin Drug Deliv,* 8**,** 1205-20.

Markham, A. & H. M. Lamb (2000) Infliximab: a review of its use in the management of rheumatoid arthritis. *Drugs,* 59**,** 1341-59.

Martuszewska, D., B. Ljungberg, M. Johansson, G. Landberg, C. Oslakovic, B. Dahlback & S. Hafizi (2009) Tensin3 is a negative regulator of cell migration and all four Tensin family members are downregulated in human kidney cancer. *PLoS One,* 4**,** e4350.

McCleverty, C. J., D. C. Lin & R. C. Liddington (2007) Structure of the PTB domain of tensin1 and a model for its recruitment to fibrillar adhesions. *Protein Sci,* 16**,** 1223-9.

Merrilees, M. J., P. S. Ching, B. Beaumont, A. Hinek, T. N. Wight & P. N. Black (2008) Changes in elastin, elastin binding protein and versican in alveoli in chronic obstructive pulmonary disease. *Respir Res,* 9**,** 41.

Mian, M. F., N. M. Lauzon, M. R. Stampfli, K. L. Mossman & A. A. Ashkar (2008) Impairment of human NK cell cytotoxic activity and cytokine release by cigarette smoke. *J Leukoc Biol,* 83**,** 774-84.

Michaeli, D. & H. H. Fudenberg (1974) Antibodies to collagen in patients with emphysema. *Clin Immunol Immunopathol,* 3**,** 187-92.

Miller, Y. I., S. Viriyakosol, D. S. Worrall, A. Boullier, S. Butler & J. L. Witztum (2005) Toll-like receptor 4-dependent and -independent cytokine secretion induced by minimally oxidized low-density lipoprotein in macrophages. *Arterioscler Thromb Vasc Biol,* 25**,** 1213-9.

Miossec, P., T. Korn & V. K. Kuchroo (2009) Interleukin-17 and type 17 helper T cells. *N Engl J Med,* 361**,** 888-98.

Mouneimne, G. & J. S. Brugge (2007) Tensins: a new switch in cell migration. *Dev Cell,* 13**,** 317-9.

Munkholm, M. & J. Mortensen (2014) Mucociliary clearance: pathophysiological aspects. *Clin Physiol Funct Imaging,* 34**,** 171-7.

Nasuhara, Y., I. M. Adcock, M. Catley, P. J. Barnes & R. Newton (1999) Differential IkappaB kinase activation and IkappaBalpha degradation by interleukin-1beta and tumor necrosis factor-alpha in human U937 monocytic cells. Evidence for additional regulatory steps in kappaB-dependent transcription. *J Biol Chem,* 274**,** 19965-72.

Nishino, T., N. Sasaki, M. Chihara, K. Nagasaki, D. Torigoe, Y. Kon & T. Agui (2012) Distinct distribution of the tensin family in the mouse kidney and small intestine. *Exp Anim,* 61**,** 525-32.

Norrby, K. (2002) Mast cells and angiogenesis. *Apmis,* 110**,** 355-71.

Noveral, J. P., A. Bhala, R. L. Hintz, M. M. Grunstein & P. Cohen (1994) Insulin-like growth factor axis in airway smooth muscle cells. *Am J Physiol,* 267**,** L761-5.

Nunez, B., J. Sauleda, J. M. Anto, M. R. Julia, M. Orozco, E. Monso, A. Noguera, F. P. Gomez, J. Garcia-Aymerich & A. Agusti (2011) Anti-tissue antibodies are related to lung function in chronic obstructive pulmonary disease. *Am J Respir Crit Care Med,* 183**,** 1025-31.

Oltmanns, U., M. B. Sukkar, S. Xie, M. John & K. F. Chung (2005) Induction of human airway smooth muscle apoptosis by neutrophils and neutrophil elastase. *Am J Respir Cell Mol Biol,* 32**,** 334-41.

Onfelt, B., S. Nedvetzki, R. K. Benninger, M. A. Purbhoo, S. Sowinski, A. N. Hume, M. C. Seabra, M. A. Neil, P. M. French & D. M. Davis (2006) Structurally distinct membrane nanotubes between human macrophages support long-distance vesicular traffic or surfing of bacteria. *J Immunol,* 177**,** 8476-83.

Opazo Saez, A. M., C. Y. Seow & P. D. Pare (2000) Peripheral airway smooth muscle mechanics in obstructive airways disease. *Am J Respir Crit Care Med,* 161**,** 910-7.

Pankov, R., E. Cukierman, B. Z. Katz, K. Matsumoto, D. C. Lin, S. Lin, C. Hahn & K. M. Yamada (2000) Integrin dynamics and matrix assembly: tensin-dependent translocation of alpha(5)beta(1) integrins promotes early fibronectin fibrillogenesis. *J Cell Biol,* 148**,** 1075-90.

Parameswaran, K., A. Willems-Widyastuti, V. K. Alagappan, K. Radford, A. R. Kranenburg & H. S. Sharma (2006) Role of extracellular matrix and its regulators in human airway smooth muscle biology. *Cell Biochem Biophys,* 44**,** 139-46.

Pelletier, A. J., S. C. Bodary & A. D. Levinson (1992) Signal transduction by the platelet integrin alpha IIb beta 3: induction of calcium oscillations required for protein-tyrosine phosphorylation and ligand-induced spreading of stably transfected cells. *Mol Biol Cell,* 3**,** 989-98.

Perkins, C., N. Yanase, G. Smulian, L. Gildea, T. Orekov, C. Potter, F. Brombacher, B. Aronow, M. Wills-Karp & F. D. Finkelman (2011) Selective stimulation of IL-4 receptor on smooth muscle induces airway hyperresponsiveness in mice. *J Exp Med,* 208**,** 853-67.

Pins, G. D., D. L. Christiansen, R. Patel & F. H. Silver (1997) Self-assembly of collagen fibers. Influence of fibrillar alignment and decorin on mechanical properties. *Biophys J,* 73**,** 2164-72.

Pollard, T. D. & J. A. Cooper (2009) Actin, a central player in cell shape and movement. *Science,* 326**,** 1208-12.

Polverino, F., L. J. Seys, K. R. Bracke & C. A. Owen (2016) B cells in chronic obstructive pulmonary disease: moving to center stage. *Am J Physiol Lung Cell Mol Physiol,* 311**,** L687-l695.

Pouwels, S. D., I. H. Heijink, N. H. ten Hacken, P. Vandenabeele, D. V. Krysko, M. C. Nawijn & A. J. van Oosterhout (2014) DAMPs activating innate and adaptive immune responses in COPD. *Mucosal Immunol,* 7**,** 215-26.

Prakash, Y. S. (2016) Emerging concepts in smooth muscle contributions to airway structure and function: implications for health and disease. *Am J Physiol Lung Cell Mol Physiol,* 311**,** L1113-l1140.

Prescott, E., P. Lange & J. Vestbo (1995) Chronic mucus hypersecretion in COPD and death from pulmonary infection. *Eur Respir J,* 8**,** 1333-8.

Profita, M., A. Bonanno, A. M. Montalbano, M. Ferraro, L. Siena, A. Bruno, S. Girbino, G. D. Albano, P. Casarosa, M. P. Pieper & M. Gjomarkaj (2011) Cigarette smoke extract activates human bronchial epithelial cells affecting non-neuronal cholinergic system signalling in vitro. *Life Sci,* 89**,** 36-43.

Pylayeva, Y. & F. G. Giancotti. 2007. Tensin relief facilitates migration. In *Nat Cell Biol*, 877-9. England.

Pype, J. L., L. J. Dupont, P. Menten, E. Van Coillie, G. Opdenakker, J. Van Damme, K. F. Chung, M. G. Demedts & G. M. Verleden (1999) Expression of monocyte chemotactic protein (MCP)-1, MCP-2, and MCP-3 by human airway smooth-muscle cells. Modulation by corticosteroids and T-helper 2 cytokines. *Am J Respir Cell Mol Biol,* 21**,** 528-36.

Qian, X., G. Li, H. K. Asmussen, L. Asnaghi, W. C. Vass, R. Braverman, K. M. Yamada, N. C. Popescu, A. G. Papageorge & D. R. Lowy (2007) Oncogenic inhibition by a deleted in liver cancer gene requires cooperation between tensin binding and Rho-specific GTPase-activating protein activities. *Proc Natl Acad Sci U S A,* 104**,** 9012-7.

Redhu, N. S., A. Saleh, A. J. Halayko, A. S. Ali & A. S. Gounni (2011) Essential role of NF-kappaB and AP-1 transcription factors in TNF-alpha-induced TSLP expression in human airway smooth muscle cells. *Am J Physiol Lung Cell Mol Physiol,* 300**,** L479-85.

Ren, X. D., W. B. Kiosses, D. J. Sieg, C. A. Otey, D. D. Schlaepfer & M. A. Schwartz (2000) Focal adhesion kinase suppresses Rho activity to promote focal adhesion turnover. *J Cell Sci,* 113 (Pt 20)**,** 3673-8.

Repapi, E., I. Sayers, L. V. Wain, P. R. Burton, T. Johnson, M. Obeidat, J. H. Zhao, A. Ramasamy, G. Zhai, V. Vitart, J. E. Huffman, W. Igl, E. Albrecht, P. Deloukas, J. Henderson, R. Granell, W. L. McArdle, A. R. Rudnicka, I. Barroso, R. J. Loos, N. J. Wareham, L. Mustelin, T. Rantanen, I. Surakka, M. Imboden, H. E. Wichmann, I. Grkovic, S. Jankovic, L. Zgaga, A. L. Hartikainen, L. Peltonen, U. Gyllensten, A. Johansson, G. Zaboli, H. Campbell, S. H. Wild, J. F. Wilson, S. Glaser, G. Homuth, H. Volzke, M. Mangino, N. Soranzo, T. D. Spector, O. Polasek, I. Rudan, A. F. Wright, M. Heliovaara, S. Ripatti, A. Pouta, A. T. Naluai, A. C. Olin, K. Toren, M. N. Cooper, A. L. James, L. J. Palmer, A. D. Hingorani, S. G. Wannamethee, P. H. Whincup, G. D. Smith, S. Ebrahim, T. M. McKeever, I. D. Pavord, A. K. MacLeod, A. D. Morris, D. J. Porteous, C. Cooper, E. Dennison, S. Shaheen, S. Karrasch, E. Schnabel, H. Schulz, H. Grallert, N. Bouatia-Naji, J. Delplanque, P. Froguel, J. D. Blakey, J. R. Britton, R. W. Morris, J. W. Holloway, D. A. Lawlor, J. Hui, F. Nyberg, M. R. Jarvelin, C. Jackson,

M. Kahonen, J. Kaprio, N. M. Probst-Hensch, B. Koch, C. Hayward, D. M. Evans, P. Elliott, D. P. Strachan, I. P. Hall & M. D. Tobin (2010) Genome-wide association study identifies five loci associated with lung function. *Nat Genet,* 42**,** 36-44.

Roach, K. M., S. M. Duffy, W. Coward, C. Feghali-Bostwick, H. Wulff & P. Bradding (2013) The K+ Channel KCa3.1 as a Novel Target for Idiopathic Pulmonary Fibrosis. *PLoS One,* 8.

Roffel, A. F., C. R. Elzinga & J. Zaagsma (1990) Muscarinic M3 receptors mediate contraction of human central and peripheral airway smooth muscle. *Pulm Pharmacol,* 3**,** 47-51.

Romer, L. H., K. G. Birukov & J. G. Garcia (2006) Focal adhesions: paradigm for a signaling nexus. *Circ Res,* 98**,** 606-16.

Rovina, N., A. Koutsoukou & N. G. Koulouris (2013) Inflammation and immune response in COPD: where do we stand? *Mediators Inflamm,* 2013**,** 413735.

Saetta, M., A. Di Stefano, G. Turato, F. M. Facchini, L. Corbino, C. E. Mapp, P. Maestrelli, A. Ciaccia & L. M. Fabbri (1998) CD8+ T-lymphocytes in peripheral airways of smokers with chronic obstructive pulmonary disease. *Am J Respir Crit Care Med,* 157**,** 822-6.

Saintigny, G., F. X. Bernard, F. Juchaux, N. Pedretti & C. Mahe (2008) Reduced expression of the adhesion protein tensin1 in cultured human dermal fibroblasts affects collagen gel contraction. *Exp Dermatol,* 17**,** 788-9.

Sakota, Y., Y. Ozawa, H. Yamashita, H. Tanaka & N. Inagaki (2014) Collagen gel contraction assay using human bronchial smooth muscle cells and its application for evaluation of inhibitory effect of formoterol. *Biol Pharm Bull,* 37**,** 1014-20.

Santos, S., A. Marin, J. Serra-Batlles, D. de la Rosa, I. Solanes, X. Pomares, M. Lopez-Sanchez, M. Munoz-Esquerre & M. Miravitlles (2016) Treatment of

patients with COPD and recurrent exacerbations: the role of infection and inflammation. *Int J Chron Obstruct Pulmon Dis,* 11**,** 515-25.

Schamberger, A. C., C. A. Staab-Weijnitz, N. Mise-Racek & O. Eickelberg (2015) Cigarette smoke alters primary human bronchial epithelial cell differentiation at the air-liquid interface. *Sci Rep,* 5**,** 8163.

Segura-Valdez, L., A. Pardo, M. Gaxiola, B. D. Uhal, C. Becerril & M. Selman (2000) Upregulation of gelatinases A and B, collagenases 1 and 2, and increased parenchymal cell death in COPD. *Chest,* 117**,** 684-94.

Selivanova, P. A., E. S. Kulikov, O. V. Kozina, I. N. Trofimenko, M. B. Freidin, B. A. Chernyak & L. M. Ogorodova (2012) Differential expression of the beta2-adrenoreceptor and M3-cholinoreceptor genes in bronchial mucosa of patients with asthma and chronic obstructive pulmonary disease. *Ann Allergy Asthma Immunol,* 108**,** 39-43.

Sethi, S. & T. F. Murphy (2008) Infection in the pathogenesis and course of chronic obstructive pulmonary disease. *N Engl J Med,* 359**,** 2355-65.

Shapiro, S. D., N. M. Goldstein, A. M. Houghton, D. K. Kobayashi, D. Kelley & A. Belaaouaj (2003) Neutrophil elastase contributes to cigarette smoke-induced emphysema in mice. *Am J Pathol,* 163**,** 2329-35.

Shaykhiev, R. & R. G. Crystal (2013) Innate immunity and chronic obstructive pulmonary disease: a mini-review. *Gerontology,* 59**,** 481-9.

Shaykhiev, R., F. Otaki, P. Bonsu, D. T. Dang, M. Teater, Y. Strulovici-Barel, J. Salit, B. G. Harvey & R. G. Crystal (2011) Cigarette smoking reprograms apical junctional complex molecular architecture in the human airway epithelium in vivo. *Cell Mol Life Sci,* 68**,** 877-92.

Shikotra, A., D. F. Choy, C. M. Ohri, E. Doran, C. Butler, B. Hargadon, M. Shelley, A. R. Abbas, C. D. Austin, J. Jackman, L. C. Wu, L. G. Heaney, J. R. Arron & P. Bradding (2012) Increased expression of immunoreactive thymic stromal lymphopoietin in patients with severe asthma. *J Allergy Clin Immunol,* 129**,** 104-11.e1-9.

Shiomi, T., D. J. Tschumperlin, J. A. Park, S. W. Sunnarborg, K. Horiuchi, C. P. Blobel & J. M. Drazen (2011) TNF-alpha-converting enzyme/a disintegrin and metalloprotease-17 mediates mechanotransduction in murine tracheal epithelial cells. *Am J Respir Cell Mol Biol,* 45**,** 376-85.

Siafakas, N. M., P. Vermeire, N. B. Pride, P. Paoletti, J. Gibson, P. Howard, J. C. Yernault, M. Decramer, T. Higenbottam, D. S. Postma & et al. (1995) Optimal assessment and management of chronic obstructive pulmonary disease (COPD). The European Respiratory Society Task Force. *Eur Respir J,* 8**,** 1398-420.

Siddiqui, S., V. Mistry, C. Doe, K. Roach, A. Morgan, A. Wardlaw, I. Pavord, P. Bradding & C. Brightling (2008a) Airway hyperresponsiveness is dissociated from airway wall structural remodeling. *J Allergy Clin Immunol,* 122**,** 335-341.e3.

--- (2008b) Airway hyperresponsiveness is dissociated from airway wall structural remodeling. *J Allergy Clin Immunol,* 122**,** 335-41, 341.e1-3.

Singh, S., A. V. Amin & Y. K. Loke (2009) Long-term use of inhaled corticosteroids and the risk of pneumonia in chronic obstructive pulmonary disease: a meta-analysis. *Arch Intern Med,* 169**,** 219-29.

Skalli, O., P. Ropraz, A. Trzeciak, G. Benzonana, D. Gillessen & G. Gabbiani (1986) A monoclonal antibody against alpha-smooth muscle actin: a new probe for smooth muscle differentiation. *J Cell Biol,* 103**,** 2787-96.

Smaldone, G. C., W. M. Foster, T. G. O'Riordan, M. S. Messina, R. J. Perry & E. G. Langenback (1993) Regional impairment of mucociliary clearance in chronic obstructive pulmonary disease. *Chest,* 103**,** 1390-6.

Smith, B. A., B. Tolloczko, J. G. Martin & P. Grutter (2005) Probing the viscoelastic behavior of cultured airway smooth muscle cells with atomic force microscopy: stiffening induced by contractile agonist. *Biophys J,* 88**,** 2994-3007.

Soler Artigas, M., L. V. Wain, E. Repapi, M. Obeidat, I. Sayers, P. R. Burton, T. Johnson, J. H. Zhao, E. Albrecht, A. F. Dominiczak, S. M. Kerr, B. H. Smith, G. Cadby, J. Hui, L. J. Palmer, A. D. Hingorani, S. G. Wannamethee, P. H. Whincup, S. Ebrahim, G. D. Smith, I. Barroso, R. J. Loos, N. J. Wareham, C. Cooper, E. Dennison, S. O. Shaheen, J. Z. Liu, J. Marchini, S. Dahgam, A. T. Naluai, A. C. Olin, S. Karrasch, J. Heinrich, H. Schulz, T. M. McKeever, I. D. Pavord, M. Heliovaara, S. Ripatti, I. Surakka, J. D. Blakey, M. Kahonen, J. R. Britton, F. Nyberg, J. W. Holloway, D. A. Lawlor, R. W. Morris, A. L. James, C. M. Jackson, I. P. Hall & M. D. Tobin (2011) Effect of five genetic variants associated with lung function on the risk of chronic obstructive lung disease, and their joint effects on lung function. *Am J Respir Crit Care Med,* 184**,** 786-95.

Spond, J., M. M. Billah, R. W. Chapman, R. W. Egan, J. A. Hey, A. House, W. Kreutner & M. Minnicozzi (2004) The role of neutrophils in LPS-induced changes in pulmonary function in conscious rats. *Pulm Pharmacol Ther,* 17**,** 133-40.

Stamatiou, R., E. Paraskeva, K. Gourgoulianis, P. A. Molyvdas & A. Hatziefthimiou (2012) Cytokines and growth factors promote airway smooth muscle cell proliferation. *ISRN Inflamm,* 2012**,** 731472.

Stanchi, F., C. Grashoff, C. F. Nguemeni Yonga, D. Grall, R. Fassler & E. Van Obberghen-Schilling (2009) Molecular dissection of the ILK-PINCH-parvin triad

reveals a fundamental role for the ILK kinase domain in the late stages of focal-adhesion maturation. *J Cell Sci,* 122**,** 1800-11.

Stockley, R. A., D. Mannino & P. J. Barnes (2009) Burden and pathogenesis of chronic obstructive pulmonary disease. *Proc Am Thorac Soc,* 6**,** 524-6.

GOLD Strategy G. 2016. From the *Global Strategy for the Diagnosis, Management and Prevention of COPD*, Global Initiative for Chronic Obstructive Lung Disease (GOLD) 2016.

Szabo, I. L., R. Pai, M. K. Jones, G. R. Ehring, H. Kawanaka & A. S. Tarnawski (2002) Indomethacin delays gastric restitution: association with the inhibition of focal adhesion kinase and tensin phosphorylation and reduced actin stress fibers. *Exp Biol Med (Maywood),* 227**,** 412-24.

Takizawa, H., M. Tanaka, K. Takami, T. Ohtoshi, K. Ito, M. Satoh, Y. Okada, F. Yamasawa, K. Nakahara & A. Umeda (2001) Increased expression of transforming growth factor-beta1 in small airway epithelium from tobacco smokers and patients with chronic obstructive pulmonary disease (COPD). *Am J Respir Crit Care Med,* 163**,** 1476-83.

Tanabe, N., S. Muro, T. Hirai, T. Oguma, K. Terada, S. Marumo, D. Kinose, E. Ogawa, Y. Hoshino & M. Mishima (2011) Impact of exacerbations on emphysema progression in chronic obstructive pulmonary disease. *Am J Respir Crit Care Med,* 183**,** 1653-9.

Tang, D. D. (2015) Critical role of actin-associated proteins in smooth muscle contraction, cell proliferation, airway hyperresponsiveness and airway remodeling. *Respir Res,* 16**,** 134.

Tang, H., J. Chen, D. R. Fraidenburg, S. Song, J. R. Sysol, A. R. Drennan, S. Offermanns, R. D. Ye, M. G. Bonini, R. D. Minshall, J. G. Garcia, R. F. Machado, A.

Makino & J. X. Yuan (2015) Deficiency of Akt1, but not Akt2, attenuates the development of pulmonary hypertension. *Am J Physiol Lung Cell Mol Physiol,* 308**,** L208-20.

Tennant, J. R. (1964) EVALUATION OF THE TRYPAN BLUE TECHNIQUE FOR DETERMINATION OF CELL VIABILITY. *Transplantation,* 2**,** 685-94.

Thornberry, N. A. & Y. Lazebnik (1998) Caspases: enemies within. *Science,* 281**,** 1312-6.

Tiddens, H. A., P. D. Pare, J. C. Hogg, W. C. Hop, R. Lambert & J. C. de Jongste (1995) Cartilaginous airway dimensions and airflow obstruction in human lungs. *Am J Respir Crit Care Med,* 152**,** 260-6.

Tjin, G., P. Xu, S. H. Kable, E. P. Kable & J. K. Burgess (2014) Quantification of collagen I in airway tissues using second harmonic generation. *J Biomed Opt,* 19**,** 36005.

Tkac, J., S. F. Man & D. D. Sin (2007) Systemic consequences of COPD. *Ther Adv Respir Dis,* 1**,** 47-59.

Tran, T., C. M. Teoh, J. K. Tam, Y. Qiao, C. Y. Chin, O. K. Chong, A. G. Stewart, T. Harris, W. S. Wong, S. P. Guan, B. P. Leung, W. T. Gerthoffer, H. Unruh & A. J. Halayko (2013) Laminin drives survival signals to promote a contractile smooth muscle phenotype and airway hyperreactivity. *Faseb j,* 27**,** 3991-4003.

Trompette, A., S. Divanovic, A. Visintin, C. Blanchard, R. S. Hegde, R. Madan, P. S. Thorne, M. Wills-Karp, T. L. Gioannini, J. P. Weiss & C. L. Karp (2009) Allergenicity resulting from functional mimicry of a Toll-like receptor complex protein. *Nature,* 457**,** 585-8.

Upham, J. W. & Y. Xi (2016) Dendritic cells in human lung disease: recent advances. *Chest*.

Van Pottelberge, G. R., K. R. Bracke, I. K. Demedts, K. De Rijck, S. M. Reinartz, C. M. van Drunen, G. M. Verleden, F. E. Vermassen, G. F. Joos & G. G. Brusselle (2010) Selective accumulation of langerhans-type dendritic cells in small airways of patients with COPD. *Respir Res,* 11**,** 35.

van Straaten, J. F., W. Coers, J. A. Noordhoek, S. Huitema, J. T. Flipsen, H. F. Kauffman, W. Timens & D. S. Postma (1999) Proteoglycan changes in the extracellular matrix of lung tissue from patients with pulmonary emphysema. *Mod Pathol,* 12**,** 697-705.

Vijayan, V. K. (2013) Chronic obstructive pulmonary disease. *Indian J Med Res,* 137**,** 251-69.

Vlahos, R., S. Bozinovski, R. C. Gualano, M. Ernst & G. P. Anderson (2006) Modelling COPD in mice. *Pulm Pharmacol Ther,* 19**,** 12-7.

Volberg, T., L. Romer, E. Zamir & B. Geiger (2001) pp60(c-src) and related tyrosine kinases: a role in the assembly and reorganization of matrix adhesions. *J Cell Sci,* 114**,** 2279-89.

Wang, Q., D. J. Miller, E. R. Bowman, D. R. Nagarkar, D. Schneider, Y. Zhao, M. J. Linn, A. M. Goldsmith, J. K. Bentley, U. S. Sajjan & M. B. Hershenson (2011) MDA5 and TLR3 initiate pro-inflammatory signaling pathways leading to rhinovirus-induced airways inflammation and hyperresponsiveness. *PLoS Pathog,* 7**,** e1002070.

Wanner, A., M. Salathe & T. G. O'Riordan (1996) Mucociliary clearance in the airways. *Am J Respir Crit Care Med,* 154**,** 1868-902.

Webber, M. M., D. Bello & S. Quader (1997) Immortalized and tumorigenic adult human prostatic epithelial cell lines: characteristics and applications Part 2. Tumorigenic cell lines. *Prostate,* 30**,** 58-64.

Weigt, C., A. Gaertner, A. Wegner, H. Korte & H. E. Meyer (1992) Occurrence of an actin-inserting domain in tensin. *J Mol Biol,* 227**,** 593-5.

Wiegman, C. H., C. Michaeloudes, G. Haji, P. Narang, C. J. Clarke, K. E. Russell, W. Bao, S. Pavlidis, P. J. Barnes, J. Kanerva, A. Bittner, N. Rao, M. P. Murphy, P. A. Kirkham, K. F. Chung & I. M. Adcock (2015) Oxidative stress-induced mitochondrial dysfunction drives inflammation and airway smooth muscle remodeling in patients with chronic obstructive pulmonary disease. *J Allergy Clin Immunol,* 136**,** 769-80.

Woodman, L., S. Siddiqui, G. Cruse, A. Sutcliffe, R. Saunders, D. Kaur, P. Bradding & C. Brightling (2008) Mast cells promote airway smooth muscle cell differentiation via autocrine up-regulation of TGF-beta 1. *J Immunol,* 181**,** 5001-7.

Xia, Y. C., N. S. Redhu, L. M. Moir, C. Koziol-White, A. J. Ammit, L. Al-Alwan, B. Camoretti-Mercado & R. L. Clifford (2013) Pro-inflammatory and immunomodulatory functions of airway smooth muscle: emerging concepts. *Pulm Pharmacol Ther,* 26**,** 64-74.

Xie, S., R. Issa, M. B. Sukkar, U. Oltmanns, P. K. Bhavsar, A. Papi, G. Caramori, I. Adcock & K. F. Chung (2005) Induction and regulation of matrix metalloproteinase-12 in human airway smooth muscle cells. *Respir Res,* 6**,** 148.

Yang, Q., N. Shigemura, M. J. Underwood, M. Hsin, H. M. Xue, Y. Huang, G. W. He & C. M. Yu (2012) NO and EDHF pathways in pulmonary arteries and veins are impaired in COPD patients. *Vascul Pharmacol,* 57**,** 113-8.

Zamir, E., M. Katz, Y. Posen, N. Erez, K. M. Yamada, B. Z. Katz, S. Lin, D. C. Lin, A. Bershadsky, Z. Kam & B. Geiger (2000) Dynamics and segregation of cell-matrix adhesions in cultured fibroblasts. *Nat Cell Biol,* 2**,** 191-6.

Zandvoort, A., D. S. Postma, M. R. Jonker, J. A. Noordhoek, J. T. Vos, Y. M. van der Geld & W. Timens (2006) Altered expression of the Smad signalling pathway: implications for COPD pathogenesis. *Eur Respir J,* 28**,** 533-41.

Zhang, J., J. He, J. Xia, Z. Chen & X. Chen (2012) Delayed apoptosis by neutrophils from COPD patients is associated with altered Bak, Bcl-xl, and Mcl-1 mRNA expression. *Diagn Pathol,* 7**,** 65.

Zhao, L., X. Zhang, H. Kuang, J. Wu, Y. Guo & L. Ma (2013) Effect of TRPV1 channel on the proliferation and apoptosis in asthmatic rat airway smooth muscle cells. *Exp Lung Res,* 39**,** 283-94.